

TECHNICAL UNIVERSITY OF MOLDOVA



With manuscript title

C.Z.U: 621.382:546:620.3(043)

MONAICO EDUARD

**MICRO- AND NANO-ENGINEERING OF SEMICONDUCTOR
COMPOUNDS AND METAL STRUCTURES BASED ON
ELECTROCHEMICAL TECHNOLOGIES**

134.01 – PHYSICS AND MATERIALS TECHNOLOGY

**Synthesis work for the title of Doctor Habilitat in Physics
(elaborated on the basis of published scientific papers)**

CHISINAU, 2024

The synthesis work was elaborated at the National Center for Materials Study and Testing, Technical University of Moldova (TUM), and is carried out as part of the postdoctoral project for period 2021-2022 „Micro- and nano-engineering of semiconductor compounds based on electrochemical technologies for electronic and photonic applications” with the code #21.00208.5007.15/PD.

The composition of the public defense Commission:

(approved by the Decision of the Scientific Council of TUM nr. 3 from 29.03.2024)

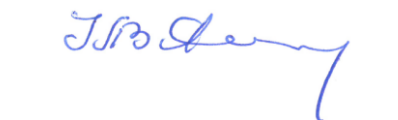
1. **ȚIULEANU Dumitru** PhD habil. in physical and mathematical sciences, prof., cor. mem. of the Academy of Sciences of Moldova, Technical University of Moldova, **president**
2. **BUZDUGAN Artur** PhD habil. in technical sciences, superior scientific researcher, Technical University of Moldova, **member, scientific secretary**
3. **TIGHINEANU Ion** PhD habil. in physical and mathematical sciences, prof., acad., Technical University of Moldova /Academy of Sciences of Moldova, **member**
4. **ACHIMOVA Elena** PhD habil. in physical and mathematical sciences, research assoc. prof., Institute of Applied Physics, Moldova State University, **member, official reviewer**
5. **CARAMAN Mihail** PhD habil. in physical and mathematical sciences, prof., Moldova State University, **member, official reviewer**
6. **DRAGOMAN Mircea** PhD, prof., National Research and Development Institute for Microtechnologies IMT Bucharest, Bucharest, Romania, **member, official reviewer**
7. **FOMIN Vladimir** PhD habil. in physical and mathematical sciences, prof., Institute for Emerging Electronic Technologies, IFW Dresden, Dresden, Germany, **member, official reviewer**

The defense will take place on **21 June 2024, at 14⁰⁰** in the meeting of the Commission for public defense within the Technical University of Moldova, Chisinau, 9/7 Studentilor str., room 3-208, MD 2048.

The synthesis work can be consulted at the National Library of Moldova and/or at the library of the Technical University of Moldova and on the website of the National Agency for Quality Assurance in Education and Research (www.anacec.md).

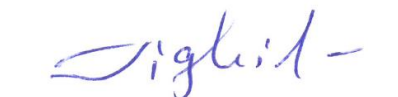
The synthesis work was sent on _____, 2024.

Scientific Secretary of the public defense Commission



BUZDUGAN Artur
PhD habil. in technical sciences,
superior scientific researcher

Scientific adviser



TIGHINEANU Ion
PhD habil. in physical and
mathematical sciences, prof., acad.
ASM

Author



MONAICO Eduard
PhD in physical and mathematical
sciences, research assoc. prof.

© Monaico Eduard, 2024

CONTENT

LIST OF ABBREVIATIONS	5
CONCEPTUAL LANDMARKS OF THE SYNTHESIS WORK.....	6
SUMMARY OF PUBLICATIONS	14
1. WIDE BANDGAP SEMICONDUCTOR NANOTEMPLATES (GaN, ZnCdS, ZnO).....	14
1.1 Electrochemical nanostructuring of gallium nitride (HVPE grown).....	14
1.2 Electrochemical nanostructuring of Zn_xCd_{1-x}S crystals	17
1.3 Electrochemical micro- and nano-structuring of ZnO crystals	19
1.4 Comparative analysis of III-V semiconductor compounds (InP, GaAs, GaN) and II-VI compounds (CdSe, ZnSe, Zn_xCd_{1-x}S)	22
1.5 Conclusions to Chapter 1	24
2. ENGINEERING OF POROUS SEMICONDUCTOR COMPOUNDS AND METALLIC STRUCTURES BY ELECTROCHEMICAL METHODS.....	25
2.1 The technology of nanotemplates fabrication with parallel pores to the surface. Cost-effective approach to control the direction of pore growth	25
2.2 From the porous structures to arrays of nanowires, nanobelts and nanomembranes.....	29
2.3 Development and demonstration of "hopping electrodeposition" mechanism of metal nanodots	32
2.4 Electrochemical etching and deposition as an efficient and accessible tool for assessing the electrical conductivity in semiconductor nanostructures	34
2.5 Control of the hydrophobic/hydrophilic properties of semiconductor structures by electrochemical techniques	37
3. RETROREFLECTION OF LIGHT IN POROUS SEMICONDUCTOR COMPOUNDS (InP, GaAs). PHOTONIC NANOSTRUCTURES (GaN, GaP, ZnSe).....	40
3.1 Anomalous retroreflection demonstrated for porous n-InP layers.....	40
3.2 Retroreflection from porous GaAs layers. Comparison with porous InP samples .	42
3.3 Bragg reflectors based on GaN multilayer structures.....	44
3.4 Integrated lenses based on GaP-metal or ZnSe-metal nanostructures.....	46
3.5 Conclusions to chapter 3	48
4. APPLICATIONS OF ELABORATED SEMICONDUCTOR NANOSTRUCTURES	49
4.1 Varicap device based on GaP-metal nanocomposites	49
4.2 Photodetectors, gas sensors based on InP and GaAs nanostructures.....	50
4.3 GaAs-Fe and GaAs-NiFe core-shell nanowire arrays fabricated by electrochemical methods.....	52

4.4	Gold coated microstructures as a platform for the preparation of semiconductor-based hybrid 3D micro-nano-architectures.....	55
4.5	Conclusions to chapter 4	58
	GENERAL CONCLUSIONS AND RECOMMENDATIONS	59
	REFERENCES.....	63
	THE LIST OF PUBLISHED SCIENTIFIC ARTICLES ON THE TOPIC OF SYNTHESIS WORK.....	70
	DECLARATION OF RESPONSIBILITY	79
	CURRICULUM VITAE.....	80
	ADNOTARE.....	82
	ANNOTATION	83

LIST OF ABBREVIATIONS

AFM – atomic force microscopy
ALD – atomic layer deposition
CA – contact angle
CE – electrochemical etching
CL – cathodoluminescence
CLO – current line oriented pores
CNSTM – National Center for Materials Study and Testing
CO – crystallographic pores
CSSNT – Center for Surface Science and Nanotechnology
CVT – chemical vapor transport
EDX – energy dispersive X-ray spectroscopy
EIS – electrochemical impedance spectroscopy
FIB – focused ion beam
FL – photolithography
HVPE – hydride vapor phase epitaxy
KPFM – Kelvin probe force microscopy
MOCVD – metal-organic chemical vapor deposition
NIM –negative index materials
PDMS – polydimethylsiloxane
PhR – photoresist
PL – photoluminescence
RR –remanent ratio M_r/M_s
TT – thermal treatment
UNSTPB – National University of Science and Technology Politehnica Bucharest
UV – ultraviolet
VSM – vibrating sample magnetometer
W – depletion region
XRD - X-ray diffraction

CONCEPTUAL LANDMARKS OF THE SYNTHESIS WORK

Starting with the rapid development of nanotechnology in the 1990s of the last century, a variety of porous materials has been reported. A considerable interest has been triggered by the discovery of macroporous Si more than three decades ago by Lehmann and Föll [1]. Nowadays, there are several well studied self-ordered porous materials finding applications in many fields, e.g.: (i) porous alumina introduced by Masuda and Fukuda in 1995 [2]; (ii) TiO₂ nanotubes presented by Macak and colleagues in 2007 [3]; and (iii) self-ordered porous III-V semiconductor compounds [4–8].

However, besides the versatility of porous alumina oxide for introducing self-ordering, its applicability is limited as a porous template to be filled in by other materials, with subsequent its removal due to the dielectric behavior leading to a passive role in the nanofabrication processes. In comparison with porous alumina, the templates based on TiO₂ nanotubes has attracted a lot of attention in research and is considered a semiconductor nanoarchitecture with potential for a variety of applications due to its unique structural, optical and electronic properties, non-toxicity, corrosion resistance, accessibility, biocompatibility, high photocatalytic characteristics, photostability, etc.

Despite the fact that TiO₂ is considered a semiconductor material, its electrical conductivity is relatively low. In connection with this, semiconductor porous structures with controlled conductivity are of major interest. Porous materials from III-V group are perfect candidates able to fill this gap. An essential contribution to the controlled nanostructuring of these materials was made by the groups of Prof. H. Föll, Prof. I. Tiginyanu, and Prof. P. Schmuki.

The authors of the Ref. [6] have focused their study on the formation of pores in III-V semiconductor compounds, highlighting the main properties of crystallographic pores "crysto pores (CO)" and current lines oriented pores "curro-pores (CLO)". The main characteristics of CO pores are as follows: (i) triangular shape in cross-section; (ii) they tend to grow along the $\langle 111 \rangle_B$ crystallographic direction independent of the initial surface orientation; (iii) are obtained at low current densities; (iv) they can intersect, leading to new three-dimensional ultra-porous architectures. Among the inherent properties of CLO pores, the following can be mentioned: (i) round shape in cross-section; (ii) their formation requires higher applied current densities; and last but not least (iii) they cannot intersect, perhaps most importantly from the point of view of the self-ordering process.

As it was established by [9], the cross-sectional shape of pores, growth rate, etc. strongly depend on the applied electrochemical parameters during anodization. Moreover, the shape of nanopores can be tuned in n-GaP substrates with different crystallographic orientations by anodization in HBr electrolyte, as it was demonstrated by [10] and [11] regarding rectangular and triangular shapes.

As a result, the problem of engineering porous semiconductor compounds at the micro- and nano-metric scale is of significant importance in the design of various electronic devices and systems. In optoelectronics, semiconductor pores can be used to improve light-material interaction. By growing pores of specific size and arrangement, it becomes possible to manipulate the behavior of photons in the semiconductor material. This opens up opportunities for applications such as photodetectors, solar cells, and light emitting devices.

Furthermore, pores in semiconductor compounds can also be used in energy storage and conversion devices such as supercapacitors and fuel cells. The growth of well-defined and uniform pores allows the effective increase in surface area, which in turn increases the efficiency of these devices. A key aspect is the ability of semiconductor pores to control the flow of ions or molecules through them. This property is particularly useful in microfluidic applications such as biosensors, where selective transport of specific analytes is required. By carefully designing and controlling the growth of these pores, it becomes possible to tailor their size, shape, and surface properties to achieve desired functionalities.

Engineering of pores in semiconductor compounds by electrochemical methods offers numerous advantages in device design. In addition, electrochemical methods allow the controlled integration of other materials into porous semiconductor compounds, paving the way for the development of hybrid or functionalized devices with potential applications in the fields of electronic, photonic, optoelectronic and energy storage devices.

The aim of the synthesis work is to develop theoretical concepts and to develop technological approaches for micro- and nano-engineering of porous semiconductor compounds and metallic nanostructures by electrochemical methods for multifunctional applications.

Achieving the goal is conditioned by the achievement of the following specific **objectives**:

- Identification of the technological conditions of the electrochemical etching to obtain templates based on wide bandgap semiconductors;
- Elaboration of concepts with further experimental demonstration for the engineering of the morphology of porous layers in semiconductor compounds by electrochemical etching;
- Comparative analysis of the nanostructuring of III-V (InP, GaAs, GaN) and II-VI semiconductor compounds (CdSe, ZnSe, $Zn_xCd_{1-x}S$);
- Investigation of the electrochemical pulse deposition of metal on porous semiconducting layers for the identification of legalities and the development of the deposition mechanism;
- Development and optimization of electrochemical technologies for switching from porous layers to arrays of nanowires with controlled alignment with respect to the surface of the substrate;

- Properties investigation of the elaborated nanostructures in order to demonstrate their applicability in micro- and nano-devices in electronics, optoelectronics, photonics, ferromagnetism.

The research hypothesis consists in exploring the mechanisms of electrochemical etching of semiconductor materials and electrochemical deposition of metals in porous semiconductor structures in order to obtain porous semiconductors with controlled morphology and design and metal-semiconductor nanocomposite materials for various applications.

Synthesis of research methodology and justification of the chosen research methods.

Electrochemical methods were used as basic techniques for the fabrication of semiconductor nanostructures, including those functionalized with metals. It should be noted that electrochemical etching in semiconductor materials is performed without lithographic means, the latter being used for the manufacture of porous layers with pores parallel to the substrate surface.

The coating of porous layers, regardless of their morphology, with a monolayer of Au nanodots was achieved by pulsed electrochemical deposition. Electrochemical methods are considered cost-effective and accessible, being available at the National Center for Materials Study and Testing (CNSTM) within the UTM.

The morphology and chemical composition study was carried out using scanning electron microscopy (SEM) and energy dispersive X-ray spectroscopy (EDX). Kelvin probe force microscopy (KPFM) was applied to the surface of HVPE-grown bulk GaN substrates to highlight non-uniform doping during HVPE growth. Photoluminescence (PL) and cathodoluminescence (CL) contributed to the study of the respective micro- and nanostructured samples.

Photoelectric characterization was used to study developed photodetectors based on ultra-thin InP nanowalls and single GaAs nanowire, using the optical filters in the IR and UV region of the spectrum placed after the Xe arc lamp. Contacting of the nanowires was performed by focused ion beam (FIB), placing the GaAs nanowire on the Si/SiO₂ chip with pre-fabricated metal contacts, or by means of laser beam lithography, the latter being an optimal method in terms of feasibility and accessibility. The current-voltage characteristics were measured in order to demonstrate the formation of the Schottky or ohmic contact.

Demonstration of retroreflection in porous InP and GaAs structures was performed by experimentally measured scattering indicatrix under laser beam illumination with wavelengths of $\lambda = 531$ nm of the Nd:LSB solid-state laser (LEMT, Belarus), laser diode (BelOMA, Belarus) $\lambda = 654$ nm and the solid-state Nd:YAG laser (Solar LS, Belarus $\lambda = 1064$ nm).

The study of metal-semiconductor structures was carried out by means of several techniques:

(i) Topographic imaging of current mapping using point contact microscopy, through which the formation of the Schottky contact at the interface of the monolayer of Au nanodots with the InP substrate was demonstrated;

(ii) Electrochemical impedance spectroscopy in 0.5 M Na₂SO₄ pH=6.5 electrolyte to identify the impact of metal nanodot functionalization;

(iii) Contact angle measurements were performed to demonstrate the impact of electrochemical nanostructuring and functionalization with metal nanodots on hydrophilic or hydrophobic properties;

(iv) Measurements of the volt-faradic characteristics to study the developed varicap based on porous GaP/Pt nanotubes;

(v) Measurements of the magnetization curves of metallic nanostructures (Fe or NiFe) deposited on GaAs nanowires were carried out by vibrating sample magnetometer (VSM) with applied magnetic fields up to ± 3 T at room temperature for “in-plane” and “out-of-plane” configurations.

The detailed description of the used semiconductor substrates, investigated electrolytes and the schematic representation of the technological set-up is reflected in the chapter 5 of the author's monograph [12].

The novelty and scientific originality of the synthesis work consists in:

- Porous templates based on wide bandgap materials (GaN, ZnCdS) and micro-nano-structures (ZnO), perspective for applications in the visible range of the spectrum, were fabricated;
- Electrochemical technological approaches have been developed to control the pore direction propagation in depth, resulting in 3D structures formed as a result of the transition from CLO to CO pores, or due to non-uniform doping in HVPE grown GaN substrates, as well as parallel to the surface of InP or ZnSe crystals by applying specially designed photolithographic masks;
- The "hopping electrodeposition" mechanism was developed and demonstrated, which allows the deposition of a monolayer of Au nanodots on porous semiconductor compounds, regardless of morphology;
- For the first time, the "abnormal" retroreflection of light on ultra-porous layers based on InP and GaAs semiconductor compounds was demonstrated;
- Optimization of the technological parameters of anodization allowed the fabrication of semiconductor nanowire arrays by electrochemical etching of InP, GaAs and ZnTe semiconductor crystals. The use of GaAs crystals with different crystallographic orientation allowed obtaining networks of nanowires tilted (100), perpendicular (111)B and predominantly parallel (001) to the substrate surface;
- For the first time, a cost-effective and original approach was proposed to estimate the electrical conductivity in InP semiconductor nanostructures with different thicknesses, by pulsed

electrochemical metal deposition. The given approach has also been shown to be effective for highlighting non-uniform doping during HVPE growth in GaN substrates. Complementarily, non-uniform doping was also demonstrated by electrochemical etching of GaN (HVPE) substrates;

- Through contact angle analysis, it has been demonstrated that the engineering of semiconductor surfaces by electrochemical methods (electrochemical etching and/or electrochemical deposition) allows the controlled switching of hydrophilic/hydrophobic properties.

The main new scientific results that led to the development of the *new research direction "Controlled micro- and nano-engineering of porous semiconductor compounds and metallic nanostructures by electrochemical methods" are:*

- (i) the developed and experimentally demonstrated concept for engineering the morphology of porous layers in semiconductor compounds by applying on the semiconductor surface the photolithographic mask with a special configuration, followed by electrochemical etching;
- (ii) elaborating the "hopping electrodeposition" mechanism involving the formation of the Schottky barrier at the Au nanodot/semiconductor interface, experimentally demonstrated by topographic current mapping imaging using point contact microscopy;
- (iii) the "hopping electrodeposition" mechanism that underpins the concept of experimental demonstration of different electrical conductivity in semiconductor nanostructures with different thicknesses;
- (iv) the "hopping electrodeposition" mechanism that experimentally demonstrates and highlights non-uniform doping during HVPE growth of GaN substrates, additionally confirmed by electrochemical etching through selective nanostructuring of regions with higher electrical conductivity;
- (v) controlling the geometrical shape of the semiconductor pores and nanowires that allows to obtain hybrid core-shell structures with triangular, square or round geometries by forming a thin metal layer inside the pores or around the nanowires by means of the "hopping electrodeposition" mechanism.

The theoretical significance of the synthesis work consists in the elaboration and demonstration of:

- (i) the "hopping electrodeposition" mechanism of Au nanodots on the surface of porous semiconductor compounds;
- (ii) the concept for engineering the pore growth direction using photolithographic processes;
- (iii) the development of the method for assessing the electrical conductivity in semiconductor nanostructures with different thickness by the electrochemical deposition of gold;
- (iv) the correspondence of the proposed mathematical model with the experimental data of the retroreflection phenomenon in ultra-porous InP and GaAs semiconductor compounds;
- (v) investigation of hydrophilic/hydrophobic surface properties of porous semiconductor compounds;

(vi) demonstration of the possibility to control the contact angle and surface engineering of porous semiconductor compounds by electrochemical etching or pulsed electrodeposition.

The applicative value of the work is emphasized by:

- The feasibility of developing multilayer structures on the basis of HVPE and MOCVD grown GaN substrates for the design of Bragg reflectors or other photonic elements was demonstrated by micro-reflectivity measurements accompanied by transfer matrix analyses and simulations by calculating optical reflection spectra.
- Demonstration of the prospect of developing new focusing elements and beam splitters based on GaP/Pt or ZnSe/Pt nanostructures for applications in the visible region of the spectrum.
- Development of the varicap device based on GaP/Pt nanostructures with a record gradient variation of the capacitance density of $6 \times 10^{-3} \text{ pF} \cdot \text{V}^{-1}$ per $1 \mu\text{m}^2$ of surface.
- Demonstration of the sensitivity of porous InP membranes functionalized with Au nanodots to H_2 and CO gases.
- Development of the IR photodetector based on an ultra-thin (10 nm) InP nanowall with photoresponse $R=1.3 \text{ A} \cdot \text{W}^{-1}$ and detectivity $D=1.28 \times 10^{10} \text{ cm} \cdot \text{Hz}^{1/2} \cdot \text{W}^{-1}$ at $P_{\text{exc}}= 800 \text{ mW} \cdot \text{cm}^{-1}$, as well as of the GaAs photodetector (single nanowire) with $R=100 \text{ mA} \cdot \text{W}^{-1}$ and $D=1.2 \times 10^9 \text{ cm} \cdot \text{Hz}^{1/2} \cdot \text{W}^{-1}$.
- Fabrication of core-shell nanowire arrays based on GaAs-Fe or GaAs-NiFe with the possibility of aligning them perpendicular/parallel to the substrate surface with a magnetic anisotropy of coercivity and remanence ratio.
- Gold nanodot functionalization of ZnO or aero-GaN micro- and nano-structures promising as platforms for the fabrication of 3D hybrid micro-nano-architectures.

The main scientific results submitted for defense:

- The "hopping electrodeposition" mechanism for the self-assembly of Au nanodots in monolayers is governed by the formation of the Schottky barrier at the interface of the semiconductor substrate with Au nanodots with diameters around 20 nm, confirmed by means of topographic imaging and current mapping measurements.
- Electrochemical methods allow the design and control of nanoscale porous structures in semiconductor and metallic materials.
- Joining the porous semiconductors and metallic structures on a nanometric scale by electrochemical methods allows the creation of hybrid materials with unique properties, having significant implications in the development of advanced devices in the field of electronics, optoelectronics and photonics.

- The concepts of the integration of electrochemical etching with patterned photolithographic masks containing opening holes provides an innovative approach for fabrication of porous domains with separate entrances for fluid manipulation at the micro- and nanoscale.
- Choosing the optimal electrochemical parameters (applied voltage, nature of the electrolyte and its concentration) offers the possibility of obtaining an enormous amount of semiconductor nanowires (InP, ZnTe, GaAs) connected to the bulk semiconductor substrate.
- The anomalous retroreflection demonstrated in nanoporous InP and GaAs materials with mesh-like morphology that strongly absorb in the visible range occurs in a narrow solid angle along with a diffuse specular reflection for all angles of incidence.
- CLO pores are characteristic of both III-V (except GaAs) and II-VI semiconductor compounds, while CO pores have only been observed in III-V semiconductor compounds.
- The presence of only CO pores in the anodization process of GaAs crystals, offers additional possibilities of aligning the nanowires obtained by electrochemical etching, by choosing the crystallographic orientation of the bulk GaAs substrate.

The results reflected in the synthesis paper were partially obtained within the **projects** in which the author was the project director: postdoctorat #21.00208.5007.15/PD (2021-2022); state program #20.80009.5007.20 (2020-2023); institutional project #15.817.02.29A (2015-2019); STCU #6222 (2017-2018); bilateral Belarus #9.80013.50.07.03A/BL (2019-2020); young researchers #11.819.05.12A (2011-2012); the Alexander von Humboldt foundation fellowship at the University of Hamburg, Germany (10.2011 – 01.2014) and at IFW Dresden, Germany (03.2018 – 05.2018).

The author's personal contribution

The work presents a systematization of the results of scientific research carried out directly by the author, whose personal contribution consists in establishing of the research objectives, justifying the methods of their implementation, performing basic experimental investigations (SEM, EDX, AFM, contact angle), analysis of the obtained results, as well as the preparation of the papers for publication. The major contribution in papers is highlighted as first author, last author, and corresponding author. The scientific supervisor acad. Ion Tighineanu participated in the discussion and formulation of the research objectives, and analysis of the obtained results. The results regarding the comparison of pore growth mechanisms in III-V and II-VI semiconductor compounds were discussed with Prof. H. Föll and Dr. Sergiu Langa. The nanostructuring processes of the GaN crystals grown by the HVPE or MOCVD method were carried out together with Dr. Fiodor Braniște, responsible for the photoelectrochemical etching, in contrast to the electrochemical etching, carried out by the author of the synthesis work. Experimental investigations of the retroreflection phenomenon observed in porous InP and GaAs samples were carried out in collaboration with acad. S. Gaponenko and Dr. S. Prislopski at the B. I. Stepanov Institute of Physics of the National Academy

of Sciences of Belarus, theoretical calculations for modeling the experimental data obtained by the author were performed by Dr. V. Sergentu. The measurement and interpretation of the PL and XRD spectra was carried out in collaboration with mem. cor. ASM V. Ursachi. The growth of bulk ZnO, ZnCdS crystals was carried out in collaboration with Dr. G. Colibaba within the State University of Moldova. Some technological optimizations of the pulse electrochemical deposition process for the formation of hybrid metal-semiconductor structures, as well as the elaboration of the top contact to the structures composed from semiconductor templates with embedded metal nanotubes, were carried out by Elena Monaico and contributed to the further development by the author of this synthesis work on concrete applications such as photonic lenses and the varicap device. The basic technological and characterization methods used in the work are part of the research infrastructure at the primary research unit (NCMST, TUM) and were used personally by the author. Topographic current mapping imaging, TEM, XRD, EIS were studied in collaboration with Prof. M. Enăchescu, Dr. Călin Moise, Dr. G. Mihai (CSSNT, UNSTPB, Romania). The investigation of the magnetic properties was carried out at IFW Dresden (Germany) in collaboration with Prof. Dr. Habil. K. Nielsch.

Dissemination and recognition of the scientific achievements. The basic results have been presented in more than 50 reports at international and national scientific conferences in Germany, France, USA, Romania, Poland, Spain, Serbia, Lithuania, Belarus, Ukraine, Armenia, Singapore and the Republic of Moldova, including 4 invited and 22 reports presented by the author of the synthesis work. 7 medals were obtained at international exhibitions of inventiveness.

Publications. The results presented in the synthesis work are systematized in 103 scientific papers, including a monograph, 1 invited chapter in Encyclopedia of Condensed Matter Physics 2nd edition, 1 monograph chapter, 1 invited review article, 43 scientific articles from the Web of Science and SCOPUS databases, 19 articles at the national and international scientific events, 3 articles in journals from the National Register, 3 invention patents and over 30 theses at international and national conferences.

The structure and volume of the work. The synthesis work consists of the introductory part with the conceptual benchmarks of the research, four chapters that reflect the synthesis of the scientific papers published on the topic, general conclusions and recommendations. The synthesis work includes 100 bibliographic references, 84 pages (70 pages of basic text), 26 figures and 3 tables.

Keywords: wide bandgap semiconductors, crystallographically oriented pores, current line oriented pores, controlling the pore growth direction, hopping electrodeposition, anomalous retroreflection, IR photodetector, integrated photonic lenses, magnetic anisotropy, hybrid core-shell structures, hydrophilic/hydrophobic properties, gas sensor, varicap.

SUMMARY OF PUBLICATIONS

1. WIDE BANDGAP SEMICONDUCTOR NANOTEMPLATES (GaN, ZnCdS, ZnO)

1.1 Electrochemical nanostructuring of gallium nitride (HVPE grown)

Due to gallium nitride's (GaN) excellent thermal and mechanical properties, chemical stability, high electron mobility and high breakdown voltage, low thermal impedance - it has become a perfect material for a wide range of applications in optoelectronics, high power devices and high frequency. Nanostructuring of GaN, especially through the use of electrochemical etching (EE), greatly expands the fields of applications such as platforms based on surface-enhanced Raman scattering, energy storage, photocatalytic, water dissociation, hydrogen generation, photodetectors, chemical and gas sensors, photonic engineering, waveguides and Bragg reflectors, etc.

The obtained porous GaN layers and reported in the literature are limited to 2 – 4 μm in depth. This is due to metal-organic chemical vapor deposition (MOCVD) growth technology on sapphire, Si or SiC substrate. Apart from this, GaN epitaxial layers suffer from internal stresses and defects due to the significant mismatch of crystal lattice parameters and thermal dilatation coefficients with the substrate material.

Nowadays, there are three main technologies used to grow bulk GaN crystals: (i) hydride vapor phase epitaxy (HVPE), (ii) sodium flux, and (iii) ammonothermal growth [13]. Among these methods, HVPE growth appears to be the best choice, while ammonothermal growth is unsuitable for mass production of GaN crystals, ensuring a low growth rate of up to several micrometers per hour. Additionally, the properties of ammonothermal GaN crystals are affected by the presence of impurities and other defects, which prevent their use for device applications [14]. On the other hand, HVPE technology offers a relatively high growth rate ($500 \mu\text{m}\cdot\text{h}^{-1}$) [13]. However, despite the important advantages of HVPE technology, achieving uniform electrical conductivity in the material is still difficult.

In the paper [15] it was demonstrated, that electrochemical etching allows to highlight three-dimensional self-organized nanostructured architectures that were attributed to the spatial modulation of electrical conductivity, generated during the HVPE growth of GaN substrates. In the study, *n*-GaN crystals with a thickness of 300 μm , having the crystallographic orientation (0001) with unpolished Ga face and polished N face, purchased from SAINT-GOBAIN Crystals, were used. Figure 1.1a,b illustrates the AFM images of the surface topology recorded on the surface of the GaN HVPE substrate where circular regions can be observed, forming concentric ring-like structures. To study the electrical properties of the sample on the surface, Kelvin probe force microscopy (KPFM) measurements were performed, also known as surface potential microscopy (Figure 1.1c).

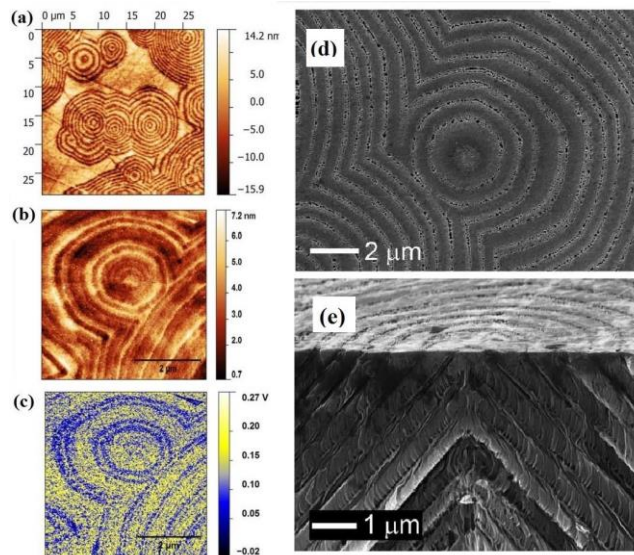


Figure 1.1. AFM images of the surface of a HVPE grown GaN substrate (a,b). (c) KPFM image of the surface shown in (b). SEM images of the GaN sample subjected to electrochemical etching: top view (d) and cross-sectional view (e) of the N surface.

Reproduced from [15]

After the electrochemical etching process, well-defined circular regions comprising concentric topographical structures, sometimes with a quasi-hexagonal shape, are observed in the image from Figure 1.1d. Since electrochemical etching techniques are very sensitive to local doping, it has been suggested that the obtained topology is due to the spatial modulation of the electrical conductivity over the entire surface and including the bulk of the HVPE grown GaN wafer. The hypothesis was confirmed by a combined study involving different characterization techniques such as AFM, KPFM, SEM and micro-CL [15]. It should be mentioned, that the electrochemical etching allowed to investigate the uniformity of the doping of the HVPE grown GaN substrate in bulk, while with KPFM only the surface can be investigated.

The configuration of the high-conductivity and low-conductivity layers, which alternate with each other with a periodicity of 80–150 nm, is different in the vicinity of the N-terminated and Ga-terminated faces of the GaN sample. The configuration is V-type, on the N face as is illustrated in Figure 1.1e, but with the increasing the growth thickness of the GaN substrates, the sharp shape of the V-type defects is attenuated, and parabolic shapes with much larger dimensions compared to the N surface are observed [15]. The results of the more detailed investigation of electrical conductivity modulation and lattice distortions in etched HVPE GaN substrates are presented in the paper [16].

In the paper [17], the capabilities of the electrochemical etching technology for the production of multilayer porous structures in HVPE grown GaN substrates were demonstrated. Electrochemical etching is nucleated at the surface of the sample with the formation of pores in the regions of the ring-shaped structures with higher conductivity and is carried out through the development of pores in

depth in the high-conductivity regions. It has been shown that the porosity of the layers in the multilayer porous structure is controlled by several technological parameters. An important parameter is the composition and the concentration of the electrolyte. Very low porosity layers are produced in the high conductivity strips upon electrochemical etching in HCl electrolyte compared to HNO₃ electrolyte at the same applied potential and duration of the anodization process. These structures obtained from layers with alternating porosity, demonstrating alternating refractive index, are promising for the design of Bragg reflectors, by cutting off the suitable regions from the multilayer porous structures produced at optimized technological parameters [17].

The applied anodization potential is another technological parameter which impacts the produced porosity. Therefore, regions with various porosities can be produced in depth of the sample by changing the anodization potential during the electrochemical etching, as demonstrated in Figure 1.2a,b. A region with high porosity is formed near the surface of the sample during the first phase of electrochemical etching under an applied anodization potential of 35 V (Figure 1.2b). Underneath, a region with the porosity similar to that obtained at an applied potential of 25 V is produced during anodization with an applied potential of 15 V (Figure 1.2b). One should note that the morphology of region 1 is no longer composed of alternating porosity layers, as both high-conductivity and low-conductivity stripes are porosified at the applied voltage of 35 V. Thus, a region with uniform porosity is obtained [17].

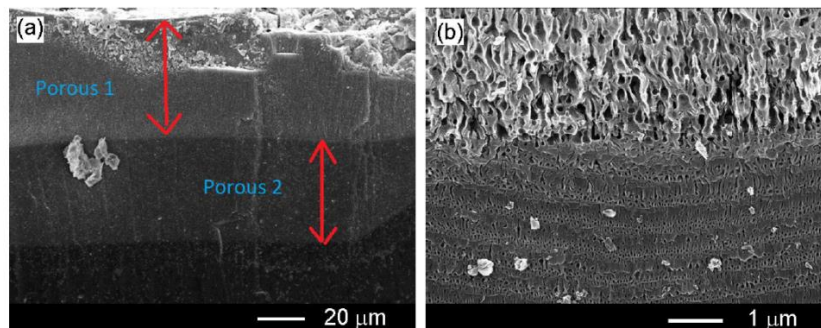


Figure 1.2. (a,b) Cross-sectional SEM images taken at different magnifications of GaN HVPE sample subjected to two-step electrochemical etching in 0.3M HNO₃ electrolyte for 2 min at anodization potential of 35 V (region 1) and 15 V (region 2). Reproduced from [17]

According to the proposed model for the growth of GaN HVPE substrates [15], the growth process of GaN by the HVPE technique is governed by the formation and subsequent growth of so-called V-type defects or pits on the crystal surface, as illustrated in the schematic presentation in the paper [15]. As previously mentioned, the morphology produced by anodization on both surfaces is different, thus it is expected that by optimizing the technological parameters during the growth of GaN HVPE substrates, the V-type defects will mostly be annihilated on the Ga-surface, representing the growth surface. Later on, in the paper [18], different porous morphologies produced by deep anodization of 300 μm thick HVPE grown GaN substrates (MTI-corporation, USA) with respect to

N or Ga face were reported. Porous structures in the form of pyramids were formed on the N face, while homogeneous porous templates with pores oriented perpendicular to the wafer surface are generated at a depth of up to 50 μm on the Ga face, the thickness of the pore walls being controlled by the value of the applied voltage. The systematic study of anodization in different electrolytes demonstrated for the first time the possibility of porous structures obtaining in ecological electrolyte based on NaCl with the preservation of the wurtzite crystalline phase of the material confirmed by HR-STEM analysis [18].

1.2 Electrochemical nanostructuring of $\text{Zn}_x\text{Cd}_{1-x}\text{S}$ crystals

II-VI semiconductors are prospective candidates for nanotemplates taking into account their large bandgap, high electron mobility, transparency in the visible region of the spectrum, etc. ZnS is a relatively large band gap II-VI compound ($E_g=3.6$ eV at 300 K) and has prominent luminescence properties that opens opportunities to use it in optoelectronics and photonics. However, electrical parameters of this material are not as good as those of the other compounds of the same group. The maximum concentration of free charge carriers in n-ZnS is less than 10^{17} cm^{-3} due to the compensation effect, and this material has extremely high contact resistance due to surface states [19,20]. On the other hand, in case of CdS ($E_g \sim 2.4$ eV), it is easy to obtain the concentration of free charge carriers up to 10^{20} cm^{-3} [19]. As a result, ZnCdS solid solution crystals are of great interest, because they may have wider bandgap and good electrical parameters necessary for efficient electrochemical treatment.

For the study [12], $\text{Zn}_x\text{Cd}_{1-x}\text{S}$ crystals with $x=0.4$; 0.5 ; and 0.67 were used, grown at the State University of Moldova by Dr. Gleb Colibaba through chemical vapor transport (CVT), using HCl as a transport agent [21,22]. The electrical resistance of $\text{Zn}_x\text{Cd}_{1-x}\text{S}$ crystals was decreased by thermal treatment in Zn + Cd vapors [22].

For the first time, the anodization of $\text{Zn}_{0.4}\text{Cd}_{0.6}\text{S}$ crystals in 5% HCl electrolyte at 16 V was reported, the porous layer being composed from pores oriented along the current lines, with a diameter of 30 nm and a wall thickness of 20 nm [23,24]. The bandgap value for the obtained compound with the value $x=0.4$ is close to the bandgap value of ZnSe. The nanostructuring of $\text{Zn}_x\text{Cd}_{1-x}\text{S}$ crystals with the value of $x \geq 0.5$ is of increased interest due to the larger bandgap.

Porous layers up to 50 μm thick were also successfully fabricated in $\text{Zn}_{0.5}\text{Cd}_{0.5}\text{S}$ substrates in 5% HCl electrolyte at the applied voltage of 40 V for 10 min (Figure 1.3a). It should be noted that similar morphology was also obtained in the case of anodized CdS crystals ($\text{Zn}_x\text{Cd}_{1-x}\text{S}$ samples with $x=0$) at an applied potential of 12 V [22].

In the case of crystals with the value of $x > 0.5$, the electrical conductivity of the grown crystals decreases monotonically. In connection with this, a much higher value of the applied potential is required for the anodization process. Nanostructuring of the even wider bandgap materials $\text{Zn}_{0.6}\text{Cd}_{0.4}\text{S}$

and $\text{Zn}_{0.67}\text{Cd}_{0.33}\text{S}$ ($E_g \sim 3.3$ eV) can only be achieved at extremely high voltages of 160 V and 180 V, respectively, as the resistivity of the $\text{Zn}_x\text{Cd}_{1-x}\text{S}$ samples increases together with the Zn content.

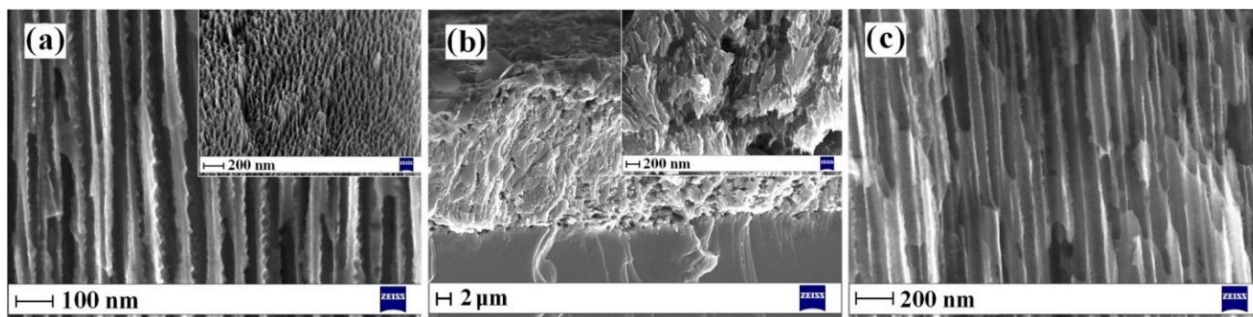


Figure 1.3. SEM images of $\text{Zn}_{0.5}\text{Cd}_{0.5}\text{S}$ porous layer anodized in 5% HCl aqueous electrolyte (40 V) (a), $\text{Zn}_{0.6}\text{Cd}_{0.4}\text{S}$ layers anodized in 5% HCl electrolyte (160 V) (b) and 0,3 M HNO_3 (70 V) (c). The insets illustrate a top view in (a) and enlarged image of the porous layer in (b).

Reproduced from [22]

According to the SEM images from Figure 1.3b, of the anodized $\text{Zn}_x\text{Cd}_{1-x}\text{S}$ samples ($x=0.6$ and 0.67) at applied voltages higher than 100 V, the fabricated porous layers are non-uniform both in the direction of pore propagation, as well as regarding the pore diameter values. The obtained morphologies represent a sponge rather than an ordered porous layer with parallel pores. Homogeneous porous layers (Figure 1.3c) were successfully fabricated by anodization of $\text{Zn}_{0.6}\text{Cd}_{0.4}\text{S}$ crystals in 0.3 M HNO_3 aqueous electrolyte, which allowed to reduce the applied anodization potential from 160 V to 70 V [22].

In order to investigate the influence of the electrolyte composition on the porous layer formation process, the $\text{Zn}_{0.5}\text{Cd}_{0.5}\text{S}$ crystals were anodized in 5 % HCl and 0.3 M HNO_3 electrolytes [12,25]. The intentional change of the anodization potential from 40 V to 30 V during the formation of the porous layer in $\text{Zn}_{0.5}\text{Cd}_{0.5}\text{S}$ crystal anodized in HCl electrolyte, leads to the change in the value of the pore diameter and degree of porosity according to the SEM image from Figure 1.4a. The porous layers obtained as a result of anodization in 0.3 M HNO_3 electrolyte (Figure 1.4b) are characterized by a much more uniform nucleation and the parallel growth of pores to each other in the second layer, in contrast to the HCl electrolyte [12].

The composition of the electrolyte also influences the rate of pore growth. For example, a porous layer with a thickness of 50 μm was obtained by electrochemical etching in HNO_3 electrolyte at an applied anodization potential of 30 V for 10 minutes, while only 20 μm in thickness was obtained at anodization with the same parameters in HCl electrolyte.

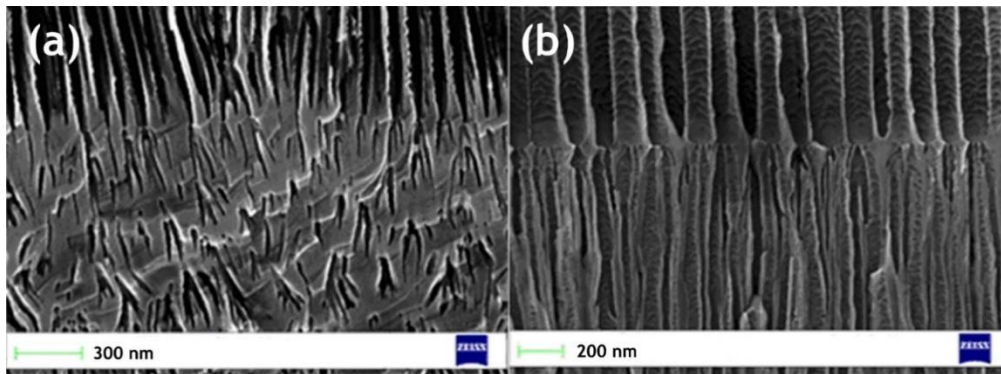


Figure 1.4. Cross-sectional SEM images of $Zn_{0.5}Cd_{0.5}S$ multilayer porous structure obtained by switching the applied voltage from 40 to 30 V during anodization in 5% HCl (a) and 0.3 M HNO_3 (b) electrolyte. Reproduced from [12,25]

The systematized parameters of the $Zn_xCd_{1-x}S$ crystals are summarized in Table 1.1

Table 1.1. Systematized results of $Zn_xCd_{1-x}S$ crystals regarding the required applied voltage for porous layers obtaining via anodization in 0.3 M HNO_3 electrolyte.

x	0	0.4	0.5	0.67
Material	CdS	$Zn_{0.4}Cd_{0.6}S$	$Zn_{0.5}Cd_{0.5}S$	$Zn_{0.67}Cd_{0.33}S$
Bandgap, eV	2.4	2.9	3.0	3.3
Applied anodization potential in HNO_3 , V	12	16	40	70 >160 (HCl)

The investigation of the chemical composition after electrochemical etching in both electrolytes, demonstrated the preservation of the stoichiometry of the samples. It should be noted that the systematic study did not revealed evidence of the crystallographic pore formation in $ZnCdS$ crystals, similar to the situation as in the case of other semiconductor compounds from II-VI group (CdS, CdSe, ZnSe).

1.3 Electrochemical micro- and nano-structuring of ZnO crystals

During the last three decades it was demonstrated that electrochemical etching represents a cost-effective and simple technology for nanostructuring of III-V and II-VI semiconductor compounds in a controlled fashion [26]. The electrochemical nanostructuring of ZnO is less studied due to its low chemical stability. To fill this gap, a cost-effective approach via anodization on O-face and Zn-face, for controlled micro- and nano-structuring of ZnO crystals, as well as the analysis of their light emission spectra were investigated and presented in paper [27].

Electrochemical etching of the O-face or the Zn-face was carried out in a stirred 5% HCl aqueous solution for 2 min, in potentiostatic mode, under different voltages, as was described in [27]. The morphologies of hexagonal pyramids obtained by electrochemical etching on the O-face of a ZnO crystal are illustrated in Figure 1.5 for crystals treated at the applied potential of 5 V (lower part) and 10 V (upper part). The value of the applied potential strongly influences the dimensions of the obtained micro- and nanostructures, the hexagonal pyramids becoming larger in diameter with the increase of the anodization potential.

The cathodoluminescence investigation demonstrated a strong dependence of the emission properties on the dimensions of ZnO micro- and nanostructures. One can see that blue emission is dominant from the area with small pyramids with a base of 1 – 5 μm (bottom of the image from Figure 1.5b), while green emission predominates in areas with large pyramids (see top of the image from Figure 1.5b).

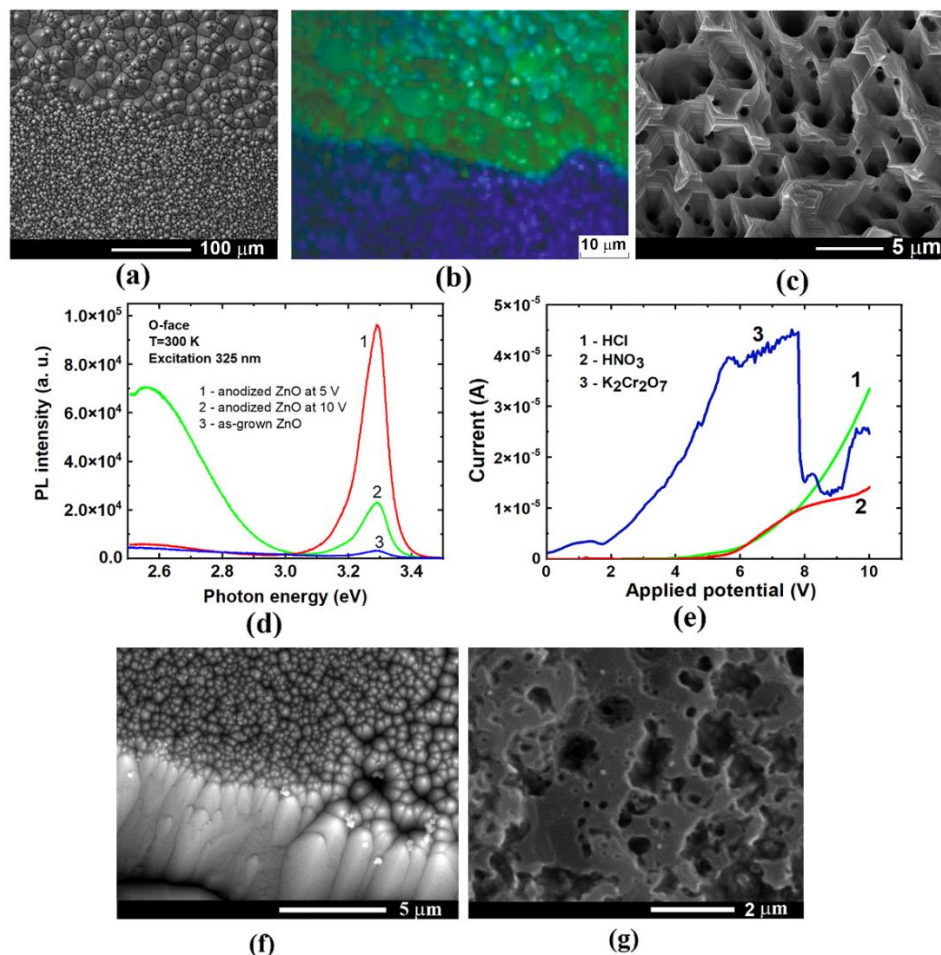


Figure 1.5. (a) SEM image of the morphology of an *n*-ZnO crystal anodized on the O-face in 5% HCl electrolyte for 2 min at the applied potential of 5 V (small pyramids) and 10 V (large pyramids). (b) CL image of the small and large pyramids from image (a). (c) SEM image of *n*-ZnO anodized on Zn-face at 10 V, showing formation of inverse pyramids. (d) PL spectra measured at room temperature from O-face of ZnO crystal before anodization (curve 3) and after anodization at 5 V (curve 1) and 10 V (curve 2). (e) The current-voltage curves measured with a slope of $10 \text{ mV}\cdot\text{s}^{-1}$ at the beginning of anodization of the ZnO crystal on the O-face in different electrolytes. (f,g) Top-view SEM images of anodized ZnO crystal on O-face in HNO_3 (f) and $\text{K}_2\text{Cr}_2\text{O}_7$ (e) electrolyte at applied potential of 8 V. Reproduced from [27,28]

The results of CL investigation are corroborated by the photoluminescence (PL) study presented in Figure 1.5d, indicating a strong influence of the applied potential on the PL spectra of the obtained microstructures. The PL spectra measured at room temperature in all three regions (bulk,

and anodized at 5 V and 10 V) consist of two bands, one of which is situated at 3.3 eV, it being associated with exciton recombination [29]. The second green luminescence broad band at 2.56 eV is typical for ZnO crystals [29,30]. The PL spectra registered on the region with morphology exhibiting small pyramids (curve 1, anodization at 5 V) is dominated by the near bandgap emission, the green emission being quenched. On the other hand, the region with big pyramids (curve 2, anodization at 10 V) shows relatively intensive green luminescence with weakened near bandgap emission.

The obtained morphology is completely different in the case of anodization on Zn-face, hexagonal pits (inverted pyramids) being reported, as is presented in Figure 1.5c. One should mention that the formation of pyramidal structures and stepped hexagonal pits on O-face and Zn-face, respectively, was also observed on ZnO and GaN thin films during wet chemical etching [31,32]. Apart from etching techniques, a novel asymmetric morphology exhibiting 1 μm hexagonal pyramids with a Zn-terminated bottom surface were obtained by means of microwave synthesis [33].

Another important study [28,34] was realized to elucidate the influence of the nature of used electrolytes as well as of the applied potential during anodization process of ZnO crystals upon the obtained morphology. Anodization of the O-face was carried out in three different aqueous solutions with 5% HCl, 1M HNO₃, and K₂Cr₂O₇ (1g K₂Cr₂O₇:10 ml H₂SO₄:100 ml H₂O) electrolytes. The applied voltages were selected based on current-voltage curves presented in Figure 1.5e, demonstrating similar dissolution behavior in HCl and HNO₃.

All three electrolytes demonstrated different morphologies as a result of electrochemical etching at the same applied potential. For the first time, the columnar morphology reaching a length of 5 μm instead of hexagonal pyramids (see Figure 1.5f), obtained in HNO₃ electrolyte was reported. However, in spite of columnar morphology, the top part exhibits a pyramid-like shape. This observation can serve as a basis for the statement that anodization in HNO₃ electrolyte weakens the dissolution along certain crystallographic directions, taking place along the current lines in comparison with the anodic etching in HCl electrolyte. The morphology looks totally different after anodization in K₂Cr₂O₇ electrolyte, showing sponge-like morphology, as presented in Figure 1.5g.

In contrast to O-face, the results of anodization on Zn-face demonstrated no to strong influence of the nature of electrolyte upon the obtained morphology demonstrating porous structure like in Figure 1.5c. Beside this, the formation of hexagonal tunnels, their growth and dissolution at the same time was observed.

With certain technological optimizations, the reported columnar morphology, obtained by anodization of bulk semiconductor substrates, could serve as an alternative to other columnar arrays obtained by much more expensive technologies [35–38], leading to contamination of nanostructures during growth that affects their properties emission [39,40]. The electrochemical etching approach is

more prospective, while it does not require a nucleation layer, high temperatures, carrier gas, etc., taking place not by growth, but by dissolution of the bulk material, so that the obtained nanostructures possess the same chemical composition and doping level as the initial crystal.

1.4 Comparative analysis of III-V semiconductor compounds (InP, GaAs, GaN) and II-VI compounds (CdSe, ZnSe, Zn_xCd_{1-x}S)

In the review paper [26], the systematization of the obtained results was carried out and it was found that CLO pores are inherent to both III-V (except for GaAs) and II-VI semiconductor compounds, while CO pores have been reported just in III-V semiconductor compounds [41,42].

Examples of CLO pores and CO pores produced in an InP anodized substrate are presented in Figure 1.6a. It should be noted that self-organization of pores during their growth leads to hexagonal packing of pores with the formation of highly ordered templates, as can be seen in the inset from Figure 1.6a. The self-ordering of CLO pores can be explained by the schematic illustration from Figure 1.6b [26].

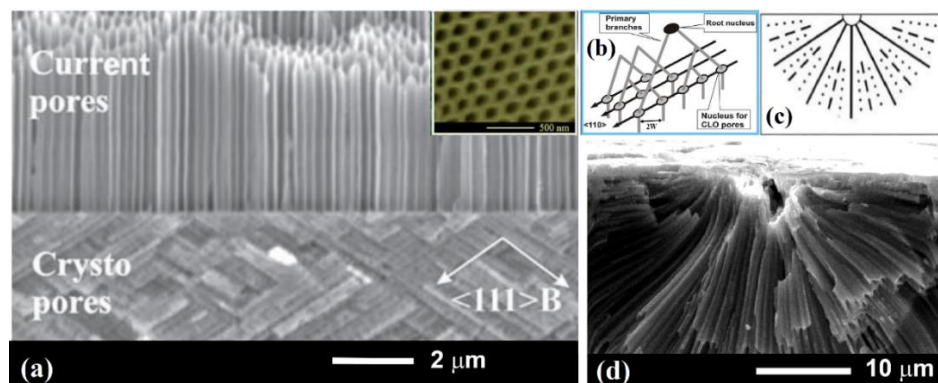


Figure 1.6. (a) SEM image of anodized porous InP layers with the applied potential changing from 7 V to 1 V, resulting in the formation of CLO pores and CO pores, respectively. The inset represents the top view of the hexagonal ordering of the porous layer. Schematic representation of the development of the porous structure in III-V (b) and II-VI (c) semiconductor compounds during anodization. (d) SEM image with experimental demonstration of pore formation in *n*-CdSe according to the proposed model in (c).

Reproduced from [26]

In contrast to III-V semiconductor compounds, the lack of cristo pores in II-VI semiconductor compounds denotes the not so high ordering of pores. In this case, the anodization starts at some imperfections at the surface and the pores grow radially away from the root nuclei, as is illustrated in Figure 1.5c. During the development of the porous structure, when the condition is fulfilled that the space between two neighboring pores is bigger than $2W$, their branching takes place. The experimental demonstration of this model by [2] is presented in Figure 1.6d based on anodized *n*-type CdSe single crystals. When the radial porous domain meets another porous domain, the pores are forced to change their direction of propagation, and after some time of anodization, a porous network

with pores parallel to each other is obtained. The formation of arrays of parallel pores starting from the nucleation layer by radial ramification was reported in other II-VI semiconductor compounds, e.g. ZnSe [43] and $Zn_xCd_{1-x}S$ solid solutions [22,44].

Let us discuss the issue of ZnO porosification. Due to the low chemical stability, the electrochemical nanostructuring of ZnO has been less investigated. In papers [27,34] discussed in chapter 1.3, was reported micro-and nano-structuring rather than pore formation in *n*-ZnO crystals. As a result of anodization nano-micro-structures with pyramidal form on the O-face, and inverted pyramids or tunnels on the Zn-face were obtained. The applied potential during anodization allows one to tune the transverse dimensions of the produced structures. Up to now, porous layers with parallel pores in ZnO were not reported in the literature. Notwithstanding this, a simple technological approach of porous ZnSe matrix transformation into porous ZnO template via thermal annealing was demonstrated [45].

The results of the comparative analysis of pore growth in II-VI and III-V semiconductor compounds as a result of electrochemical etching are summarized in Table 1.2.

Table 1.2. Systematization of type of pores that can be obtained in semiconductor compounds
[26]

Type of pores	II-VI				III-V				
	ZnO	ZnSe	CdSe	$Zn_xCd_{1-x}S$	InP	GaAs	GaP	GaN	InAs
Crysto pores (CO)	No	No	No	No	Yes, Low volt.	Yes	Yes, Low volt.	Yes, Low volt.	No
Determining factor	High ionicity degree				Low ionicity degree				Low bandgap
Curro pores (CLO)	No	Yes	Yes	Yes	Yes, High volt.	No	Yes, High volt.	Yes, High volt.	No
Determining factor	Not influenced by the ionicity degree								High bandgap
Fractal	No	Yes	No	No	No	Yes	No	No	No
Determining factor	Not identified								

In recent years, considerable research activity has been focused on the fabrication of ordered three-dimensional (3D) porous structures that possess electrical conductivity. In the paper [42], the results of the formation of 3D structures, representing a smooth Bragg-like structure, fabricated by modulation of the external current density (Figure 1.7a) were systematized. Unlike galvanostatic anodization, in which the formation of parallel layers with different degrees of porosity takes place, potentiostatic anodization of the InP substrate, with the consecutive application of voltages of 2 V, 4 V and 6 V (see the insert in Figure 1.7b), leads to the spatial nanostructuring of the material by modulation of the porous layers. At the same time, the morphology changes considerably due to the

induced self-organization of the pores governed by the transition from CO pores to CLO pores (Figure 1.7b).

An interesting finding was established during the successive anodization of ZnSe at applied voltage 15 V followed by the anodization at 8 V. The experimental demonstration of porous layer formation with two different pore diameters in the same plane is presented in Figure 1.7c. During the first anodization of the *n*-ZnSe crystal at 15 V, a porous layer with 500 nm pore diameter and thick skeleton walls is formed (see the upper porous layer in the inset of Figure 1.7c). As the applied voltage is reduced to 8V, a new porous layer is created with pore diameters up to 50 nm and much thinner pore walls compared to the previous anodization (see the lower porous layer in the inset of Figure 1.7c). At the same time, 50 nm pores are also formed in the skeleton walls of the first porous layer. The observed successive nanostructuring of the same layer at two different length scales opens new possibilities for the design and fabrication of device structures based on porous semiconductor compounds.

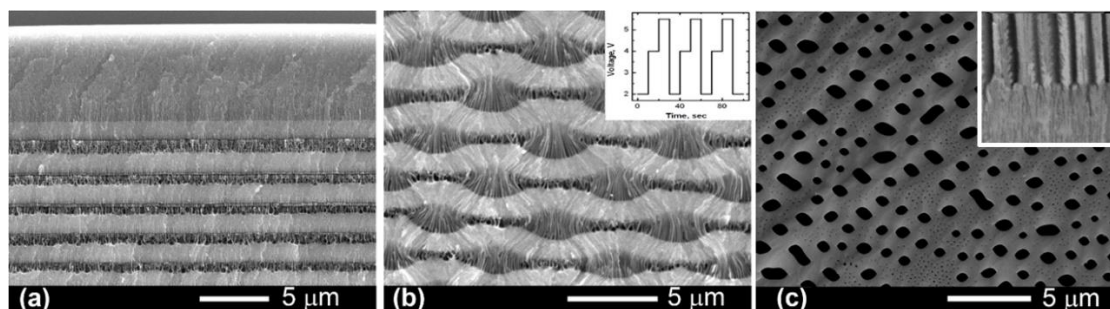


Figure 1.7. SEM images of InP crystal anodized in 3.5 M NaCl electrolyte (a) in galvanostatic regime at $100 \text{ mA}\cdot\text{cm}^{-2}$ followed by consecutive anodization at low/high current densities ($50 \text{ mA}\cdot\text{cm}^{-2}/500 \text{ mA}\cdot\text{cm}^{-2}$) resulting in several porous layers in the same plane with different degrees of porosity; (b) in potentiostatic regime at consecutively changed anodization potential of 2 V, 4 V and 6 V with demonstration of modulation of the porous layer. (c) Top-view SEM image and cross-section view in the inset, after successive anodization of ZnSe crystals, leading to the perforation of the primary pore walls. Reproduced from [42]

1.5 Conclusions to Chapter 1

In this chapter, the results of wide bandgap semiconductor compounds nanostructuring via electrochemical etching of: (i) HVPE grown GaN substrates; (ii) $\text{Zn}_x\text{Cd}_{1-x}\text{S}$ solid solutions; (iii) ZnO crystals were systematized.

Different porous morphologies were produced by anodization of HVPE-grown GaN substrates with respect to the N or Ga face. Complex pyramid-type porous structures are formed at a depth of several tens of micrometers from the N face, while homogeneous porous templates with pores oriented perpendicular to the wafer surface are generated at a depth of up to $50 \mu\text{m}$ on Ga face.

These characteristics are explained by the variations in electrical conductivity along the wafer resulting from the growth mechanisms of the HVPE technology. The possibilities of producing porous GaN structures in neutral NaCl electrolyte were demonstrated. HR-STEM analysis of porous GaN structure demonstrates the preservation of the high quality wurtzite crystalline phase of the material.

The selectivity of ZnO micro- and nano-structures obtaining with different shapes by anodization on different surfaces of ZnO crystal was demonstrated. The obtained microstructures have a pyramidal shape on the O-face, and inverted pyramids or tunnels were produced on Zn-face. The obtained morphologies corroborate with previously reported results for wet chemical etching, but we demonstrated additionally that the size of the formed microstructures can be controlled with the applied potential during anodization, as well as by the selection of the used electrolyte for anodization.

At the same time, $Zn_xCd_{1-x}S$ solid solution crystals with composition in the range of $0.4 \leq x \leq 0.6$, which possess a wider bandgap than ZnSe, have been shown to be a promising material for the fabrication of nanoporous templates with pore diameters up to 30 nm and 20 nm wall thickness via electrochemical etching. The anodization of samples with the composition $x > 0.6$ is limited by the low electrical conductivity inherent in these materials.

From the comparative analysis, it was established that the absence of CO pores in II-VI semiconductor compounds and the possibility of their growth in III-V semiconductor compounds is explained by the degree of ionicity of the chemical bonds. The CLO pores grow in almost all semiconductor compounds, except GaAs. However, in II-VI semiconductor compounds, CLO pores grow over a wide range of applied potential during electrochemical etching, while in III-V compounds they grow only at high values of the applied potential. The absence of CLO pores in GaAs requires further investigation.

The absence of CO pores in II-VI semiconductor compounds is confirmed by anodization on ZnSe and $Zn_xCd_{1-x}S$ crystals, in which during consecutive anodization at high and low voltage values, only layers with different degrees of porosity are formed, in contrast to the case of consecutive anodization of InP substrates.

2. ENGINEERING OF POROUS SEMICONDUCTOR COMPOUNDS AND METALLIC STRUCTURES BY ELECTROCHEMICAL METHODS

2.1 The technology of nanotemplates fabrication with parallel pores to the surface.

Cost-effective approach to control the direction of pore growth

To make use of industrial approaches of planar semiconductor technologies, it is important to develop methods for the preparation of templates with pores oriented parallel to the top surface of the

substrate. These types of porous structures are of particular interest for the fabrication of two-dimensional and three-dimensional photonic crystals, including metal-dielectric ones, because this geometry allows a wide implementation of the structures due to the large surface area of the samples compared to the traditional geometry, where the pores propagate perpendicularly to the surface.

A technological approach was elaborated and described in paper [46], for the fabrication of porous structures with pores oriented parallel to the top surface of the n -InP or n -ZnSe substrate, as is illustrated in Figure 2.1a, taking into account that CLO pores always grow in a direction perpendicular to the equipotential lines inside the anodized sample, which means that the crystallographic orientation of the substrate does not play any role for such kind pores.

According to this approach, some areas of the top surface of the substrate are covered with a photoresist (PhR), while other areas are exposed to the electrolyte in the anodization process. In such a case, the pores will initially grow from the surface exposed to the electrolyte in a direction perpendicular to the surface. However, with the further propagation of pores, they will be deflected in directions parallel to the top surface, and will grow under the regions covered by the photoresist. An experimental demonstration of this approach is presented for n -InP in Figure 2.1b and for n -ZnSe in Figure 2.1c,d.

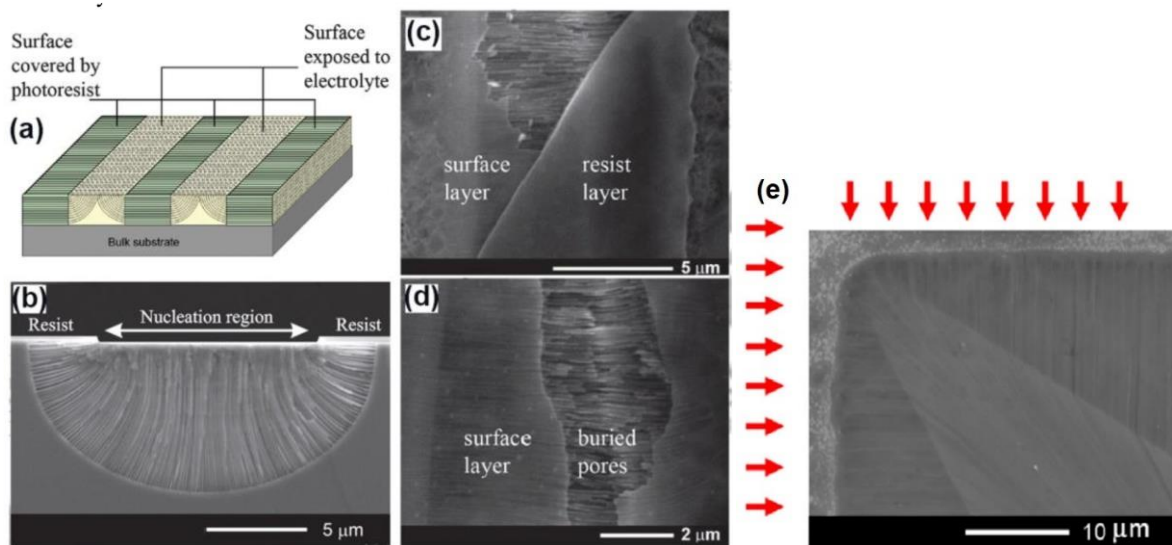


Figure 2.1. (a) Illustration of the approach for the preparation of porous templates with pores parallel to the top surface of the sample. SEM images of pores produced with the approach from (a) in InP (b) and ZnSe (c,d) substrates. Reproduced from [26,46]. (e) SEM view of anodized InP surface through rectangular photoresist mask, demonstrating the change of the propagation direction of the pores. The red arrows indicate the direction of electrochemical etching from the two photoresist edges. Reproduced from [28].

An interesting feature of porous structures obtained by this method is the fabrication of buried porous layers, as illustrated in Figure 2.1b,c. The pores grow under a thin surface layer which remains intact during the electrochemical treatment. The thickness of this surface layer is of the order of the

surface depletion region (W), i.e. from several tens to several hundreds of nanometers, depending on the conductivity of the anodized substrate. Figure 2.1c shows three layers present at the surface of the produced structure: a resist layer is reminiscent on a part of the sample, a virgin ZnSe layer determined by the depletion region as described above, and the porous structure buried under this surface layer.

The pore morphology becomes completely different, if the photoresist strips are replaced by a PhR mask in the form of squares, a spectacular porous architecture is obtained [37]. In such a case, the pores are forced to develop by the self-ordering process in the restricted space under the PhR. The wonderful play of pores is conditioned by the feature that curro pores cannot intersect. If in the case of using the PhR mask in the form of strips, the pores grow from both opposite sides, growing both parallel to themselves and parallel to the surface, the changing of the shape of the mask introduces major changes in the morphology because it invokes more sides from which the pores start to grow. It is obvious that the pores at the corners will meet each other faster than the pores growing in the middle of the PhR edge, and they will push each other keeping $2W$ between them (see Figure 2.1e) [28].

Taking into consideration the fight of pores in the restricted space under the PhR leading to fascinating morphologies depending on the shape and dimension of the used PhR mask, the recent study demonstrated that the direction of pore propagation can be strongly influenced by the introduction of holes in the PhR mask, as is illustrated in Figure 2.2 [28]. Let's examine the situation when nearly the whole surface of a semiconductor sample is covered by PhR except for a region exposed to anodization (left side in Figure 2.2a) and an open window with round shape ($1\ \mu\text{m}$ in diameter) in the PhR. Because of anodization, the formed "primary pores" on the unprotected surface will be deflected under the PhR and will propagate from the right to the left. At the same time, in the open hole with round shape, "secondary pores" will start to grow in all directions, forming a porous domain. These secondary pores will interact with the primary pores, changing their direction of propagation to avoid the intersection of pores (see Figure 2.2a). It should be noted that the primary pores are isolated by $2W$ -thick walls from the secondary pores, thus opening the possibility for application of this structures in microfluidics [28]. The morphology becomes more complex when several open holes are introduced in the PhR mask (see Figure 2.2b). This approach leads to the formation of several porous domains, filling the space under the PhR mask, and making flow of primary pores more difficult or even resulting in their annihilation [28].

The flexibility of this approach can amaze one even more. Unlike the case when the anodization is performed from the four PhR edges (Figure 2.1e), or one PhR edge (Figure 2.2a,b), with anodizing performed from two opposite PhR edges it is possible to influence the shape of the porous domain formed through an open hole in the PhR mask (Figure 2.2c) [28]. Despite the round shape of the hole (see Figure 2.2c the left side), applying a simple design of a PhR mask during the

etching will lead to the formation of a porous domain with a more complex shape (see Figure 2.2c in the middle). This phenomenon can be explained as follows: the pores propagating in both directions to the mask edges from the open hole (white arrows) will meet the primary pores much earlier than pores propagating laterally away (blue arrows). Once the pores from the porous domain meet with the primary pores (yellow arrows), both pores will stop growing, leaving a double space charge region between them. The growth of the laterally oriented pores (green and blue arrows) and the primary pores will continue until all free space is filled, therefore resulting in an “eye-like” porous structure, as is presented in the right part of Figure 2.2c. A simple combination of art with material science and technology is a perfect visual aid for education in Nanoscience and Nanotechnology named NanoArt. It can be concluded that anodization in combination with photolithographic means opens a new avenue for controlling the self-organization of the pores leading to new topologies obtained by design.

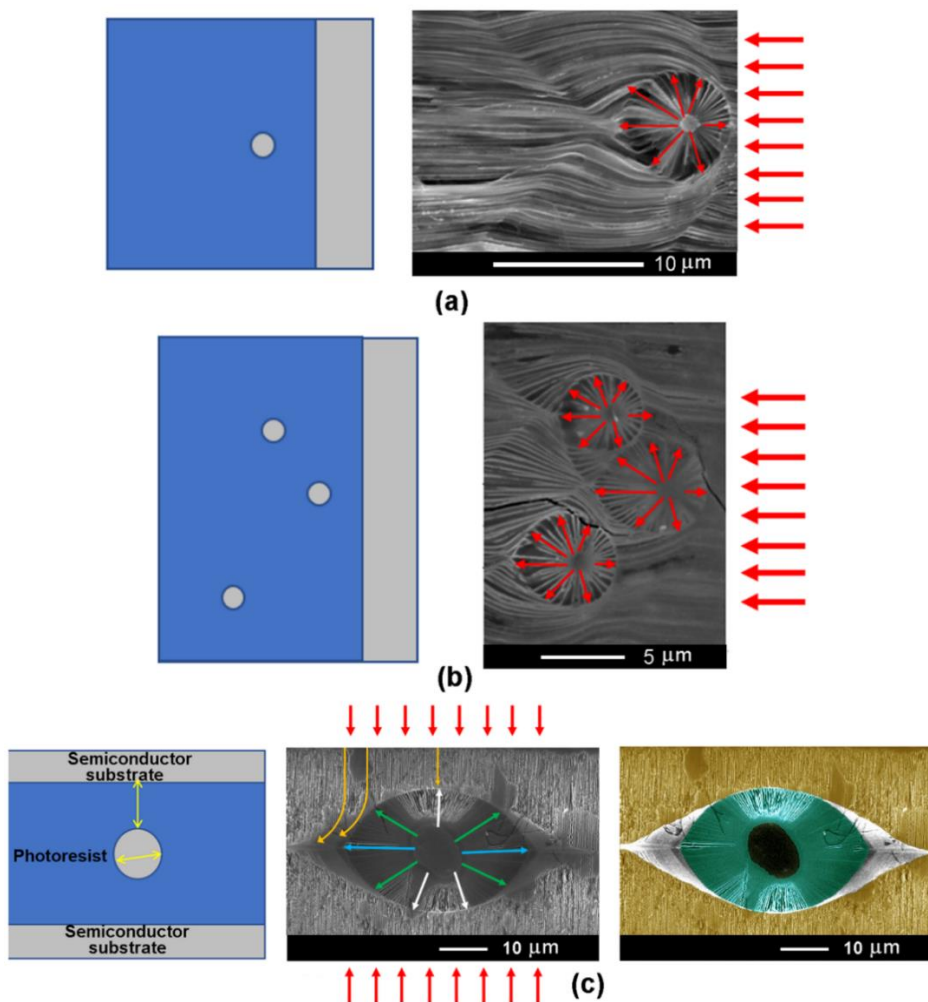


Figure 2.2. Schematic design (left) and (right) SEM image of anodized n -InP from one side using PhR masks with one (a) and three (b) open holes in the PhR. (c) Schematic design of the mask (left side), SEM image of anodized InP from two opposite PhR edges using PhR mask with one open hole in the PhR leading to the “eye-like” porous structure (center part), and NanoArt visualization of the SEM image (right side). Reproduced from [28]

2.2 From the porous structures to arrays of nanowires, nanobelts and nanomembranes

Considerable research efforts have been focused in the last decade on one-dimensional (1-D) nanostructures. Semiconductor nanowires with different compositions have been fabricated by a variety of methods, including laser ablation, templated electrochemical deposition, chemical transport, chemical vapor deposition, and solvothermal methods. However, nanowires obtained using these techniques possess crystallographic defects due to impurities from electrolytes, precursors, and various transport gases in the growth process.

All mentioned above technologies represent bottom-up approaches. An alternative and cost-effective technology for the fabrication of low-dimensional nanostructures proves to be anodic etching of bulk semiconductor crystals. By choosing the optimal electrochemical conditions, it is possible to obtain a huge amount of semiconductor nanowires connected to the bulk substrate. Usually, the wire formation procedure passes through the pore formation in the anodization process, but it is relatively difficult to identify the time when the electropolishing process starts.

Li *et al* applied simple and cost-effective technology for obtaining triangular GaAs nanowires through electrochemical etching of (100) GaAs surfaces in aqueous KOH solutions [47]. Nonetheless, this was a hardly controlled process, the bundles of GaAs nanowires being formed only in some regions of the surface and the orientation of the arrays was basically random. From the comparative study of the anodization processes occurring at the (111)A and (111)B GaAs surfaces with a free electron concentration of $2 \times 10^{18} \text{ cm}^{-3}$ subjected to electrochemical etching in neutral NaCl and acidic HNO₃ based aqueous electrolytes, the GaAs nanowires obtaining in HNO₃ electrolyte that are oriented perpendicular to the sample surface was reported [48].

In order to clarify the orientation of the nanowires with respect to the substrate, a detailed study was carried out in this work of the anodization of *n*-GaAs crystals with different crystallographic orientations (111)B, (001) [49] and (100) [12,42]. Anodization of *n*-GaAs crystals with (100) crystallographic orientation in 1 M HNO₃ electrolyte for 15 min at 4 V results in the formation of an array of nanowires oriented at an angle to the substrate surface, as shown in Figure 2.3a, while the anodization of (111)B and (001) crystals under the same technological conditions leads to the formation of nanowire arrays oriented perpendicularly (Figure 2.3b) and respectively predominantly parallel to the wafer surface (Figure 2.3c).

The mechanism of nanowire formation by electrochemical etching can be explained by the images in Figure 2.3d,e that represent the top view of porous GaAs after successive anodization at an applied potential from 4 V to 3 V of (111)B and (001) GaAs substrates, respectively. The process was followed by sonication for 1 min for detaching the nanowires from the substrate, to disclose the growth direction of pores. From Figure 2.3d, it can be seen that pores pose a triangular cross-sectional shape due to the formation of CO pores, in contrast to a round cross-sectional shape inherent to CLO

pores. Note that the formation of pores with the round shape in GaAs was not reported up until now. With the increase in applied potential, the transverse dimensions of triangular pores increase, leading to the overlapping of pores. As a result, the non-etched island having the same triangular shape remains as an individual nanowire [49].

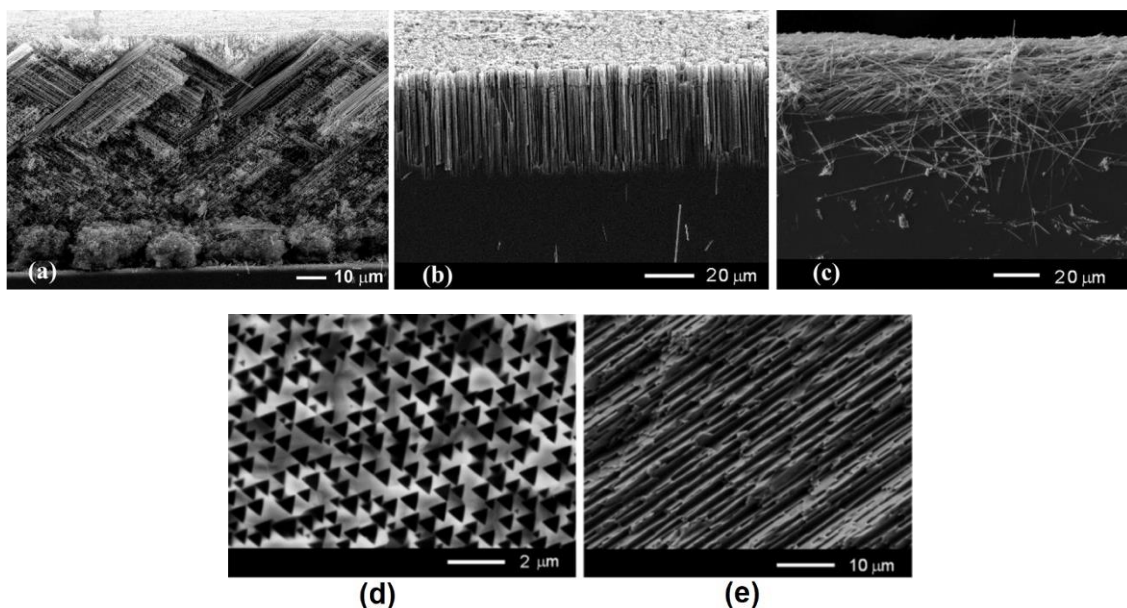


Figure 2.3. Cross-sectional SEM images of GaAs nanowires produced by anodization of *n*-GaAs crystals with crystallographic orientation (100) (a), (111)B (b) and (001) (c) in 1 M HNO₃ electrolyte at applied voltage 4 V. (d,e) Top-view SEM images of the samples from (b) and (c) after successive anodization at 4 V and 3 V followed by detaching the nanowires by sonication. Reproduced: (a) from [28]; (b-e) from [49]

In the paper [50] it was demonstrated that pulsed electrochemical etching, proved to be efficient for anodization of *p*-type ZnTe, resulting in the formation of 10 μm long nanowires with the diameter of 50 nm. As in the study of Zenia *et al* [51], an electrolyte based on HNO₃:HCl:H₂O with the ratio 5:20:100 was used, but under the application of 0.3 s voltage pulses with the frequency of 1 Hz and amplitude of 5 V (the pause between pulses was of 1 s). The high quality of the produced ZnTe nanowires was demonstrated by photoluminescence investigations since the emission intensity and spectral distribution of PL are practically identical to those of the initial bulk material.

It is well known, that preparation of nanowires through described above approaches requires at least half an hour of anodization duration. In the paper [52], it was demonstrated the possibility to fabricate InP nanomembranes and nanowires using fast anodic etching of *n*-InP single crystalline substrates. The term “fast anodic etching” was used because 2-μm long nanowires are obtained in just 3 s of anodization, which means that the rate of etching in depth direction is about 40 μm·min⁻¹.

Applying anodization under 5 V potential to *n*-InP samples with the carrier density of 1x10¹⁸ cm⁻³, one can fabricate porous layers with pore diameter and wall thickness about 80 nm and 40 nm, respectively (see Figure 2.4a). Increase in the applied potential up to 7 V gives rise to pronounced

fluctuations in the pore diameter and leads to the formation of highly porous layers, the porous skeleton being characterized by percolation, see Figure 2.4b. Further, by applying a high-voltage pulse during the anodization it is possible to detach the obtained porous layer from the substrate, i.e. to fabricate a highly porous membrane. To demonstrate the diversity of structures that can be obtained by electrochemical etching, a conventional photolithography was used to open rectangular windows with a breadth of 35 μm in the photoresist covering the top surface of n -InP samples. In this way, porous membranes with predefined width can be easily obtained. Moreover, applying a high-voltage short pulse via photolithographically defined windows before the anodization process leads to the formation of InP nanowalls and nanowires. It was established that the morphology depends drastically upon the value of the applied voltage pulse. As one can see from Figure 2.4c, the etching results in the formation of mosaic structures consisting of ultrathin semiconductor walls. At the same time, a relatively large number of nanowires simultaneously form with diameters of about 50 nm (Figure 2.4c). The formation of nanowires starts to predominate with further increase of the applied voltage. Figure 2.4d illustrates a uniform network of parallel nanowires fabricated by applying pulse voltage of 15 V.

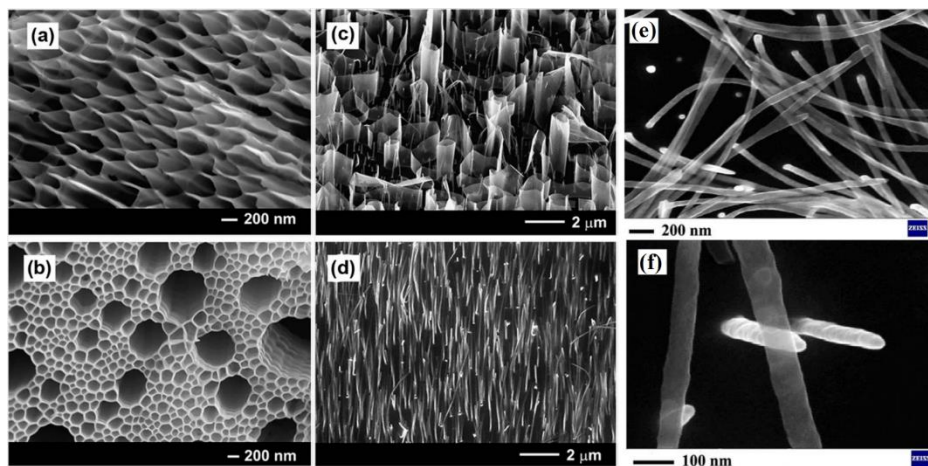


Figure 2.4. SEM images of porous layers fabricated by anodization of n -InP crystals at different applied voltages: (a) $U = 5$ V; (b) $U = 7$ V; (c) $U = 10$ V; (d) $U = 15$ V. (e) SEM image of the InP mosaic architecture after anodization at 13 V demonstrating the formation of a mixture of nanowires and nanobelts. (f) Enlarged SEM image from (e). Reproduced from [52]

Using this approach, a new type of nanostructures were identified in the InP mosaic architecture produced using electrochemical etching, namely nanobelts, which are generated at an anodization voltage of 13 V. InP nanobelts are formed simultaneously with nanowires and nanowalls (Figure 2.4e), their width being equal to the diameter of the nanowires (about 50 nm), while the thickness of the nanobelts is less than 10 nm, as suggested by their transparency in the SEM image in Figure 2.4f. The SEM, TEM, EDX characterization of the InP-based nanostructures was described in the paper [52]. The electrical and optical properties of nanobelts have been shown to be different

from those of nanowires, the experimental demonstration of which is disclosed in [53] and chapter 2.4.

2.3 Development and demonstration of "hopping electrodeposition" mechanism of metal nanodots

Electrochemical deposition of metal nanodots proves to be one of the most effective techniques, especially when the deposition is realized on semiconductor substrates or matrices that possess electrical conductivity. The possibility of covering an extensive surface inherent in porous GaP and InP structures with a self-assembled monolayer of Au nanodots by pulsed electrochemical deposition was demonstrated [54].

The so-called "hopping electrodeposition" mechanism was proposed to explain the deposition of a monolayer of gold nanodots on porous semiconductor structures. In the paper [54], pulsed electrochemical deposition of gold was used and it was determined that after nucleation, each nanodot grows up to a critical diameter of about 20 nm, which is determined by the height of the Schottky barrier at the interface with the semiconductor substrate. This value corroborates with previously published data for Pt electrodeposition on bulk *n*-InP wafers, being evidence that the height of the Schottky barrier depends on the size of Pt nanodots [55]. As the diameter of the metal dots increases, the surface barrier height increases rapidly up to the Mott–Schottky threshold value of 1.1 eV which is reached at the Au nanodot diameter about 23 nm. Subsequently, the formation of a new metal nanoparticle is initiated, and the deposition process continues until the entire surface exposed to the electrolyte is covered by a monolayer of self-assembled gold nanodots (see Figure 2.5a,b).

The schematic representation of "hopping electrodeposition" mechanism is presented in Figure 2.5c. At the initial phase of deposition, the process of nucleation of gold dots takes place along with the gradual increase in their size. As the diameter of the nanoparticle reaches the threshold value, a Schottky barrier appears, the barrier potential being oriented opposite to the applied cathodic voltage. Thus, the modified local potential "stops" electrodeposition in the region of this dot. To keep the process going, the system initiates the nucleation of new dot. In other words, electrodeposition is a jumping process: gold deposition "jumps" to other areas on the surface as soon as one or more dots reach the threshold diameter. The "stopping" and "jumping" processes continue until the entire surface exposed to the electrolyte is covered by a monolayer of self-assembled Au nanodots. It was established that after the formation of the self-assembled monolayer the process of further electrodeposition of gold is spatially non-uniform and leads to the deposition of large particles with diameters of 100-300 nm. Subsequently, the "hopping electrodeposition" mechanism was used to obtain the perforated gold nanomembranes [56].

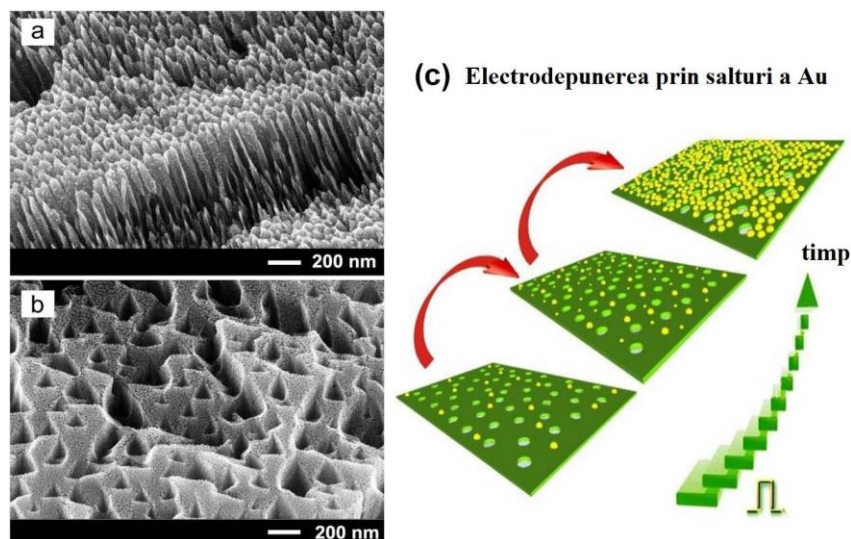


Figure 2.5. SEM images of porous GaP after electrochemical deposition of Au dots for 5 s (a) and 100 s (b) and schematic illustration of the “hopping electrodeposition” mechanism (c).

Reproduced from [54]

The type of the contact, i.e., ohmic or Schottky, can be estimated from the analysis of the difference between the work function of the metal (ϕ_m) and the value of the electron affinity of InP (χ_s). One can expect the formation of a Schottky contact on an *n*-type material when $\phi_m - \chi_s > 0$. Among metals (such as Mg, Zn, Al, Cr, Ni, Pt), Pt exhibits the highest value of $\phi_m - \chi_s$ which equals 1.3 eV, followed by Ni (0.81 eV) and Au (0.63 eV) [57,58].

In the paper [59], the topography imaging and Point Contact Microscopy (PCM) measurements were performed to experimentally demonstrate the formation of the Schottky barrier at the metal-semiconductor interface. A layer of Au nanoparticles with different thicknesses was electroplated on the surface of a porous InP sample with pores parallel to the surface, obtained according to the approach from Figure 2.1. The analysis of Current Mapping images from Figure 2.6 suggests the variation of the Au nanoparticle layer thickness over the substrate surface. The regions with red color (high current densities) correspond to a monolayer of Au nanodots with the size of around 20 nm. The regions with blue color in the Current Mapping images correspond to thicker Au layers formed from larger Au particles, with the size around 100–300 nm deposited on the monolayer of Au nanodots according to the previously discussed "hopping electrodeposition" mechanism.

The formation of Schottky barriers is indicated by the analysis of I–V curves from Figure 2.6. Measurements in the point 3 from Figure 2.6 with high value of the current demonstrate an I–V curve typical for Schottky diodes, which confirms deposition of a monolayer of 20 nm Au nanodots. The breakdown of the Schottky barrier at a voltage of 5 V at the cantilever tip leads to current flow in these regions, which produces a red color in the current mapping image. The I–V curves measured in regions with a thicker metal layer (point 2) or at a larger metal particle of 200 nm (point 1) in Figure 2.6, suggests a much higher electrical resistance than the measurements on the monolayer of Au

nanodots (point 3). We can assume that a more difficult current flow is caused by the insufficiency of the 5 V voltage used for the investigation to break the Schottky barrier.

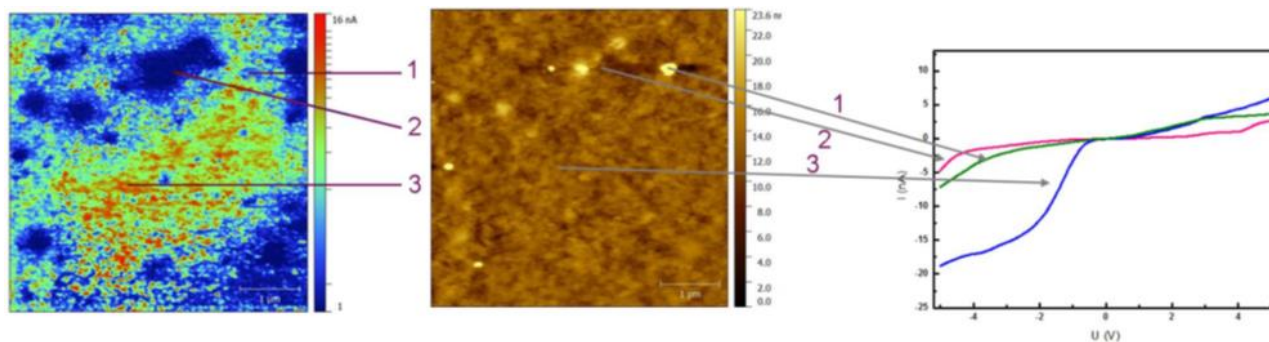


Figure 2.6. Current–voltage curves (right) measured in indicated points on the topography image (center) and current mapping image (left) of the porous InP sample with Au nanodots. Scan size of $5\times 5\ \mu\text{m}$. Reproduced from [59]

Later on, a comparative analysis of electrochemical impedance spectroscopy (EIS) characterization was performed in porous GaN and GaP templates with and without metal nanostructured layers deposited by pulsed electroplating. It is found that the EIS data of porous electrodes without electroplating are best fitted with equivalent electrical circuit with both the charge transfer and mass transfer components of the Faradaic impedance, while electroplating reduces the importance of the mass transport component, i.e. of the Warburg impedance, associated with diffusion, in favor of the charge transport phenomena [60].

2.4 Electrochemical etching and deposition as an efficient and accessible tool for assessing the electrical conductivity in semiconductor nanostructures

Development of devices based on nanomaterials such as nanowires, nanotubes, membranes, etc, requires a deep understanding of charge carrier dynamics and transport in these structures. To understand these properties, the deposition of an electrical contacts at the nanoscale is required. However, measurements can be influenced by artifacts generated by electrical contacts deposited on individual nanoobjects.

An original and innovative method for estimating the electrical conductivity in 1D and 2D semiconductor nanostructures by pulsed electrochemical deposition of metal nanodots is reflected in the paper [53]. The essence of the estimation method according to the geometrical dimensions of the nanostructure is the "hopping electrodeposition" mechanism [54], previously discussed in chapter 2.3. Figure 2.7a shows the SEM image of an *n*-InP nanowire and several nanobelts on bulk InP substrate after pulsed electrochemical deposition for 120 s. It is clearly seen that after gold electroplating the surface of the nanowire as well as the surface of the bulk substrate is covered by a uniform monolayer of 20 nm gold nanodots and some 300 nm particles. This issue is better illustrated in Figure 2.7b. More 300 nm Au particles are formed because the deposition time is longer than that

required to deposit a single monolayer of 20 nm Au nanodots. In contrast to nanowires, the surface of nanobelts remains intact, i.e. no electrochemical deposition occurs on them.

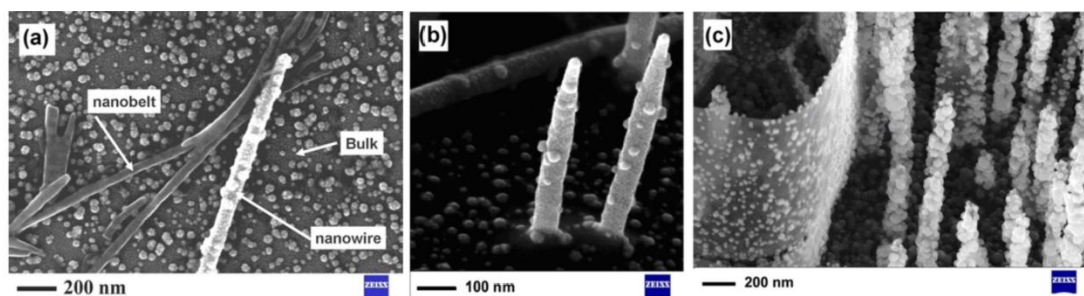


Figure 2.7. (a) SEM image of n -InP nanowire and nanobelts on bulk InP substrate after pulsed electrochemical deposition for 120 s; (b) Magnified image of a few nanowires after electrochemical deposition for 120 s; (c) SEM view of a nanowall and several nanowires after electrochemical deposition for 300 s. The measured thickness of the nanostructures is: nanowire – 50 nm; nanowall – 10 nm; nanobelts – a few nanometers. Reproduced from [53]

Figure 2.7c compares the electrodeposition of gold on InP nanowires and on a nanowall, which by thickness represents an intermediate nanostructure between nanowires and nanobelts. Comparing Au depositions on nanowires (SEM images in Figure 2.7b and Figure 2.7c), it can be confirmed that less 300 nm Au nanoparticles are deposited on the monolayer of 20 nm Au nanodots within 120 s (Figure 2.7 b), while the number of nanoparticles with a diameter of 300 nm deposited on the nanowires increases significantly after deposition for 300 s (Figure 2.7c). Also, from Figure 2.7b can be seen that the density of 300 nm Au nanoparticles on the nanowires and on the bulk InP substrate is almost the same, which suggests that the electrical conductivity of the nanowires is comparable to that of the bulk n -InP semiconductor crystals. In contrast, the surface of the nanowall in Figure 2.7c is only partially covered by Au nanodots, i.e., a monolayer of 20 nm Au nanodots is not completely formed on the surface of the nanowall. This indicates that the conductivity of the nanowalls has an intermediate value of electrical conductivity between InP nanowire and nanobelt [53,61].

In the recent work [62], the electrochemical deposition of gold, governed by the “hopping electrodeposition” mechanism, was also used to highlight the modulation of the electrical conductivity in HVPE-grown GaN crystals. Previously, by means of electrochemical etching, three-dimensional self-organized nanostructured architectures were revealed that were attributed to the spatial modulation of the electrical conductivity, generated during the HVPE growth of GaN [15], discussed in more detail in the chapter 1.1.

During the electrochemical deposition of gold, as in the case of the electrochemical etching, the current flows through the electrical path with the lowest resistance. Thus, experimentally optimizing the parameters of the electrochemical deposition, especially the value of the pulse voltage

amplitude, it was demonstrated the predominant deposition of gold specifically on the regions with higher electrical conductivity, forming concentric structures similar to those from Figure 2.8b. It should be noted that the regions with different electrical conductivity can also be distinguished with the electron microscope, observing different contrast in the SEM images as shown in Figure 2.8a. The experimental demonstration that electrical conductivity modulation occurs not only on the surface is presented in the cross-sectional study of GaN samples subjected to electrochemical etching (Figure 2.8c) and pulsed electrochemical deposition (Figure 2.8d) [62].

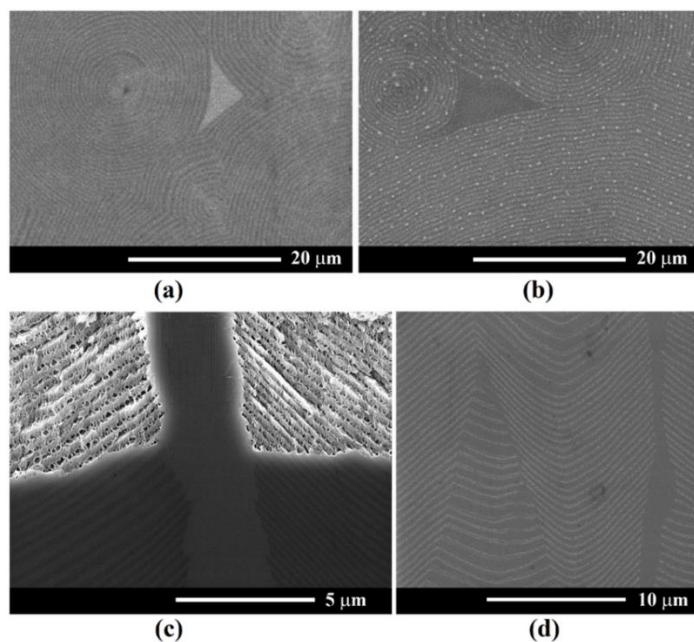


Figure 2.8. (a) Top-view SEM image (registered using a detector with backscattered electrons) of the as-grown HVPE GaN free-standing substrate revealing alternating concentric rings with different electrical conductivities. The dark regions exhibit higher conductivity. (b) Gold nanodots electroplated for 100 s on the surface of the HVPE as-grown GaN substrate at 50 μs pulse width, 1 s pause between the pulses, and pulse amplitude - 15 V for 100 s of electrodeposition. (c) Cross-sectional SEM view of HVPE GaN substrate after electrochemical etching in 1 M HNO₃ at 25 V for 10 min. (d) The electrochemical deposition of Au nanodots on freshly cleaved as-grown HVPE GaN substrate demonstrating the nonuniformity of doping during the HVPE growth. Reproduced from [62]

As another way of deposition along certain lines has been demonstrated by combining the electrochemical technologies, namely, in the first step, the formation of pores parallel to the surface of the *n*-InP substrate takes place, buried under a thin layer on the surface, as described in the chapter 2.1, later on the Au nanodots are deposited by pulsed electrochemical deposition [62]. Since the surface layer is depleted of charge carriers, its resistivity is high and metal deposition does not occur on it. On the other hand, the thickness of the pore walls that are buried under this layer is twice as high, being characterized by higher electrical conductivity. As a result, arrays of Au nanodots are

deposited on these conductive regions during electroplating. The density of Au nanodots in the matrix is controlled by the number of pulses applied during electroplating. The mechanism of Au deposition along the lines is described in more detail in the paper [63].

2.5 Control of the hydrophobic/hydrophilic properties of semiconductor structures by electrochemical techniques

Nowadays, hydro insulation is very important technological step intended to protect electrical components embedded in consumer devices, such as computers, smartphones, smart watches, medical examination devices and more. To protect the microchips from contact with water, hydrophobic polymers such as polydimethylsiloxane (PDMS) are usually used, but they are characterized by low thermal conductivity, leading to poor heat dissipation. The idea of III-V semiconductor impermeability has been previously reported, involving the transfer of epitaxially grown III-V structures to flexible and impermeable substrates such as PDMS [64]. However, these processes are complicated from the point of view of realization. In the following study, the GaAs and InP semiconductor compounds were selected because they represent an important class of materials for the high-frequency microelectronics and optoelectronics industry.

The anodization and electroplating of metals on the bulk or porous semiconductor layers have a great impact upon the wetting properties of surfaces leading to pronounced hydrophilic or hydrophobic behavior as was demonstrated in papers [28,65].

To establish how the deposition of metal influence the wetting properties of semiconductor crystals surface (GaAs in our case), the contact angle of bulk GaAs substrates and bulk GaAs decorated with deposited gold nanodots was investigated [65]. The measured contact angle of bulk *n*-GaAs substrate is 80.4°. The electrochemical deposition of gold on bulk *n*-GaAs substrate with pulse duration of 50 μ s resulted in formation of thin layer consisting of closely packed 20 nm Au nanodots. In this case, the measured contact angle decreased to 73.9° due to the small voids between the deposited Au nanodots. The increase of the pulse duration up to 300 μ s during electrochemical deposition leads to the formation of perforated Au membrane on the surface of GaAs semiconductor substrate with the thickness about 100 nm [56]. The measured contact angle about 42.7° indicate the hydrophilic properties of GaAs surface decorated by perforated gold membrane. The formation of pores in deposited Au film was explained and demonstrated in the paper [56].

Introducing porosity on the semiconductor surface is another way to control the wetting properties [65]. It was recently demonstrated that anodization on different (111)GaAs surfaces resulting in different orientation of pores to the surface [48]. The measured contact angle on these porous structures demonstrated the possibility of switching from hydrophobic (137.5°) to hydrophilic (37.5°) behavior by controlling the degree of porosity as well as the alignment of the obtained pores with respect to the sample surface [65].

Even greater flexibility to control the contact angle can be achieved by functionalization of the porous layer with a monolayer of Au nanodots via pulsed electrochemical deposition. The porous layer decorated with 20 nm gold nanodots demonstrated an increase in the contact angle up to 117.6° , compared to the porous GaAs layer (33.6°) or bulk (80.4°) [28].

In contrast to the random orientation of GaAs pores investigated above, the anodization of *n*-InP substrates leads to the formation, underneath of top nucleation layer, of self-ordered hexagonally packed pores with a diameter of 80 nm, oriented perpendicularly to the substrate surface [26]. The removal of the top nucleation layer is a very important step, since it allows chemical dissolution of a thin layer with branched pores, reaching the opened self-ordered perpendicular pores [57,66]. These porous InP structures, after removal of the top nucleation layer, demonstrated an CA about 151.6° , while bulk InP samples showed an CA of 95.7° , as can be seen in Figure 2.9a,b, with the real image of the water drop shape in Figure 2.9c,d [28].

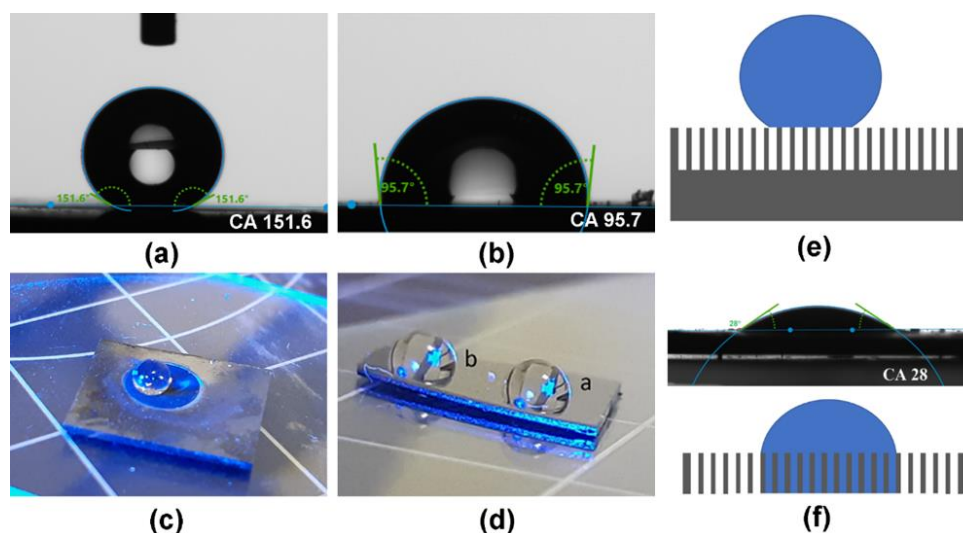


Figure 2.9. CA measurements on the porous *n*-InP (a) and bulk (b) substrate. Real photo images demonstrating pronounced hydrophobic properties for porous *n*-InP layer (c) in contrast to bulk InP substrate (d). (e) Schematic representation of the water drop measured on a porous *n*-InP layer filled with air on a bulk substrate. (f) Schematic representation and measured CA on free-standing InP membrane, demonstrating the filling of the membrane with water due to the open pores from both sides. Reproduced from [28]

In the case of detachment of the porous InP layer from the substrate, the CA decreases to 28° in comparison with the same porous layer on the bulk substrate (see Figure 2.9f). To explain this behavior, we will examine both cases. (i) The porous layer with a thickness of $100\ \mu\text{m}$ represents a network of parallel tubes isolated from each other by pore walls. From the top, the pores are open because of removal of the top nucleation layer, while from the bottom, the pores are closed by the bulk InP substrate. Normally, the porous structures are filled by air, which is trapped in channels

between the water drop and bulk substrate (see Figure 2.9e). (ii) When the porous layer is detached from the substrate, we get a membrane with open channels from both sides. In this case we consider that hydrophilic behavior is facilitated by the better conditions for water drop to flow inside due to the open pores at the bottom surface (Figure 2.9f). Thus, it can be concluded that wetting properties of semiconductor surfaces can be engineered by anodization or electrochemical deposition of metal nanodots.

Conclusions to chapter 2

It was demonstrated that self-organization proved to be a powerful and cost-effective tool for developing a new class of semiconductor-based nanotemplates for nanofabrication. Anodic etching of semiconductor compounds under specific conditions enabled one to fabricate two-dimensional single crystals of nanopores which seemed impossible without application of lithography.

Porosification of semiconductor compounds combined with the application of special masks brought to light a variety of fascinating morphologies, including formation of networks of pores oriented parallel to the top surface of the semiconductor substrate and of porous domains excluding pore percolation between them.

Anodic etching of bulk crystalline substrates of *n*-InP via photolithographically defined windows leads to the formation of nanomembranes and nanowires being promising for device applications. Under potentiostatic etching conditions, the morphology of etched samples strongly depends on the applied voltage. It was found that anodization at 5–7 V results in the formation of highly porous layers with mechanically stable skeletons exhibiting percolation, which easily detach from the substrate thus representing nanomembranes. At the same time the predominant formation of nanowires was evidenced at further increase of the applied voltage up to 15 V.

The obtaining of semiconductor nanowires by anodization and on *n*-GaAs crystals in nitric acid electrolyte, with the possibility of controlling the orientation of the nanowires with respect to the substrate surface was demonstrated. As a result, tilted to the surface nanowires were obtained using substrates with (100) crystallographic orientation, perpendicular to the surface nanowires for (111)B orientation and predominantly parallel to the substrate surface nanowires formed in the case of crystals with (001) orientation.

Electrochemical deposition of Au has proven to be an effective tool for evaluation of the electrical conductivity of *n*-InP nanostructures, fabricated by electrochemical etching of semiconductor crystals. The comparison of the electrochemical deposition of metals on nanowires and on bulk InP wafers demonstrates that the electrical conductivity of nanowires is similar to that of bulk crystals. At the same time, the comparison of pulsed electrodeposition of gold on nanowires and on nanowalls demonstrates that the conductivity of nanowalls is much lower than that of nanowires.

Since the electrodeposition of metals on the InP nanobelts does not occur, we conclude that there are no charge carriers in the semiconductor nanobelts with a few nanometers thick. Electrochemical etching or electrochemical deposition can be used as a cost-effective and accessible method to highlight the doping fluctuations in GaN semiconductor crystals during HVPE growth.

The anodization and electroplating of metals on the bulk or porous semiconductor layers have a great impact upon the wetting properties of surfaces leading to pronounced hydrophilic or hydrophobic behavior. It was demonstrated that the morphology of pores, tilted or perpendicular to the surface, play an important role in switching from the hydrophobic to hydrophilic properties.

3. RETROREFLECTION OF LIGHT IN POROUS SEMICONDUCTOR COMPOUNDS (InP, GaAs). PHOTONIC NANOSTRUCTURES (GaN, GaP, ZnSe)

3.1 Anomalous retroreflection demonstrated for porous n-InP layers

In the paper [67], anomalous retroreflection has been discovered in 2011 for a fishnet nanoporous semiconductor material strongly absorbing in the visible range. Retroreflection occurs in a narrow solid angle along with a diffusive specular reflection for all angles of incidence. Porous InP samples were fabricated by anodization of *n*-InP:Si crystals with (100) and (111) crystallographic orientations, with free charge carrier concentration of $3 \times 10^{18} \text{ cm}^{-3}$, at different anodization voltages applied (4 V – 8 V) resulting in porous layers with morphologies possessing different degrees of porosity [67]. It should be noted that the crystallographic orientation does not strongly influence the morphology, because the value of the anodization voltages used cause the growth of CLO pores. Remarkable is a more pronounced retroreflection for samples having pore parameters of the mesh-like morphology comparable to or smaller than the wavelengths for visible light, being a non-trivial and unexpected behavior. From the set of eight samples, pronounced retroreflection of light was observed on six of them [67].

From the analysis of the results of the scattering diagram (Figure 3.1a-c) for different incidence angles and polarizations of the incident light for porous InP layer, it was established that at an incidence angle close to normal ($\alpha = 60^\circ \dots 80^\circ$), retroreflection dominates over the specular reflection. At grazing angle of incidence ($\alpha = 15^\circ - 30^\circ$), retroreflection remains, and specular reflectance for *s*-polarized light rises while falling for *p*-polarized light. The latter is expected from the standard theory of light reflection. Notably, retroreflection is persistent in every case, showing neither noticeable dependence on angle of incidence nor on *s/p*-type polarization of incident light [67].

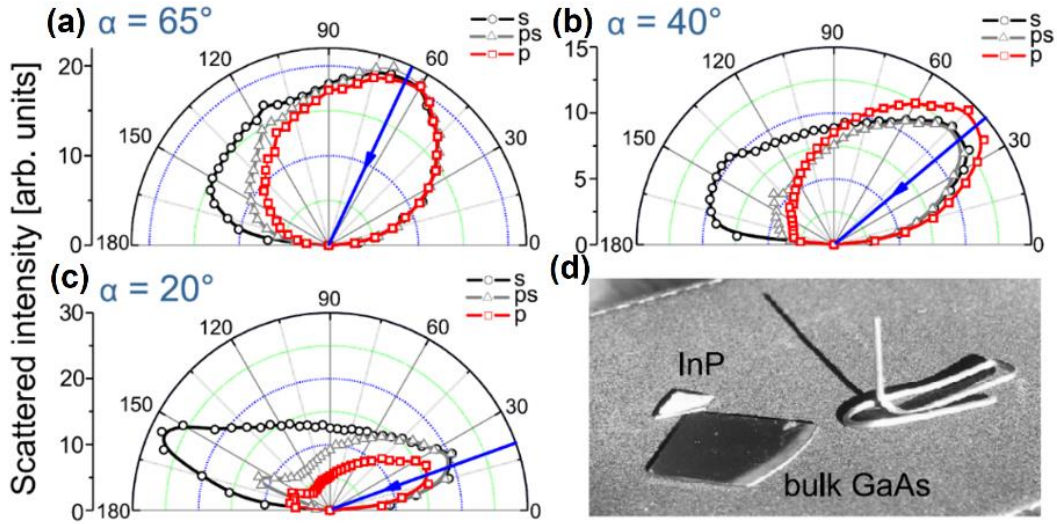


Figure 3.1. (a–c) Scattering diagrams for s , p and mixed ps polarization of incident light for porous n -InP sample for three values of incidence angle α . The incidence direction is indicated by arrows. (d) Observation of retroreflection in daylight with a paper clip indicating incidence direction and a bulk GaAs sample shown for comparison. The scattering diagrams were measured at wavelength of 531 nm, where the real n and imaginary κ parts of the complex refractive index are $n=3.8$ and $\kappa=0.5$. Reproduced from [67]

Among the disordered absorbent materials, porous Si should be mentioned. But none of the tens of porous Si samples examined showed retroreflective behavior [68]. Thus, we suppose both a specific mesh structure and strong absorption are significant in understanding retroreflection.

Later, in contrast to the case of anomalous retroreflection demonstration in spectral domain of interband transitions with high values of the refractive index ($n=3.8$) and the absorption coefficient ($\alpha=10^5 \text{ cm}^{-1}$) [67], in the paper [69] it was continued the investigation of retroreflection and scattering properties of fishnet nanoporous semiconductor InP not only in the spectral range of interband optical transitions where multiple scattering is inhibited by strong absorption, but also in the infrared spectral region where this material is transparent.

Remarkable is the systematic manifestation of retroreflection in scattering diagrams of every sample for the wavelengths 531 nm and 654 nm (some representative diagrams are shown in Figure 3.2) where the optical absorption (interband) is high, $\alpha=1.3 \times 10^5 \text{ cm}^{-1}$ and respectively $\alpha=0.6 \times 10^5 \text{ cm}^{-1}$. At the same time, retroreflective feature vanishes for 1.064 nm wavelength, where the absorption is negligible according to Ref. [70]. The diffuse reflection for 1.064 nm shows an angular dependence close to that typically observed in porous materials with low absorption, the reference diagrams being presented in the paper [67].

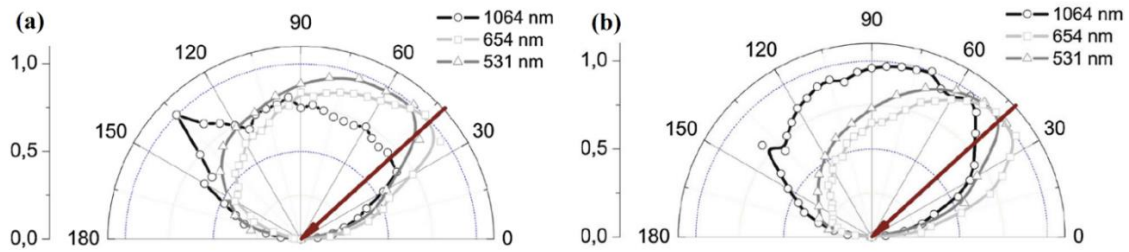


Figure 3.2. Scattering diagrams for two porous InP samples investigated at three laser wavelengths. The red arrow line represents the direction of the incident laser beam.

Reproduced from [69]

Later, in the paper [71], the formation of longitudinal electromagnetic waves was suggested as a possible reason for the observed phenomenon, considering two cases: *s* polarization with the excitation of only transverse waves in the material ("bright modes") and the case of polarization *p*, which allows the excitation of both longitudinal and transverse waves in the medium ("dark modes" and "bright modes"). In the paper, the concept of coherent scattering, the mathematical model, as well as the results of theoretical calculations were described in detail [71].

A summary of experimental data obtained for a nanoporous InP sample is presented in Figure 3.3 to show the principal regularities of the observed 'anomalous' backscattering. In these experiments, the fundamental (1064 nm) or the second (532 nm) harmonics of a Nd-based solid state laser have been used corresponding to photon energy well below and well higher the InP bandgap energy, respectively.

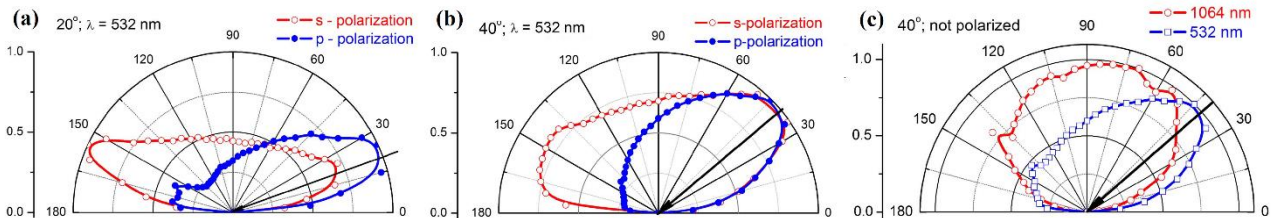


Figure 3.3. Angular dependent scattering diagram of a nanoporous InP sample for different angles of incident light (20° (a) and 40° (b,c)) for *s*- and *p*-polarization, and different wavelengths corresponding to low (1064 nm) and high (532 nm) intrinsic interband absorption in InP. Reproduced from [71]

Backscattering is more pronounced for *p*-polarized compared to *s*-polarized radiation (according to Figure 3.3a,b), it shows an apparent tendency to increase when the angle of incidence moves from normal to oblique incidence (compare the data for 20° and 40°) and vanishes for wavelengths corresponding to low intrinsic absorption (1064 versus 532 nm, from Figure 3.3c) [71].

3.2 Retroreflection from porous GaAs layers. Comparison with porous InP samples

After a series of works regarding the experimental observation of retroreflection from porous InP layers [67,69,71,72], the phenomenon was experimentally demonstrated also on porous GaAs

layers [73,74]. At room temperature InP and GaAs have $E_g=1.34$ eV (corresponding to 925 nm) and 1.42 eV (corresponding to 873 nm), respectively. At $\lambda = 532$ nm optical parameters of solid GaAs are $n=4$ și $\alpha=6 \times 10^4$ cm⁻¹, both values are very high and close to the parameters of InP. The high absorption and refraction in both materials result from the direct interband optical transitions because the photon energy is considerably higher than the bandgap energy. Porous GaAs layers with different degrees of porosity were obtained by electrochemical etching of (100) GaAs crystals with $n=2 \times 10^{18}$ cm⁻³ in the galvanostatic regime at current densities from 100 mA·cm⁻² to 600 mA·cm⁻² in HCl or HNO₃ electrolyte.

In Figure 3.4, a variety of scattering polar diagrams are presented for seven GaAs samples with various degrees of porosity and morphologies, obtained by anodizing under different conditions, indicated in more detail in Table 1 from Ref. [73]. Data for the original crystalline GaAs (#1) are not presented because this sample showed typical mirror-like Fresnel reflection.

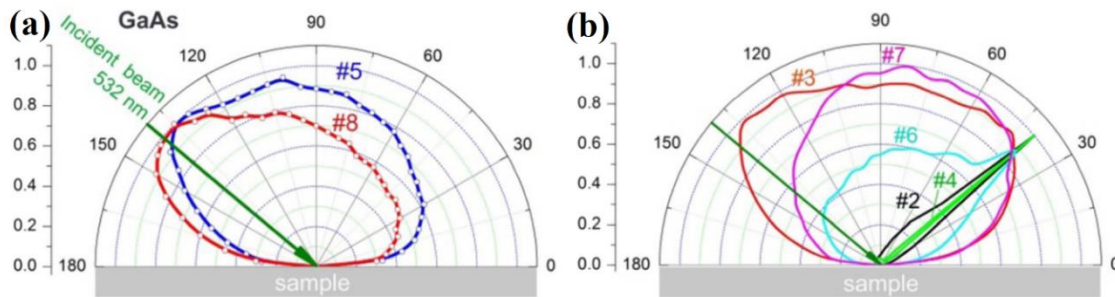


Figure 3.4. Polar diagrams of scattering intensity versus detection angle for seven porous GaAs samples. The direction of the incident beam is indicated by the green arrow (140°). Samples #5 and #8 show the highest retroreflection intensity. Samples #2 and #4 show diffuse reflectance due to scattering inhomogeneities due to low porosity, while the other samples show a combination of these two cases. Reproduced from [73]

From the comparison of the results of samples anodized in HCl [#2 (100 mA·cm⁻²), #3 (200 mA·cm⁻²), #4 (300 mA·cm⁻²) with #5 (600 mA·cm⁻²)] and in NHO₃ [#6 (100 mA·cm⁻²) with #8 (600 mA·cm⁻²)] it can be seen that, for each of the two sets of samples, anodization current of 600 mA·cm⁻² results in a pronounced enhancement of retroreflected (backscattered) light for samples #5 and #8. Scattering diagrams similar to those on sample #8 were recorded in four of eight porous InP samples previously examined [67,69].

In the paper [74], the angular dependence of the scattering intensity was studied in more detail for porous GaAs samples (#5 and #8) with retroreflection behavior. Polarization of the scattered light was considered as the critical parameter in evaluation of possible retroreflection mechanisms. In this regard, the dependence of the backscattered light intensity versus the angle between polarizer (incident beam) and analyzer (backscattered light) was measured. For the porous InP sample and the

GaAs sample no. #8, which showed the most pronounced retroreflection feature, the parallel arrangement of the polarizer and analyzer provides a backscattered light intensity several times higher than in the crossed one. It means that the backscattered light has a high degree of linear polarization, for GaAs being equal to 72% and for InP to 47% [74].

It is obvious that observation of high retroreflection of light and conservation of its linear polarization for strongly absorbing nanoporous systems based on the two different III–V semiconductor materials cannot be accidental. These properties are considered as a signature of the coherent backscattering phenomenon. Two modes of coherent scattering development are assumed. (i) The first path is the development from the shortest possible loop paths in the porous skeleton. In this case, one round-trip is sufficient. (ii) The second way is developing from the multiple scattering which becomes possible owing to emergence of longitudinal electromagnetic waves, so-called “dark modes” as was reported in the paper [71].

Subsequently, a mathematical model for calculation of the scattered radiation by a highly absorbing porous medium with dark modes was proposed [75]. The contribution of the scattered light from two areas with the same slope was taken into account. It was shown that the previously discovered anomalous retroreflection phenomenon can be observed only in the case when in the porous material the interface between the medium and the vacuum is maintained. Based on these calculations, a new technology for obtaining highly porous materials with the preservation of the interface between the medium and the vacuum was proposed, which involves the development of the technology to obtain ultra-porous materials with the preservation of the interface between the environment and the vacuum, for example the backside anodization of the sample. As a suitable technological alternative could serve the approach of fabrication of pores parallel to the surface with the involvement of photolithographic processes described in paragraph 2.1 and Ref. [28,46]. Accordingly, using this technology, the formation of the porous layer takes place under a thin layer on the surface with a thickness of 20 nm - 60 nm.

3.3 Bragg reflectors based on GaN multilayer structures

The porous GaN layers with alternating porosity, based on anodized HVPE grown GaN substrates elaborated in chapter 1.1, do not allow the fabrication of the multilayer porous structure in a totally controlled way. Controlled fabrication of multilayer porous structures can be achieved in MOCVD grown samples. Therefore, in the paper [76], technological conditions for MOCVD epitaxial grown GaN layers with charge carrier concentration from 10^{17} cm^{-3} (undoped) up to $5 \times 10^{19} \text{ cm}^{-3}$ in alternating layers were developed. In this study the results were obtained on two types of samples: the first sample marked as #1 consists of 5 layers of GaN with charge carrier concentration of $5 \times 10^{18} \text{ cm}^{-3}$ and 5 layers of undoped GaN; the second sample marked as #2 consists of 5 GaN layers with a charge carrier concentration of $1.2 \times 10^{19} \text{ cm}^{-3}$ and 5 layers with a charge carrier

concentration of $5 \times 10^{17} \text{ cm}^{-3}$. The multilayer structures were grown on an undoped GaN substrate. The thickness of the alternating high-conductivity/low-conductivity layers is 100 nm/50 nm, and the undoped GaN substrate is 2 μm thick. In order to identify the best technological conditions for the selective porosification of GaN structures, several electrolytes were investigated, such as 0.1 M KOH, 0.3 M oxalic acid and 0.3 M HNO_3 . The best results were obtained using oxalic acid electrolyte, where the doped layers are porosified during anodization, while the undoped layers, including the undoped substrate, remained intact (Figure 3.5a).

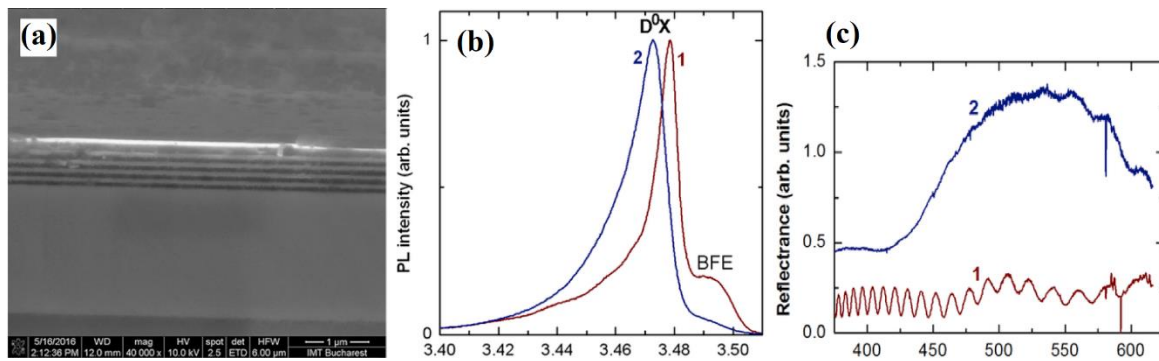


Figure 3.5. (a) Cross-sectional SEM image, (b) PL spectra measured at 10 K and (c) reflection spectra measured at 300 K of porous structure fabricated by electrochemical etching in 0.3 M oxalic acid electrolyte at the anodization applied voltage of 5 V on MOCVD grown GaN sample (#2) consisting of 5 GaN layers with carrier concentration of $1.2 \times 10^{19} \text{ cm}^{-3}$ and 5 GaN layers with carrier concentration of $5 \times 10^{17} \text{ cm}^{-3}$. In the spectra (curve 1) before and (curve 2) after anodization. Reproduced from [76]

The identified possibilities to control the morphology of porous layers by selecting the doping level and electrochemical etching are important for the design of various photonic structures based on porous multilayer GaN structures, for example Bragg reflectors.

The PL spectra of the sample #1 (lower carrier concentration) is totally dominated by the emission related to the recombination of excitons with a predominant contribution from recombination of neutral donor bound excitons D^0X in both the initial and etched samples, which is an indication of the preservation of the high quality of the GaN material after porosification. On the other hand, the position of the D^0X peak is shifted from 3.480 eV to 3.473 eV upon porosification, which is indicative of the relaxation of strains in the electrochemically etched sample. The same is true for the sample #2 with higher carrier concentration (Figure 3.5b) [76]. However, this sample contains an additional higher energy PL band at 3.493 eV which comes from the highly doped layers due to the Burstein shift and it is governed by the band filling effects. But, the intensity of this band is reduced in the electrochemically etched sample, due to the etching of the layers with higher carrier concentration.

The feasibility of the produced structures for the design of Bragg reflectors or other photonic elements has been demonstrated by micro-reflectivity measurements accompanied by transfer matrix analysis (Figure 3.5c) and simulations by a method developed for calculation of optical reflection spectra described in more detail in the paper [76].

3.4 Integrated lenses based on GaP-metal or ZnSe-metal nanostructures

Negative refractive index materials (NIMs) introduced by Veselago in 1968 [77], are artificial materials that exhibit amazing optical properties and offer the possibility for fabrication of "perfect lens" that can focus electromagnetic waves to a spot size much smaller than wavelength of electromagnetic radiation (called superlensing effect). It should be noted that Veselago's work did not arouse the interest of researchers for a relatively long period of time. Decades later, thanks to the development of nanotechnologies and small-sized materials, a great deal of interest and effort has been focused on lens simulations based on metamaterials with different configurations and compositions capable of operating especially in the visible region of the spectrum.

Sergentu and colleagues [78], proposed the assembly of NIMs from TiO₂ nanotubes with inner and outer surfaces coated with a thin metal layer. The high electrical resistance of TiO₂ nanotubes implies expensive and sophisticated deposition techniques for metallization, such as atomic layer deposition (ALD) which ensures uniform deposition along the entire depth of the nanotubes.

On the other hand, porous templates based on III-V and II-VI semiconductor compounds can be easily filled with metal nanotubes, nanowires or nanodots by pulsed electrochemical deposition due to the high electrical conductivity of the pore walls [26,46,79]. For the development of photonic lenses working in the visible region of the electromagnetic spectrum, materials possessing a wider bandgap should be used, for example GaP and ZnSe [80].

In order to investigate the photonic properties of materials assembled from porous templates with metallized pores, a simplified method was used which is based on the analysis of a parameter f describing the difference from the point of view of light scattering properties between the investigated material and a similar one with identical geometrical parameters but assembled from rods with the refractive index $n = -1$:

$$f = \max |D_m^{ni} - D_m|_{10 > m > -10} \quad (3.1)$$

where D_m^{ni} and D_m are the parameters determining the light scattering properties of the material assembled from rods with $n = -1$ and the investigated material, respectively; m is the index of the cylindrical function [78,81].

In the paper [79], the results of calculation demonstrated good focusing properties of planar photonic lenses assembled from Ag metallized porous GaP slabs, especially at long wavelengths, including the far infrared spectral range. The calculations were performed for templates with different pore diameters (250 nm and 500 nm) packed in a triangular lattice with the lattice parameter of 500

nm. The metallization with Ag was chosen because the plasmonic frequency is in the near UV spectral range. The simulation results demonstrated much better focusing properties for the lens based on the metallized GaP porous template with close packing of pores, i.e., for the pore diameter equal to the lattice parameter.

New focusing elements and beam splitters based on porous metallized ZnSe structures for applications in the visible region of the spectrum was demonstrated and reported [46]. It has been reported that the focusing properties of a planar photonic lens assembled from clusters of metallized ZnSe nanotubes with 40 nm inner diameter and 20 nm wall thickness with a design illustrated in Figure 3.6b are better than those of a fabricated planar lens of a porous ZnSe slab with regular pore arrangement of 40 nm diameter and 40 nm wall thickness in Figure 3.6a, both pores and nanotubes being metallized with a 6 nm thick Ag film.

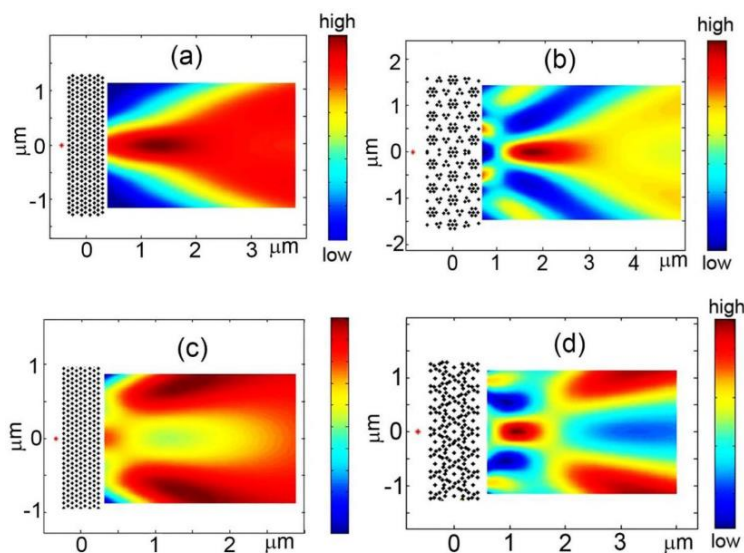


Figure 3.6. Electric field intensity maps of cross-sectional views of the 2D source–image system at the photon energy of 1.48 eV for a triangular lattice planar lens consisting of (a) metallized ZnSe pores with 40 nm pore diameter; (b) the slab assembled from clusters of metallized ZnSe nanotubes with 40 nm inner diameter. (c,d) Same as pore arrangement configurations and metallized ZnSe nanotubes in (a,b) but with the following parameters: photon energy of 1.45 eV and inner diameter of 22 nm. Reproduced from [26]

The photonic properties of porous structures and metallized nanotubes were found to be determined both by the arrangement of the nanopores or nanotubes, as well as by their geometrical dimensions and the used semiconductor material. By decreasing the pore diameter or inner diameter of the nanotubes by a factor of two, the function of the photonic slab can be changed from a focusing lens (Figure 3.6a,b) to a beam splitter (Figure 3.6c,d).

The obtained results were compared with the results of flat lenses based on TiO₂ nanotubes [80], demonstrating a similar focusing of porous ZnSe flat lens with the triangular arrangement of

pores, but the focus is at a larger distance from the lens, while the sample with clusters of titania nanotubes arranged in a superlattice demonstrates clear superlensing effect.

It should be mentioned that the shape of the pores in the elaborated semiconductor templates within the given theme can be adjusted from circular to triangular or square, using substrates with different crystallographic orientations, subjected to anodization in different electrolytes as reported in more details in recent work [28]. The high conductivity of the porous skeleton provides perfect conditions for a uniform metal deposition on the internal surface of porous template, regardless of the geometric shape of pores, the deposited metal nanotubes taking over the geometrical shape of pores, as demonstrated in the paper [79,82]. Moreover, in order to avoid the need for cleavage of porous layer, the technological method for the preparation of templates with pores oriented parallel to the upper surface of the substrate was developed, as described in chapter 2.1 and papers [26,46], with the possibility of engineering the morphology of pores from the point of view of their propagation direction [28].

3.5 Conclusions to chapter 3

The observed retroreflection phenomenon for light scattered by nanoporous GaAs and InP sample is realized in the case of high values of the absorption and refractive indices of material. The observed retroreflection can be taken into account in optical circuits based on InP and GaAs. Under certain conditions, retroreflection can be used in optoelectronic components to improve the efficiency of light extraction.

A pronounced linear polarization coinciding with that of the incident radiation was observed which is indicative of the coherent backscattering implying generation of longitudinal electromagnetic waves at interfaces. The angular scattering diagram is generally asymmetric which is explained by contribution from incoherent scattering from an anisotropic medium with losses at oblique incidence of radiation.

The possibilities to produce multilayer porous structures in both HVPE and MOCVD-grown GaN by means of electrochemical etching were demonstrated. While multilayer porous structure is obtained in HVPE-grown GaN due to uncontrolled self-modulation of doping during the crystal growth, multilayer porous structures with a controlled spatial design can be fabricated in MOCVD grown GaN.

The optimization of technological conditions of electrochemical etching in oxalic acid and KOH electrolytes allowed one to obtain good-quality multilayer porous structures suitable for applications in distributed Bragg reflectors. The feasibility of the produced structures for the design of Bragg reflectors or other photonic elements has been demonstrated by micro-reflectivity measurements accompanied by transfer matrix analysis and simulations by a method developed for calculation of optical reflection spectra.

The importance of hybrid structures based on semiconductor nanotemplates with metal nanotubes grown inside the pores for photonic applications was demonstrated by photonic property calculations. On the basis of GaP/Pt or ZnSe/Pt the prospects for the development of beam splitters and focusing elements with a clear superlensing effect have been demonstrated.

4. APPLICATIONS OF ELABORATED SEMICONDUCTOR NANOSTRUCTURES

4.1 Varicap device based on GaP-metal nanocomposites

In the work [79], the formation of a semiconductor-metal Schottky barrier junction with a huge internal contact area involving an enormous capacitance was reported, subsequently exploited in a variable capacitance device based on two-dimensional metal-semiconductor arrays, fabricated by pulsed electrochemical deposition of platinum on the pore walls inside the GaP template with parallel pores [82].

In the process of developing the variable capacitance device, two important aspects were taken into account, namely: (i) ensuring the high value of the Schottky barrier (about 1.1-1.3 eV for Pt-GaP) and (ii) the correct choice of the width of the walls of porous skeleton, to ensure the overlap of the two depletion regions in the walls of skeleton, starting from a certain applied potential. Therefore, the width of a pore wall cannot be less than two charge-depleted regions with no applied potential. The thickness of the porous GaP layer was 70 μm in the 500 μm thick substrate.

The Schottky contact was formed on the inner surface and subsequently on the top surface of the GaP pores by successive pulsed electrochemical deposition of Pt. Successive electrochemical deposition means that after the formation of Pt nanotubes on the internal surface of pores by applying pulses with duration of 100 μs and a pause between pulses of 1 s (region 2 in Figure 4.1a), the pause between pulses was reduced to 10 ms with the aim to not allow the penetration of metal ions inside the porous layer [66]. In this regime, the deposition at the interface of the porous layer and the electrolyte was ensured, thus interconnecting each Pt nanotube with a thin Pt film deposited on the surface (region 3 in Figure 4.1a). The ohmic contact on the back side of the sample was made by deposition of indium (region 4 in Figure 4.1a).

The measured current-voltage and capacitance-voltage characteristics of the elaborated device are presented in Figure 4.1b and Figure 4.1c, respectively. From the capacitance-voltage characteristic, it can be seen that the capacitance starts to decrease sharply from 12 to 2 nF under the applied negative potential in the range from 0.5 to 4 V, indicating that the device reaches a capacitance density variation of about $6 \times 10^{-3} \text{ pF} \cdot \text{V}^{-1}$ per $1 \mu\text{m}^2$ [79,80].

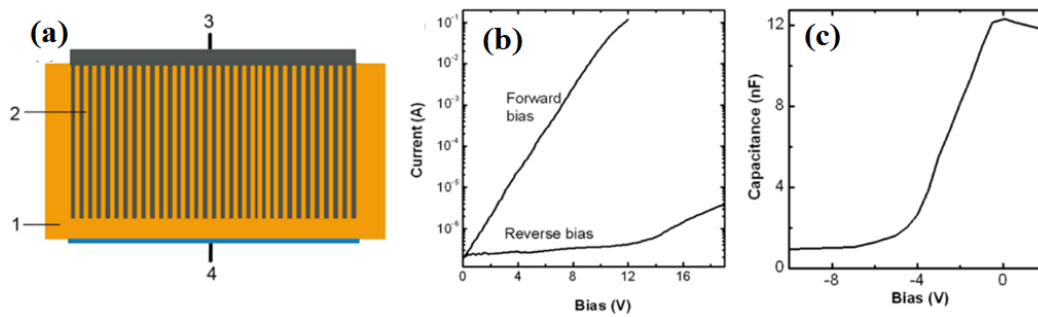


Figure 4.1. (a) Schematic representation of the device with variable capacity: 1 - GaP substrate; 2 – porous GaP template with Pt nanotubes; 3 – Pt Schottky contact deposited inside the pores and on the top surface of the template; 4 - ohmic contact. (b) Current-voltage characteristics. (c) Capacitance-voltage characteristic. Reproduced: (a) from [80], (b,c) from [79]

This value is much higher compared to other variable capacitance devices based on planar p - n junction or two-dimensional metal film deposited on the semiconductor surface. Recently, with the aim of further increase of the effective capacity, the technological approach of pulsed electrochemical deposition in porous GaP template with the depth of 300 μm [83] compared to 70 μm [79] has been proposed and optimized. Optimization of electrodeposition parameters demonstrated that uniform deposition of Pt nanotubes inside 300 μm long GaP pores occurs at 100 μs pulse duration and 3 s pause between pulses during the 15 hours.

4.2 Photodetectors, gas sensors based on InP and GaAs nanostructures

The porous semiconductor compounds from III-V group developed in this work, especially InP and GaAs have been shown to be attractive for optoelectronic applications as photodetectors [83,84], due to their much more advanced properties than Si. Apart from this, due to the large internal surface area, porous semiconductors are of interest for the development of gas sensors [85].

In the paper [85], porous InP membranes with controlled morphology have been fabricated by electrochemical etching of n -InP substrates in NaCl electrolyte, being subsequently functionalized with Au nanodots by electroplating in pulsed voltage regime. The photoluminescence and photoelectric characterization of the fabricated membranes demonstrated the preservation of the high crystalline quality of the porous template, the effective passivation of the porous surface, and light trapping inside the porous network. Exposure of the huge internal surface of the porous template to hydrogen environment leads to further passivation of the porous surface. It was also shown that the interaction of gas molecules with the porous surface is also influenced by Au nanodots deposited inside the pores, the Au dots possessing high catalytic activity during the interaction with H₂ and CO gases, thus enhancing the response and reduce the response time (5 s). It was established that these properties strongly depend on the morphology of deposited gold, which is controlled by the deposition time (10 min or 30 min) and the concentration of free charge carriers in the porous semiconductor

template, especially for $n=1 \times 10^{18} \text{ cm}^{-3}$. The improvement of the sensory properties upon deposition for 30 min is explained by interconnection of Au nanodots, forming Au nanotubes inside the InP pores according to the "hopping electrodeposition" mechanism [54].

The integration of semiconductor nanostructures into electronic and optoelectronic devices, become a challenge from the point of view of electrical contact elaboration. In the paper [84], the applicability of an ultra-thin InP nanowall (Figure 2.4c and Figure 2.7c), with lateral dimensions of several micrometers and thickness of 10 nm, as a photodetector in the IR region was demonstrated. In contrast to the case examined above, in which porous InP membranes were used, the contacts being made with the Ag paste, the InP nanowall was contacted by means of focused ion beam (FIB) using Pt as contact metal. From the photocurrent dependence in the dark and illumination at the applied voltage of 10 V under the excitation power of $800 \text{ mW} \cdot \text{cm}^{-2}$ the parameters of the photodetector based on the ultra-thin InP nanowall were calculated: the photoresponse $R=1.3 \text{ A} \cdot \text{W}^{-1}$ and detectivity $D=1.28 \cdot 10^{10} \text{ cm} \cdot \text{Hz}^{1/2} \cdot \text{W}^{-1}$.

Later, the applicability of GaAs nanowires developed in chapter 2.2 (Figure 2.3b) as a photodetector in the IR region of the spectrum was demonstrated [83]. Moreover, the feasibility of three methods for contacting the individual GaAs nanowire was studied.

The first one is fabrication using the FIB. In this case, the measured I-V characteristic of the elaborated photodetector demonstrated formation of Schottky contact due to the use of Pt, requiring an applied voltage with amplitude about 8 V for fabricated device. It is worth to mention that the fabrication of contacts with FIB it is very expensive while require a lot of work-hours in clean room and expensive equipment. The second approach is based on contacts fabrication via Laser Beam Lithography. Used equipment in this case is not so expensive. The possibilities to choose the deposited material in magnetron sputtering (e.g. Cr/Au) give the advantage to obtain ohmic contact resulting in linear dependence of photodetector, being possible to operate at a voltage of 5 V, reaching a photoresponse of $100 \text{ mA} \cdot \text{W}^{-1}$ and $D=1.2 \cdot 10^9 \text{ cm} \cdot \text{Hz}^{1/2} \cdot \text{W}^{-1}$. The investigation of the parameters as a function of the diameter of GaAs nanowires with an optimized contact design was studied in another PhD thesis [86], the results being published in the paper [48].

As another approach, representing a low-cost fabrication, could serve the deposition of nanowires on Si/SiO₂ chips with prefabricated contacts on the surface of the substrate. Despite the accessibility and the low cost of this method, it should be mentioned that the photodetector manufactured by this approach demonstrated a degradation over the time after 3 months. We assume that the cause is the formation of unstable contact, the nanowire is just placed on the contact and any mechanical action, electrical stress, and temperature gradient can affect the integrity of the contact between the nanowire and the contact pad. So, this method could be recommended just for rapid

investigation of electrical properties of fabricated nanowires with further deposition of contacts by Laser Beam Lithography or FIB [83].

4.3 GaAs-Fe and GaAs-NiFe core-shell nanowire arrays fabricated by electrochemical methods

In this paragraph, the systematic results of the deposition of Fe [49] and NiFe layers [87,88] with Ni contents of 65%, 80% and 100%, both on planar GaAs substrates and on nanowire arrays fabricated by anodization of n-GaAs substrates with (111)B and (001) crystallographic orientation will be discussed. The optimization of Ni deposition process in porous InP layers was also carried out [57].

Figure 4.2a shows hysteresis loops measured using a vibrating sample magnetometer (VSM) in an in-plane configuration on a nanowires array fabricated on GaAs (111)B substrate, the anodization procedure being described in more detail in chapter 2.2 and Ref. [49].

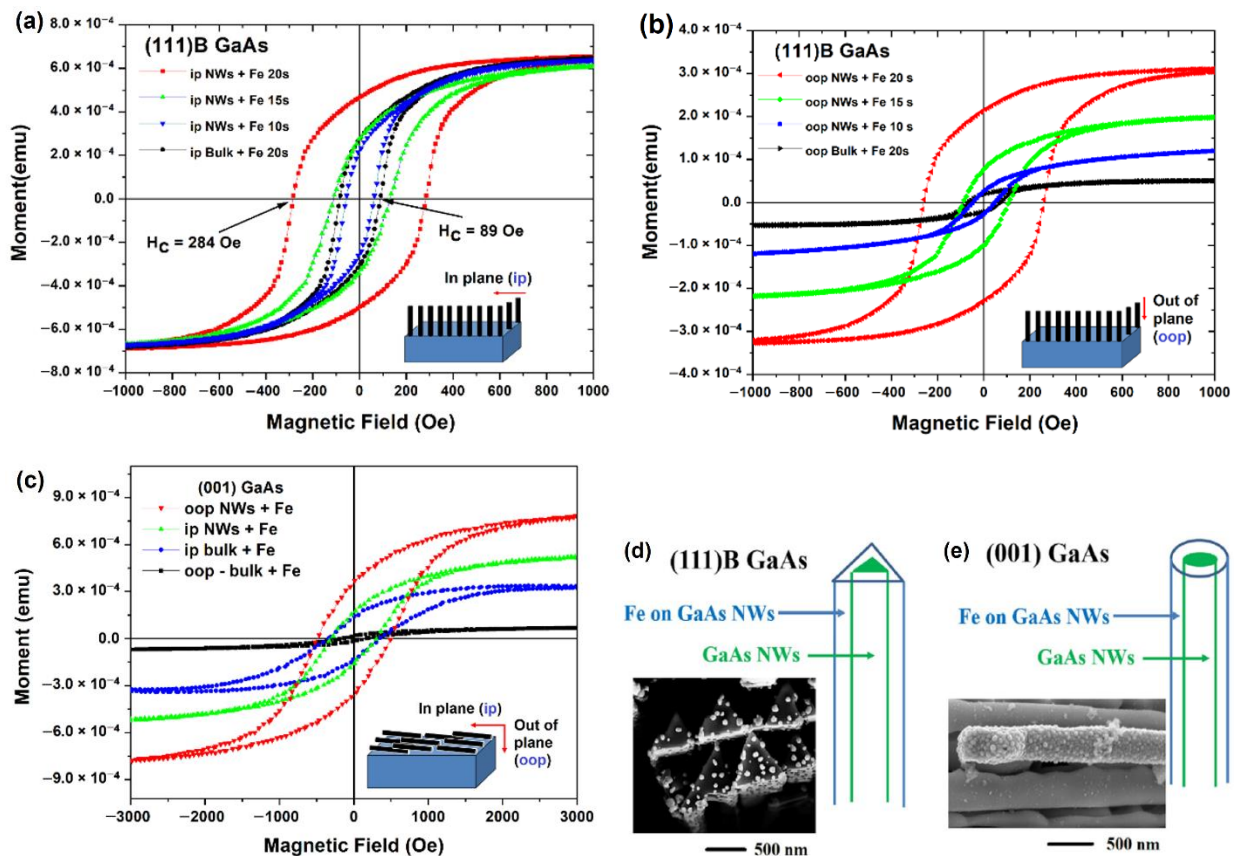


Figure 4.2. Hysteresis loops measured in "in-plane" (a,c) and "out-of-plane" (b,c) configurations on a nanowires array fabricated on GaAs (111)B substrates (a,b) and (001) in (c) compared with measured planar substrates coated with a Fe film. (d,e) Schematic representation and experimental demonstration of nanowires formation with different geometric shape and resulting metal coating. Reproduced: (a-c) from [49], (d,e) from [42]

In such a case, the magnetic field is applied perpendicular to the nanowire array. The hysteresis loops measured on the substrate covered by a polycrystalline Fe film are shown for comparison. One can see that the coercivity of nanowires after Fe deposition for 10 s is nearly the same as that of the substrate after Fe deposition for 20 s, and it increases from 62 to 284 Oe when increasing the Fe deposition time from 10 to 20 s. The remanence ratio $M_r/M_s = RR$ (squareness) also increases from 0.35 to 0.70 with the increase in the deposition time.

Similarly to the case of in-plane magnetization, for the out-of-plane magnetization, the coercivity of nanowires after Fe deposition for 10 s is nearly the same as that of the substrate after 20 s Fe deposition, and it increases from 46 to 260 Oe when increasing the Fe deposition time from 10 to 20 s (Figure 4.2b). The remanence ratio also increases from 0.22 to 0.68 with an increase in the deposition time.

For the nanowires array prepared on (001) GaAs, i.e., for those oriented parallel to the wafer surface, all of the magnetic parameters (the saturation moment, the coercivity, and the remanence) are higher in the out-of-plane configuration, i.e., when the magnetic field is perpendicular to the nanowire array, compared to the case of in-plane magnetization (Figure 4.2c). If one compares the magnetic characteristics of the nanowires array with those of the magnetic film on planar substrate, one can see that they do not differ significantly for the in-plane configuration, but the magnetic characteristics of the nanowires array are much higher than those of the film on the substrate for the out-of-plane configuration. In particular, the remanence ratio is two times higher, and the coercive force is three times higher [49].

In the paper [87], was performed a comparative analysis of the magnetic properties for in-plane configuration, in terms of saturation and remanence moment, squareness ratio and coercivity, for GaAs/Ni core-shell structures with different contents by Ni. Research has been focused on nanowires obtained by anodizing GaAs (111)B substrate because the nanowires have a triangular geometric shape compared to circular nanowires obtained by anodization of GaAs substrates with (001) orientation according to Figure 4.2d,e [42].

It was established that both the magnetic moment and the coercive force are much larger for nanowire arrays than for planar substrates with similar coating thicknesses (Figure 4.3a). The coatings of $Ni_{0.65}Fe_{0.35}$ alloys on GaAs nanowires (Figure 4.3b) are more sensitive to the deposition time as compared with permalloy coatings. However, the magnetic parameters have close values for coatings after 60 s deposition. The magnetic parameters (the magnetic moment and the coercive force) of Ni coatings on GaAs nanowire arrays are also not very much different from those of $Ni_{0.65}Fe_{0.35}$ coatings after the same deposition of 60 s (Figure 4.3c). However, the remanence ratio M_r/M_s (squareness) is lower for the Ni coating as compared to the $Ni_{0.65}Fe_{0.35}$ and permalloy coatings [87].

Systematized data of magnetic parameters for planar GaAs substrates and nanowires with metal coating are elucidated in tables from the paper [49] for GaAs-Fe, [87] for GaAs-NiFe with different Ni content, as well as for the comparative systematization of coatings of Fe and NiFe in the paper [88]. It was established that the magnetic parameters are better for NiFe and Fe coated nanowires as compared to coated planar structures. The coercivity is larger than 170 Oe for both magnetic field configurations on GaAs nanowires coated with NiFe for 60 s in the potentiostatic mode, while the remanence ratio is around 0.7 for both configurations. The same remanence ratio of around 0.7 is measured for both magnetic field configurations on GaAs nanowires prepared on (111)B GaAs substrates and coated with Fe for 20 s in the galvanostatic mode, while the coercivity is by a factor of around 3 larger than that measured on planar structures with the same coating. The largest value of coercivity (around 500 Oe) was reached on GaAs nanowires prepared on (001) GaAs substrates, when measured with out-of-plane magnetic field configuration, i.e. with the magnetic field perpendicular to the nanowires axis. However, the remanence ratio is around 0.5 for this case, which is less than 0.7 measured for NiFe and Fe coatings on nanowires prepared on (111)B GaAs substrates.

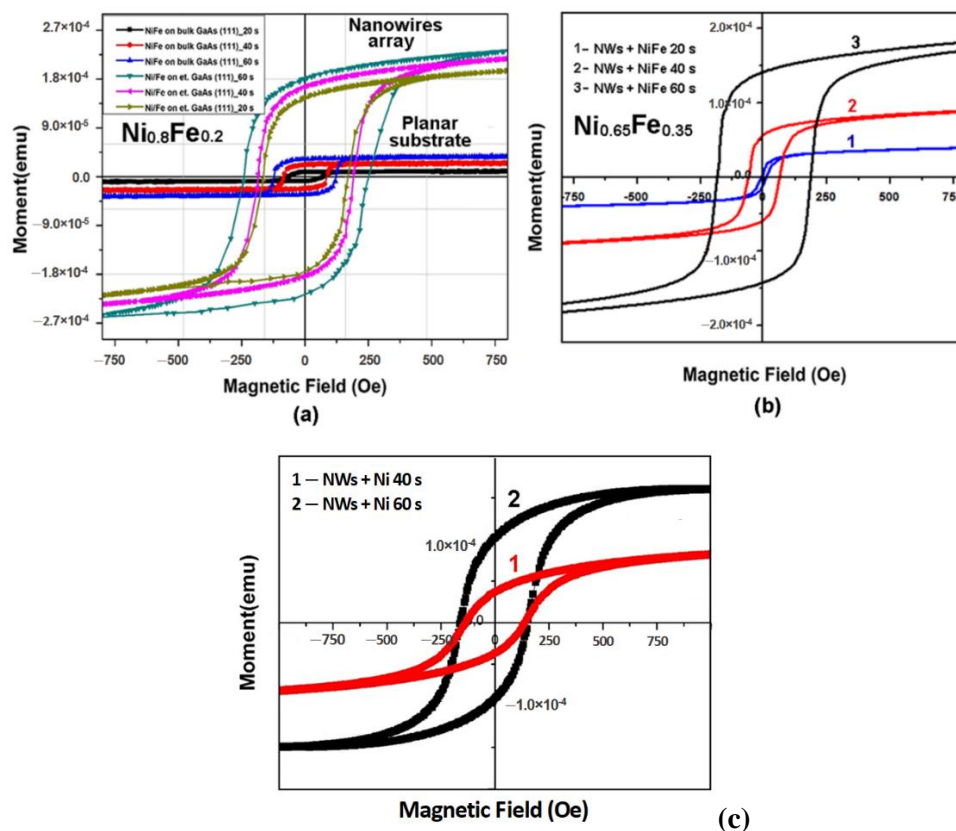


Figure 4.3. Hysteresis loops measured on GaAs (111)B substrates: (a) coated with permalloy (Ni_{0.80}Fe_{0.20}) planar substrates and anodized (nanowires) GaAs substrates; (b,c) GaAs nanowire arrays coated with Ni_{0.65}Fe_{0.35} (b) and Ni (c). Reproduced from [87]

In the paper [57], another possibility of depositing Ni nanodots inside porous InP templates was demonstrated. In this case, metal nanodots are deposited on the inner walls of the pores, the diameter of the pores being controlled in the range of 80 nm – 500 nm, and the thickness of the walls, i.e. the distance between the pores from 100 nm – 700 nm, by choosing InP semiconductor substrates with the free carrier concentration of $2 \times 10^{18} \text{ cm}^{-3}$ or $2 \times 10^{17} \text{ cm}^{-3}$. The given approach offers greater possibilities from the point of view of choosing the spatial distribution of metal nanodots, especially due to the approaches developed in chapter 2.1 that allow the fabrication of pores parallel to the surface [46] and controlling their growth direction [28].

4.4 Gold coated microstructures as a platform for the preparation of semiconductor-based hybrid 3D micro-nano-architectures

Recently, an improvement in the photocatalytic performances of a newly developed material, called *aero-Ga₂O₃*, due to functionalization with noble metals has been demonstrated [89]. In their study [89], the authors used an approach based on a template composed of a network of ZnO microtetrapods. The technological process consisted of four technological stages. In the first step, gold sputtering was performed on ZnO microtetrapods. In the second step, a GaN layer was deposited by HVPE over the Au-functionalized ZnO microtetrapods. During the HVPE growth of GaN, the simultaneous dissolution of ZnO occurred, which resulted in the formation of GaN microtubes, decorated with Au on the internal surface. In the third step, another functionalization with Au by sputtering was carried out, already on the external surface of the GaN microtubes. Finally, the GaN/Au microtubes were subjected to heat treatment in air to transform into *aero-Ga₂O₃/Au*. However, it should be noted that it is impossible to achieve uniform deposition by sputtering along the depth of the template. In addition, this technological process is quite complex.

Due to the fact that gallium oxide possesses high electrical resistivity, functionalization with noble metals by electrochemical deposition is challenging. Further, a feasible and cost-effective approach was demonstrated that allows uniform functionalization of Ga₂O₃ nanowire arrays with Au nanodots by electrochemical methods [66]. The technological flow of the process consists of two stages: (i) electrochemical deposition of Au nanodots ($U = -16 \text{ V}$, $t_{\text{on}} = 100 \text{ } \mu\text{s}$, $t_{\text{off}} = 1 \text{ s}$ for 300 s) on a semiconductor nanowires array produced by anodization of the *n*-GaAs (111)B substrates (as described in chapter 2.2, Figure 2.3b); (ii) followed by the oxidation of Au-functionalized semiconductor nanowires by heat treatment in air at 800 °C for one hour.

The deposition of Au nanodots on ZnO microtetrapod networks with controlled density both will result in hybrid structures that can be further used as catalyst nucleation points for the growth of semiconductor nanowires with needed composition. Considering that the preferential direction of nanowires growth is perpendicular to the used substrate, it is expected that their growth in radial directions of the tetrapod arms will result in the fabrication of more complex micro-nano-structure

assemblies with controlled design and morphology, for various applications. However, the ZnO tetrapods grown by the flame transport method are considered to possess high electrical resistance [90].

In recent paper [91], by applying pulsed electrochemical deposition at 50 μ s pulse length, it was experimentally demonstrated that ZnO tetrapods possess sufficient conductivity for uniform functionalization with Au nanodots. It was established that the density of the deposited Au nanodots is different for different microtetrapods in the same sample. The deposition of very rarely Au nanodots on microtetrapod 1 in Figure 4.4a indicates its high electrical resistivity, as previously observed [90,92,93], while the deposition of Au nanodots on microtetrapod 2 suggests moderate electrical conductivity. The image in Figure 4.4b demonstrates that the conductivity of ZnO microtetrapods can even reach a value high enough for the deposition of a monolayer of Au nanodots, as observed for microtetrapod 3. The image in Figure 4.4b demonstrates that the conductivity of ZnO microtetrapods can even reach a value high enough to deposit a monolayer of self-assembled Au nanodots, as observed for microtetrapod 3. These observations suggest that additional investigations are necessary to elaborate technological conditions enabling to produce ZnO microtetrapods networks with controlled electrical conductivity, which could be suitable for the production of complex micro-nano-structure assemblies with controlled design by means of VLS growth of semiconductor nanowires with various chemical composition on the surface of ZnO microtetrapods arms.

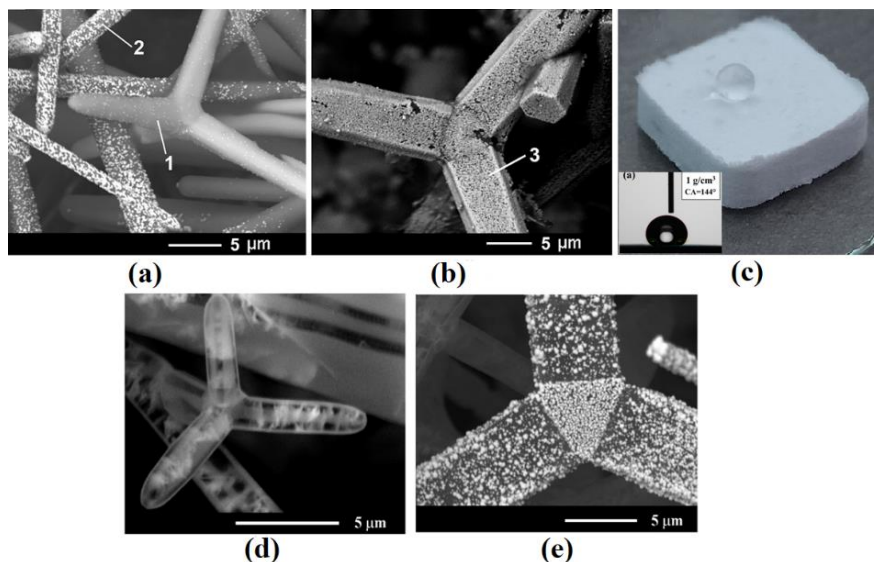


Figure 4.4. (a,b) SEM images of ZnO microtetrapods covered with Au nanodots taken on different regions of a pressed pellet from (c). (c) Photo image of a water droplet on the surface of ZnO tetrapods before heat treatment, indicating an CA=144°. SEM images of the hollow GaN tetrapod from aero-GaN sample before (d) and after pulsed electrochemical deposition (e). Electrodeposition parameters: $t_{on}=50 \mu$ s; $t_{off}=1$ s; $U= -15$ V, $t_{dep}=120$ s. Reproduced: (a,b) from [91], (c) from [94], (d,e) from [62]

It should be noted that the pressed ZnO pellets with a density of $1 \text{ g}\cdot\text{cm}^{-3}$ demonstrated hydrophobic properties (Figure 4.4c), being unsuitable for electrochemical deposition that involves the penetration of the electrolyte inside the ultra-porous 3D architecture. In recent work [94], the possibility of controlling the hydrophobic/hydrophilic properties of ZnO microtetrapod networks by means of thermal treatment (TT) was demonstrated. ZnO microtetrapod networks produced by flame transport synthesis were found to be hydrophobic but became super-hydrophilic upon annealing at $950 \text{ }^\circ\text{C}$ for 1 h in air. From the beginning, TT was only intended to ensure the welding of the arms of ZnO microtetrapods after pressing into pellets, providing higher mechanical stability.

Functionalization with Au nanodots by electrodeposition has also been shown to be feasible on ultra-porous 3D nanoarchitectures composed of micro-nano-tetrapods of aero-GaN [62]. The SEM image of a hollow GaN microtetrapod, extracted from aero-GaN material, is presented in Figure 4.4d. Pulsed electrodeposition of Au on such a microtetrapod with a pulse length of $50 \mu\text{s}$ resulted in its coating with Au nanodots, as shown in Figure 4.4e. In this work, pulsed electrodeposition was used to estimate the electrical conductivity (proposed and demonstrated approach in chapter 2.4) of aero-GaN microtetrapods, a higher density of Au nanodots being observed, specifically in the region where the arms of the microtetrapods intersect, which indicates a higher electrical conductivity of this region compared to the conductivity of the microtetrapod arms.

Table 4.1. Systematized results of porous III-V and II-VI semiconductor compounds with engineered morphology elaborated in this work by electrochemical methods [42]

Semiconductor compound	E_g , (eV)	Concentration of charge carriers, (cm^{-3})	Pore diameter, required applied voltage, other details.	Typical electrolyte	Ref.
GaAs	1.42	2×10^{18} (111)B, (111) and (001)	100 - 400 nm triangular shape nanowires oriented perpendicular, tilted or parallel to the substrate surface, 4 V.	HNO_3	[48,49]
InP	1.34	$1,3 \times 10^{18}$	Pores parallel to the substrate surface	NaCl	[46]
		$1,3 \times 10^{18}$	Morphologies by design with photolithographic processes.	NaCl	[28,42]
		$1,7\text{-}3 \times 10^{18}$	100-150 nm; 3D porous structures at 100 – 350 mA cm^{-2} , or successive applied potential of 2 V- 4 V - 6 V.	NaCl, HCl	[28,42]
		$1,3 \times 10^{18}$	Nanowires - 50 nm; 10 nm thick nanowalls; nanobelts with thickness about several nm at 15 V for 3 seconds.	HCl	[52]
		2×10^{17}	Self-ordered porous layers with 200 nm pore diameter at 20 V.	NaCl	[57]
GaP	2.26	$2\text{-}8 \times 10^{17}$	Pores with circular shape and 300-500 nm diameter, 25 V.	H_2SO_4	[79]
		$2\text{-}8 \times 10^{17}$ (100)	Pores with rectangular shape and 100 nm diameter, 15 V.	HBr	[28]
		3×10^{17} (111)	Pores with triangular shape and 100 nm diameter, 15 V.	HBr	[28]

GaN	3.4	MOCVD 2.5×10^{18}	Multilayer porous structures, 50-100 nm, 15 – 25 V	HNO ₃	[17]
		HVPE	Porous concentric pyramidal structures, < 50 nm, 25 V.	HNO ₃	[15]
		HVPE > 5×10^{17}	Uniform pores, 50 nm at 70 V on Ga-face; 10 nm at 15 V on N-face.	HNO ₃ , HCl, NaCl	[18]
		HVPE > 5×10^{17}	Multilayer porous structures, 25 V.	HNO ₃	[76]
ZnSe	2.7	3.0×10^{17} 2.1×10^{18}	Pores, 100 nm at 9 V; pores, 40 nm at 6 V.	K ₂ Cr ₂ O ₇ :H ₂ SO ₄ :H ₂ O	[28]
ZnTe	2.3	3×10^{18}	<i>p</i> -type, nanowires, 50 nm, applied voltage in pulse, 5 V.	HNO ₃ :HCl: H ₂ O	[50]
ZnO	3.37	3×10^{18}	Pyramids on the O-face, 1–5 μm at 5 V; or 10–50 μm at 10 V, inverted pyramids or tunnels on Zn-face.	HCl	[27,28]
		3×10^{18}	Columnar morphology on O-face.	HNO ₃	[28]
ZnCdS	2.9 3.0 3.3	2×10^{18}	30 nm–120 nm; wide bandgap template Zn _{0.4} Cd _{0.6} S – 16 V; Zn _{0.5} Cd _{0.5} S – 40 V; Zn _{0.67} Cd _{0.33} S – 70 V.	HCl, HNO ₃	[22,24, 25]

4.5 Conclusions to chapter 4

Fabrication of two-dimensional metal-semiconductor arrays with Pt nanotubes in porous GaP template has been shown to be feasible for the development of variable capacitance devices with improved capacitance density variation up to 6×10^{-3} pF·V⁻¹ per square micrometer under a small change in voltage (up to – 4 V).

The developed nanostructures based on ultrathin InP nanowall or GaAs nanowire were used for elaboration of IR photodetectors that demonstrated a photoresponse $R=1.3$ A·W⁻¹ and detectivity $D=1.28 \cdot 10^{10}$ cm·Hz^{1/2}·W⁻¹ or, respectively, $R=100$ mA·W⁻¹ and $D=1.2 \cdot 10^9$ cm·Hz^{1/2}·W⁻¹ at the optical excitation power of 800 mW·cm⁻².

GaAs-Fe or GaAs-NiFe core-shell nanowire arrays together with the possibility of aligning the nanowires perpendicular or parallel to the substrate surface demonstrated magnetic anisotropy of coercivity and remanence ratio.

A two-step technological approach for Ga₂O₃ nanowire arrays functionalization with Au nanodots by pulsed electrochemical deposition has been proposed and demonstrated, with the high electrical resistance of the nanowire arrays being one of the critical factors in this process. The first technological step consists in the deposition of Au nanodots on GaAs nanowires, and the second step involves thermal treatment, during which the oxidation of GaAs nanowires takes place. Thus, additional technological steps of sensitization and activation of the gallium oxide surface were avoided, which could lead to contamination and the formation of unwanted residues.

GENERAL CONCLUSIONS AND RECOMMENDATIONS

1. Semiconductor templates based on wide bandgap materials, promising for applications in the visible range of the spectrum, have been fabricated by electrochemical etching of GaN (HVPE) or ZnCdS crystals possessing a deepness of porous layer of 70 μm , in contrast to 2 – 4 μm for MOCVD grown GaN layers. It has been demonstrated the obtaining by electrochemical etching of multilayer porous structures based on GaN grown by the HVPE method, due to the uncontrolled self-modulation of doping during the growth of the substrates. On the other hand, the fabrication of multilayer porous structures with a controlled spatial design was achieved by anodization of MOCVD grown GaN, with two different electrical conductivities of layers. The feasibility of the produced structures for the design of Bragg reflectors was demonstrated by optical micro-reflection measurements. By anodization of ZnO crystals, the selectivity of ZnO micro-nano-structures obtaining with different shapes was demonstrated. Pyramidal microstructures were obtained on the O face, and inverted pyramids were produced on the Zn face. It was shown that the dimensions of microstructures can be controlled by varying the applied potential during anodization, thus demonstrating a strong influence on the photoluminescence spectra of the obtained microstructures. It was found that the photoluminescence spectra recorded on the region with morphology in the form of small pyramids (obtained at 5 V) is dominated by emission with the photon energy of 3.3 eV, close to the value of the band gap, the green emission at 2.56 eV being attenuated compared to the emission from large pyramids (10 V), which show relatively intense green luminescence. The possibility of control with the morphology obtained by using different electrolytes in the anodization process was demonstrated, and columnar morphologies were produced for the first time by electrochemical methods in HNO_3 electrolyte. The results were discussed in paragraphs 1.1; 1.2; 1.3; 1.4; 3.3 and were published in papers [12,15–18,22–28,34,76].
2. The successful combination of electrochemical etching and pulsed electrodeposition led to the solution of an important technological problem, namely, the possibility of non-lithographic fabrication of two-dimensional periodic metal-dielectric structures for micro-opto-electronic and photonic applications, an important precondition for this achievement being the development of the so-called "hopping electrodeposition" mechanism of Au nanodots, described in paragraph 2.3 [54]. The prospect of developing new focusing elements and beam splitters based on GaP/Pt or ZnSe/Pt nanostructures, for applications in the visible region of the spectrum, was demonstrated. The photonic properties of porous structures metallized with nanotubes were found to be determined by both the spatial distribution of the nanopores or nanotubes and their geometrical dimensions, as well as the composition of the semiconductor material used. By decreasing the pore diameter or inner diameter of the nanotubes by a factor of two, the purpose of the photonic

slab can be changed from a focusing lens to a beam splitter. Another important compartment of semiconductor compound engineering for nano-micro-electronics was demonstrated by the development of varicap device based on GaP/Pt nanostructures with a record capacitance density variation of $6 \times 10^{-3} \text{ pF} \cdot \text{V}^{-1}$ per $1 \text{ } \mu\text{m}^2$ of surface area. The results were discussed in paragraphs 2.3; 3.4 and 4.1 and were published in papers [26,46,54,59,60,79,80,82,83].

3. In premiere, the "abnormal" retroreflection of light from ultra-porous layers based on InP and GaAs semiconductor compounds was demonstrated. As a result, the following regularities were established: (i) Only ordinary transverse waves ("bright modes") and their associated backscattered radiation can be excited with an incident *s*-polarized wave. Absorption strongly modifies the scattering indicatrix, suppressing scattered radiation at small incidence/scattering angles. (ii) Ultrashort modes ("dark modes") and ordinary transverse waves ("bright modes"), as well as their associated backscattered radiation, can be excited with an incident *p*-polarized wave. The contribution from "dark modes", which is practically independent of absorption, is predominant at high incidence/scattering angles. The results were discussed in paragraphs 3.1; 3.2 and were published in papers [67,69,71-74].
4. Using the developed "hopping electrodeposition" model, a cost-effective and original approach for assessing the electrical conductivity in InP semiconductor nanostructures with different thicknesses, such as those fabricated by electrochemical etching of *n*-InP crystals with free carrier concentration of $1.3 \times 10^{18} \text{ cm}^{-3}$, discussed in paragraph 2.4, was proposed. This statement is confirmed by the results of Au nanodots electrodeposition concomitantly on 10 nm thick nanowall nanostructures, nanowires with 50 nm diameter and 2 nm thick InP nanobelts, as well as on bulk *n*-InP substrate. Comparison of the electrodeposition of 20 nm diameter Au nanodots on InP nanowires and on bulk InP suggests that the electrical conductivity of nanowires is similar to that of bulk crystals. At the same time, the comparison of the electrochemical coating of Au nanodots on nanowires and nanowalls indicates a much lower conductivity of nanowalls compared to that of nanowires, and the absence of deposition of Au nanodots on InP nanobelts demonstrates that there are no free charge carriers in nanobelts with a thickness of several nanometers. The given approach has also been shown to be effective for highlighting non-uniform doping during HVPE growth in GaN substrates. Complementarily, non-uniform doping was also demonstrated by electrochemical etching of GaN (HVPE) substrates. The developed "hopping electrodeposition" model was used for Au nanodot functionalization of promising ZnO or aero-GaN micro- and nano-structures as platforms for the fabrication of 3D hybrid micro-nano-architectures. The results were discussed in paragraphs 2.3; 2.4 and 4.4 and were published in papers [53,54,61,62,66,91,94].

5. It has been shown that combining possibilities to produce two types of pores (CLO and CO) with generating porous arrays by design significantly enlarges the variety of produced porous morphologies and topologies. As a result, possibilities to control the physical properties of semiconductor porous structures, such as optical, vibrational, photonic and luminescence properties, are widened, therefore opening new prospects for practical applications. The systematized results demonstrated that rectangular, triangular, and circular shape of pores, as well as nanowires with controlled sizes can be produced by adjusting the crystallographic orientation of the substrate and the technological conditions of anodization (paragraph 2.2). The optimization of technological parameters of anodization allowed the fabrication of semiconductor nanowire arrays by electrochemical etching of InP, GaAs and ZnTe semiconductor crystals. The use of GaAs crystals with different crystallographic orientation allowed to obtain nanowire arrays tilted (100), perpendicular (111)B and predominantly parallel (001) to the substrate surface by electrochemical etching at applied voltage 4 V in nitric acid with a concentration of 1M for 30 min. The feasibility of applying the developed nanostructures as photodetectors in IR region was demonstrated based on an ultra-thin (10 nm) InP nanowall, which demonstrated a photoresponse $R=1.3 \text{ A}\cdot\text{W}^{-1}$ and detectivity $D=1.28\times 10^{10} \text{ cm}\cdot\text{Hz}^{1/2}\cdot\text{W}^{-1}$, as well as GaAs photodetector (single nanowire) with values $R=100 \text{ mA}\cdot\text{W}^{-1}$ and $D=1.2\times 10^9 \text{ cm}\cdot\text{Hz}^{1/2}\cdot\text{W}^{-1}$ at optical excitation power $P_{\text{exc}}=800 \text{ mW}\cdot\text{cm}^{-2}$. The results were discussed in paragraphs 2.2; 4.2 and were published in papers [12,28,42,49,50,52,83,84].
6. An important compartment of semiconductor compound engineering has been demonstrated which consists in the development of electrochemical technological approaches to control the direction of pore propagation both in depth, being produced 3D structures as a result of the transition from CLO to CO pores, or due to non-uniform doping in GaN HVPE grown substrates, as well as parallel to the surface of InP or ZnSe crystals by applying photolithographic masks. Using the properties of CLO pores to not intersect during growth, combined with the formation of pore networks propagating in planes parallel to substrate surface, were obtained morphologies by-design determined by the shape of photolithographic mask used, which open new perspectives for microfluidic applications (paragraph 2.1). An additional tool for such applications is the possibility to control the hydrophilic or hydrophobic properties of the produced structures, discussed in paragraph 2.5. It has been demonstrated by contact angle analysis that the engineering of semiconductor surfaces by electrochemical methods (etching and/or electrochemical deposition) allows the controlled change of hydrophilic/hydrophobic properties. It was demonstrated that the morphology of GaAs pores, tilted or perpendicular to the surface, plays an important role in the transition from hydrophobic to hydrophilic properties, demonstrating contact angles of 137.5° and 37.5° respectively. Even greater flexibility of contact

angle control was demonstrated by functionalization of porous layer with a monolayer of Au nanodots. The results were discussed in paragraphs 2.1; 2.5 and were published in papers [28,37,42,46,65].

7. It has been demonstrated that the elaborated "hopping electrodeposition" mechanism provides an efficient platform for functionalization and modification of nanostructured surfaces, which enables precise control over the process parameters. It has been shown that using pulses can avoid some of the adverse effects associated with continuous deposition, such as formation of nonuniform layers, diffusion-limited phenomena, and supersaturation. It has been demonstrated the possibility of gold nanodots deposition with controlled density on various nano-micro-structured semiconductor substrates such as: (i) hollow GaN microtetrapods arrays from aero-GaN, (ii) porous microdomains with a controlled design produced by anodization of InP substrates and (iii) complex microdomains composed of strips with alternating electrical conduction based on HVPE grown GaN substrates. The self-assembled gold nanodots can serve as catalyst nucleation sites for growth of nanowires with different chemical compositions to form complex 3D hybrid micro-nano-architectures, promising for photocatalytic applications. The results were discussed in paragraphs 2.3; 4.4 and were published in papers [54,62,66,90,91,94].
8. It was demonstrated the possibility of core-shell nanowires networks fabrication based on GaAs-Fe or GaAs-NiFe, with the possibility of aligning perpendicularly or parallel to the substrate surface, which revealed a magnetic anisotropy of coercivity and remanence ratio. The magnetic parameters for both Fe and NiFe coatings were found to be more advantageous for coaxial core-shell structures compared to planar structures. At the same time, these parameters are higher for the configuration with the magnetic field oriented in the radial direction of the coaxial core-shell structures compared to the orientation along the axis of the nanowires. It was determined that by controlling the deposition duration, resulting in a larger thickness of the Fe coating on GaAs nanowire arrays, is assured an increase in coercivity and remanence ratio from 62 to 284 Oe and from 0.35 to 0.70 respectively. Controlling with geometrical shape of pores or semiconductor nanowires, which are used as templates for the deposition of metals with magnetic properties by means of the "hopping electrodeposition" mechanism, allows obtaining hybrid core-shell structures with triangular, square or round geometries, by forming a thin metal layer inside the pores or around the nanowires. The results were discussed in paragraphs 2.2; 4.3 and were published in papers [28,42,49,57,63,87,88].

The results of synthesis work are obtained after the defense of the PhD thesis in 2009, but they are compared with the results on the subject from the last 30 years. As a result of analysis carried out and obtained conclusions, the following **recommendations** are proposed:

1. It remains to be understood why no CO pores are generated in II-VI semiconductor compounds and solid solutions, possessing the same sphalerite crystal structure as III-V semiconductor compounds. In fact, this problem was analyzed only from the consideration of the percentage value of the degree of ionicity in the chemical bonds. The reason why CLO pores do not grow in GaAs crystals should also be elucidated.
2. Despite the fact that FL mask-assisted electrochemical etching is a cost-effective and versatile tool for the preparation of porous structures with specific morphologies, its exploration is still in the primary phase. The results obtained in paragraph 2.1 demonstrated that the design of the porous morphology depends on several factors, namely: from how many and which edge of the FL mask is anodized; size and location of open holes in FL mask, etc. It is proposed to develop a mathematical model for simulation with visualization of anodization results through FL mask with a special design, which, reaching a desired morphology as a result of the simulation, can be repeated experimentally. The following laws and parameters can be recommended as boundary conditions for the simulation: (i) pores can be formed in the space under the specially designed FL mask; (ii) in CLO pore formation regime, which assumes that the pores cannot intersect each other; (iii) once the thickness of 60 nm is reached, the pores change their propagation direction in the free (non-etched) semiconductor space but in the same plane (these concrete values depend on the conductivity of the material). In the case of the meeting of two neighboring pores tip-to-tip, they will stop growing, leaving a space of 60 nm between them. (iv) the growth rate for all pores is constant, regardless of the number of edges of the FL mask.
3. Since electrochemical etching is carried out by breaking the chemical bonds between atoms due to the extraction of electrons, it is recommended to carry out the anodization process by combining it with surface charge lithography, which involves the additional introduction of negative charges on the surface that stop the material dissolution process, being previously demonstrated on MOCVD grown GaN substrates. Thus, supplying the surface with excess free charges in a controlled manner will allow to expand the possibility of engineering porous semiconductor compounds.

REFERENCES

1. LEHMANN, V., FÖLL, H. Formation Mechanism and Properties of Electrochemically Etched Trenches in N-type Silicon. In: *J. Electrochem. Soc.* 1990, Vol. 137, p. 653, doi:10.1149/1.2086525.
2. MASUDA, H., FUKUDA, K. Ordered Metal Nanohole Arrays Made by a Two-Step Replication of Honeycomb Structures of Anodic Alumina. In: *Science* 1995, Vol. 268, p. 1466–1468, doi:10.1126/science.268.5216.1466.
3. MACAK, J.M., ALBU, S.P., SCHMUKI, P. Towards Ideal Hexagonal Self-Ordering of TiO₂ Nanotubes. In: *physica status solidi (RRL) – Rapid Research Letters* 2007, Vol. 1, p. 181–183, doi:10.1002/pssr.200701148.

4. CHRISTOPHERSEN, M., LANGA, S., CARSTENSEN, J., TIGINYANU, I.M., FÖLL, H. A Comparison of Pores in Silicon and Pores in III–V Compound Materials. În: *physica status solidi (a)* 2003, Vol. 197, p. 197–203, doi:10.1002/pssa.200306499.
5. FÖLL, H., LEISNER, M., COJOCARU, A., CARSTENSEN, J. Self-Organization Phenomena at Semiconductor Electrodes. În: *Electrochimica Acta* 2009, Vol. 55, p. 327–339, doi:10.1016/j.electacta.2009.03.076.
6. FÖLL, H., LANGA, S., CARSTENSEN, J., CHRISTOPHERSEN, M., TIGINYANU, I. m. Pores in III–V Semiconductors. În: *Advanced Materials* 2003, Vol. 15, p. 183–198, doi:10.1002/adma.200390043.
7. FÖLL, H., CARSTENSEN, J., LANGA, S., CHRISTOPHERSEN, M., TIGINYANU, I.M. Porous III–V Compound Semiconductors: Formation, Properties, and Comparison to Silicon. În: *physica status solidi (a)* 2003, Vol. 197, p. 61–70, doi:10.1002/pssa.200306469.
8. LANGA, S., TIGINYANU, I.M., CARSTENSEN, J., CHRISTOPHERSEN, M., FÖLL, H. Self-Organized Growth of Single Crystals of Nanopores. În: *Appl. Phys. Lett.* 2003, Vol. 82, p. 278–280, doi:10.1063/1.1537868.
9. LANGA, S., CARSTENSEN, J., TIGINYANU, I.M., CHRISTOPHERSEN, M., FÖLL, H. Formation of Tetrahedron-like Pores during Anodic Etching of (100) Oriented n-GaAs. În: *Electrochem. Solid-State Lett.* 2002, Vol. 5, p. C14, doi:10.1149/1.1423803.
10. WLOKA, J., MUELLER, K., SCHMUKI, P. Pore Morphology and Self-Organization Effects during Etching of n-Type GaP(100) in Bromide Solutions. În: *Electrochem. Solid-State Lett.* 2005, Vol. 8, p. B72, doi:10.1149/1.2103507.
11. MÜLLER, K., WLOKA, J., SCHMUKI, P. Novel Pore Shape and Self-Organization Effects in n-GaP(111). În: *J Solid State Electrochem* 2009, Vol. 13, p. 807–812, doi:10.1007/s10008-008-0771-4.
12. MONAICO, E.V. *Micro- and Nano-Engineering of III-V and II-VI Semiconductor Compounds and Metal Nanostructures Based on Electrochemical Technologies for Multifunctional Applications*; Bons Offices: Chisinau, Moldova, 2022; ISBN 978-9975-166-63-8.
13. BOCKOWSKI, M., IWINSKA, M., AMILUSIK, M., FIJALKOWSKI, M., LUCZNIK, B., SOCHACKI, T. Challenges and Future Perspectives in HVPE-GaN Growth on Ammonothermal GaN Seeds. În: *Semicond. Sci. Technol.* 2016, Vol. 31, p. 093002, doi:10.1088/0268-1242/31/9/093002.
14. SUIHKONEN, S., PIMPUTKAR, S., SINTONEN, S., TUOMISTO, F. Defects in Single Crystalline Ammonothermal Gallium Nitride. În: *Advanced Electronic Materials* 2017, Vol. 3, p. 1600496, doi:10.1002/aelm.201600496.
15. TIGINYANU, I., STEVENS-KALCEFF, M.A., SARUA, A., BRANISTE, T., MONAICO, E., POPA, V., ANDRADE, H.D., THOMAS, J.O., RAEVSCHI, S., SCHULTE, K., ADELUNG, R. Self-Organized Three-Dimensional Nanostructured Architectures in Bulk GaN Generated by Spatial Modulation of Doping. În: *ECS J. Solid State Sci. Technol.* 2016, Vol. 5, p. P218, doi:10.1149/2.0091605jss.
16. WOLFF, N., JORDT, P., BRANISTE, T., POPA, V., MONAICO, E., URSAKI, V., PETRARU, A., ADELUNG, R., MURPHY, B.M., KIENLE, L., TIGINYANU, I. Modulation of Electrical Conductivity and Lattice Distortions in Bulk HVPE-Grown GaN. În: *ECS J. Solid State Sci. Technol.* 2019, Vol. 8, p. Q141, doi:10.1149/2.0041908jss.
17. BRANISTE, T., MONAICO, E., MARTIN, D., CARLIN, J.-F., POPA, V., URSAKI, V.V., GRANDJEAN, N., TIGINYANU, I.M. Multilayer Porous Structures on GaN for the Fabrication of Bragg Reflectors. In Proceedings of the Nanotechnology VIII; SPIE, May 30 2017; Vol. 10248, pp. 83–89.
18. MONAICO, E., MOISE, C., MIHAI, G., URSAKI, V.V., LEISTNER, K., TIGINYANU, I.M., ENACHESCU, M., NIELSCH, K. Towards Uniform Electrochemical Porosification of Bulk HVPE-Grown GaN. În: *J. Electrochem. Soc.* 2019, Vol. 166, p. H3159, doi:10.1149/2.0251905jes.

19. HANDLER, P. Properties of Compounds: Physics and Chemistry of II-VI Compounds. M. Aven and J. S. Prener, Eds. North-Holland, Amsterdam; Interscience (Wiley), New York, 1967. 862 Pp., Illus. \$30. În: *Science* 1968, Vol. 159, p. 185–185, doi:10.1126/science.159.3811.185.
20. AVEN, M., MEAD, C.A. ELECTRICAL TRANSPORT AND CONTACT PROPERTIES OF LOW RESISTIVITY n-TYPE ZINC SULFIDE CRYSTALS. În: *Appl. Phys. Lett.* 1965, Vol. 7, p. 8–10, doi:10.1063/1.1754243.
21. COLIBABA, G., GONCEARENCO, E., NEDEOGLO, D., NEDEOGLO, N.D. Growth of ZnO Crystals by CVT Methods. În: *Mold. J. Phys. Sci.* 2012, Vol. 11, p. 366–370.
22. COLIBABA, G.V., MONAICO, E.V., GONCEARENCO, E.P., NEDEOGLO, D.D., TIGINYANU, I.M., NIELSCH, K. Growth of ZnCdS Single Crystals and Prospects of Their Application as Nanoporous Structures. În: *Semicond. Sci. Technol.* 2014, Vol. 29, p. 125003, doi:10.1088/0268-1242/29/12/125003.
23. MONAICO, E., COLIBABA, G., NEDEOGLO, D., NIELSCH, K. Porosification of III–V and II–VI Semiconductor Compounds. În: *Journal of Nanoelectronics and Optoelectronics* 2014, Vol. 9, p. 307–311, doi:10.1166/jno.2014.1581.
24. COLIBABA, G., GONCEARENCO, E., NEDEOGLO, D., NEDEOGLO, N., MONAICO, E., TIGINYANU, I. Obtaining of II-VI Compound Substrates with Controlled Electrical Parameters and Prospects of Their Application for Nanoporous Structures. În: *physica status solidi c* 2014, Vol. 11, p. 1404–1407, doi:10.1002/pssc.201300590.
25. COLIBABA, G.V., MONAICO, E.V., GONCEARENCO, E.P., INCULET, I., TIGINYANU, I.M. Features of Nanotemplates Manufacturing on the II-VI Compound Substrates. In Proceedings of the 3rd International Conference on Nanotechnologies and Biomedical Engineering; Sontea, V., Tiginyanu, I., Eds.; Springer: Singapore, 2016; pp. 188–191.
26. MONAICO, E., TIGINYANU, I., URSAKI, V. Porous Semiconductor Compounds. În: *Semicond. Sci. Technol.* 2020, Vol. 35, p. 103001, doi:10.1088/1361-6641/ab9477.
27. ZALAMAI, V.V., COLIBABA, G.V., MONAICO, E.I., MONAICO, E.V. Enhanced Emission Properties of Anodized Polar ZnO Crystals. În: *Surf. Engin. Appl. Electrochem.* 2021, Vol. 57, p. 117–123, doi:10.3103/S1068375521010166.
28. MONAICO, E.V., MONAICO, E.I., URSAKI, V.V., TIGINYANU, I.M. Porous Semiconductor Compounds with Engineered Morphology as a Platform for Various Applications. În: *physica status solidi (RRL) – Rapid Research Letters* 2023, p. 2300039, doi:10.1002/pssr.202300039.
29. ÖZGÜR, Ü., ALIVOV, Ya.I., LIU, C., TEKE, A., RESHCHIKOV, M.A., DOĞAN, S., AVRUTIN, V., CHO, S.-J., MORKOÇ, H. A Comprehensive Review of ZnO Materials and Devices. În: *Journal of Applied Physics* 2005, Vol. 98, p. 041301, doi:10.1063/1.1992666.
30. MEYER, B.K., ALVES, H., HOFMANN, D.M., KRIEGSEIS, W., FORSTER, D., BERTRAM, F., CHRISTEN, J., HOFFMANN, A., STRASSBURG, M., DWORZAK, M., HABOECK, U., RODINA, A.V. Bound Exciton and Donor–Acceptor Pair Recombinations in ZnO. În: *physica status solidi (b)* 2004, Vol. 241, p. 231–260, doi:10.1002/pssb.200301962.
31. HAN, S.-C., KIM, J.-K., KIM, J.Y., KIM, K.-K., TAMPO, H., NIKI, S., LEE, J.-M. Formation of Hexagonal Pyramids and Pits on V-/VI-Polar and III-/II-Polar GaN/ZnO Surfaces by Wet Etching. În: *J. Electrochem. Soc.* 2009, Vol. 157, p. D60, doi:10.1149/1.3253564.
32. MEHTA, M., MEIER, C. Controlled Etching Behavior of O-Polar and Zn-Polar ZnO Single Crystals. În: *J. Electrochem. Soc.* 2010, Vol. 158, p. H119, doi:10.1149/1.3519999.
33. KLICH, W., INADA, M., GAO, H., SAITO, H., OHTAKI, M. Microwave Synthesis of ZnO Microcrystals with Novel Asymmetric Morphology. În: *Advanced Powder Technology* 2021, Vol. 32, p. 4356–4363, doi:10.1016/j.apt.2021.09.038.
34. MONAICO, E.V., COLIBABA, G.V. Impact of the Electrolyte and Electrochemical Parameters upon the Morphology of Anodized Zinc Oxide.; Минск : БГУ, 2022.

35. NOMAN, M.T., AMOR, N., PETRU, M. Synthesis and Applications of ZnO Nanostructures (ZONSs): A Review. *In: Critical Reviews in Solid State and Materials Sciences* 2022, Vol. 47, p. 99–141, doi:10.1080/10408436.2021.1886041.
36. LE PIVERT, M., MARTIN, N., LEPRINCE-WANG, Y. Hydrothermally Grown ZnO Nanostructures for Water Purification via Photocatalysis. *In: Crystals* 2022, Vol. 12, p. 308, doi:10.3390/cryst12030308.
37. SANKUSH KRISHNA, M., SINGH, S., BATOOL, M., MOHAMED FAHMY, H., SEKU, K., ESMAIL SHALAN, A., LANCEROS-MENDEZ, S., NADEEM ZAFAR, M. A Review on 2D-ZnO Nanostructure Based Biosensors: From Materials to Devices. *In: Materials Advances* 2023, Vol. 4, p. 320–354, doi:10.1039/D2MA00878E.
38. ASPOUKEH, P.K., BARZINJY, A.A., HAMAD, S.M. Synthesis, Properties and Uses of ZnO Nanorods: A Mini Review. *In: Int Nano Lett* 2022, Vol. 12, p. 153–168, doi:10.1007/s40089-021-00349-7.
39. RAI, H., PRASHANT, KONDAL, N. A Review on Defect Related Emissions in Undoped ZnO Nanostructures. *In: Materials Today: Proceedings* 2022, Vol. 48, p. 1320–1324, doi:10.1016/j.matpr.2021.08.343.
40. PEKAR, G.S., SINGAEVSKY, A.F., LOKSHIN, M.M., VASIN, I.A., DUBIKOVSKYI, O.V. Improved Efficiency of ZnO and Ge Purification. *In: Journal of Crystallization Process and Technology* 2020, Vol. 9, p. 39–47, doi:10.4236/jcpt.2019.93003.
41. LANGA, S., TIGINYANU, I.M., MONAICO, E., FÖLL, H. Porous II-VI vs. Porous III-V Semiconductors. *In: physica status solidi c* 2011, Vol. 8, p. 1792–1796, doi:10.1002/pssc.201000102.
42. TIGINYANU, I.M., MONAICO, E.V. Self-Organized Porous Semiconductor Compounds. *In Encyclopedia of Condensed Matter Physics (Second Edition)*; Chakraborty, T., Ed.; Academic Press: Oxford, 2024; pp. 350–374 ISBN 978-0-323-91408-6.
43. LANGA, S., TIGINYANU, I.M., MONAICO, E., FÖLL, H. Porous II-VI vs. Porous III-V Semiconductors. *In: physica status solidi c* 2011, Vol. 8, p. 1792–1796, doi:10.1002/pssc.201000102.
44. MONAICO, E., COLIBABA, G., NEDEOGLO, D., NIELSCH, K. Porosification of III–V and II–VI Semiconductor Compounds. *In: Journal of Nanoelectronics and Optoelectronics* 2014, Vol. 9, p. 307–311, doi:10.1166/jno.2014.1581.
45. URSAKI, V.V., ZALAMAI, V.V., BURLACU, A., KLINGSHIRN, C., MONAICO, E., TIGINYANU, I.M. Random Lasing in Nanostructured ZnO Produced from Bulk ZnSe. *In: Semiconductor science and technology* 2009, Vol. 24, p. 085017.
46. TIGINYANU, I.M., URSAKI, V.V., MONAICO, E., ENACHI, M., SERGENTU, V.V., COLIBABA, G., NEDEOGLO, D.D., COJOCARU, A., FÖLL, H. Quasi-Ordered Networks of Metal Nanotubes Embedded in Semiconductor Matrices for Photonic Applications. *In: Journal of Nanoelectronics and Optoelectronics* 2011, Vol. 6, p. 463–472, doi:10.1166/jno.2011.1197.
47. LI, X., GUO, Z., XIAO, Y., UM, H.-D., LEE, J.-H. Electrochemically Etched Pores and Wires on Smooth and Textured GaAs Surfaces. *In: Electrochimica Acta* 2011, Vol. 56, p. 5071–5079, doi:10.1016/j.electacta.2011.03.084.
48. MONAICO, E.I., MONAICO, E.V., URSAKI, V.V., HONNALI, S., POSTOLACHE, V., LEISTNER, K., NIELSCH, K., TIGINYANU, I.M. Electrochemical Nanostructuring of (111) Oriented GaAs Crystals: From Porous Structures to Nanowires. *In: Beilstein J. Nanotechnol.* 2020, Vol. 11, p. 966–975, doi:10.3762/bjnano.11.81.
49. MONAICO, E.V., MORARI, V., URSAKI, V.V., NIELSCH, K., TIGINYANU, I.M. Core–Shell GaAs-Fe Nanowire Arrays: Fabrication Using Electrochemical Etching and Deposition and Study of Their Magnetic Properties. *In: Nanomaterials* 2022, Vol. 12, p. 1506, doi:10.3390/nano12091506.
50. MONAICO, E., SYRBU, N.N., COSEAC, V., URSAKI, V.V., TIGINYANU, I.M. Photoluminescence of ZnTe Nanowires Prepared by Electrochemical Etching of Bulk ZnTe. *In*

Proceedings of the ICMCS-2009: 6th international conference on microelectronics and computer science; Technical University of Moldova: Moldova, Republic of, October 1 2009; pp. 150–153.

51. ZENIA, F., LÉVY-CLÉMENT, C., TRIBOULET, R., KÖNENKAMP, R., ERNST, K., SAAD, M., LUX-STEINER, M.C. Electrochemical Texturization of ZnTe Surfaces. În: *Appl. Phys. Lett.* 1999, Vol. 75, p. 531–533, doi:10.1063/1.124438.
52. MONAICO, E., TIGINYANU, I., VOLCIUC, O., MEHRTENS, T., ROSENAUER, A., GUTOWSKI, J., NIELSCH, K. Formation of InP Nanomembranes and Nanowires under Fast Anodic Etching of Bulk Substrates. În: *Electrochemistry Communications* 2014, Vol. 47, p. 29–32, doi:10.1016/j.elecom.2014.07.015.
53. MONAICO, E.V., TIGINYANU, I.M., URSAKI, V.V., NIELSCH, K., BALAN, D., PRODANA, M., ENACHESCU, M. Gold Electroplating as a Tool for Assessing the Conductivity of InP Nanostructures Fabricated by Anodic Etching of Crystalline Substrates. În: *J. Electrochem. Soc.* 2017, Vol. 164, p. D179, doi:10.1149/2.1071704jes.
54. TIGINYANU, I., MONAICO, E., NIELSCH, K. Self-Assembled Monolayer of Au Nanodots Deposited on Porous Semiconductor Structures. În: *ECS Electrochem. Lett.* 2015, Vol. 4, p. D8, doi:10.1149/2.0041504eel.
55. HASEGAWA, H., SATO, T. Electrochemical Processes for Formation, Processing and Gate Control of III–V Semiconductor Nanostructures. În: *Electrochimica Acta* 2005, Vol. 50, p. 3015–3027, doi:10.1016/j.electacta.2004.11.066.
56. MONAICO, E.V., MONAICO, E.I., URSAKI, V.V., TIGINYANU, I.M. Free-Standing Large-Area Nanoperforated Gold Membranes Fabricated by Hopping Electrodeposition. În: *ECS J. Solid State Sci. Technol.* 2020, Vol. 9, p. 064010, doi:10.1149/2162-8777/aba6a2.
57. MOISE, C.C., MIHAI, G.V., ANICĂI, L., MONAICO, E.V., URSAKI, V.V., ENĂCHESCU, M., TIGINYANU, I.M. Electrochemical Deposition of Ferromagnetic Ni Nanoparticles in InP Nanotemplates Fabricated by Anodic Etching Using Environmentally Friendly Electrolyte. În: *Nanomaterials* 2022, Vol. 12, p. 3787, doi:10.3390/nano12213787.
58. HÖLZL, J., SCHULTE, F.K. Work Function of Metals. In *Solid Surface Physics*; Hölzl, J., Schulte, F.K., Wagner, H., Eds.; Springer Tracts in Modern Physics; Springer: Berlin, Heidelberg, 1979; pp. 1–150 ISBN 978-3-540-35253-2.
59. MONAICO, E., BRINCOVEANU, O., MESTERCA, R., URSAKI, V., PRODANA, M., ENACHESCU, M., TIGINYANU, I. Pulsed Electroplating of Metal Nanoparticles Form DODUCO Electrolytes. In Proceedings of the 9th International Conference on Microelectronics and Computer Science; Chisinau, Republic of Moldova, October 19-21, 2017; pp. 16–20.
60. ANICAI, L., GOLGOVICI, F., MONAICO, E., URSAKI, V., PRODANA, M., ENACHESCU, M., TIGINYANU, I. Influence of Metal Deposition on Electrochemical Impedance Spectra of Porous GaP and GaN Semiconductors. In Proceedings of the 9th International Conference on Microelectronics and Computer Science,; Chisinau, Republic of Moldova, October 19-21, 2017; pp. 60–64.
61. MONAICO, E., URSACHI, V., TIGHINEANU, I. Frontierele Electrochimiei Şi Aplicații În Nanotehnologii. În: *Fizica și Tehnologiile Moderne* 2020, Vol. 18, p. 8–18.
62. MONAICO, E.V., URSAKI, V.V., TIGINYANU, I.M. Gold Coated Microstructures as a Platform for the Preparation of Semiconductor-Based Hybrid 3D Micro-Nano-Architectures. În: *Eur. Phys. J. Plus* 2023, Vol. 138, p. 827, doi:10.1140/epjp/s13360-023-04462-8.
63. MONAICO, Ed., MONAICO, E.I., URSAKI, V.V., TIGINYANU, I.M., NIELSCH, K. Electrochemical Deposition by Design of Metal Nanostructures. În: *Surf. Engin. Appl. Electrochem.* 2019, Vol. 55, p. 367–372, doi:10.3103/S1068375519040070.
64. KIM, R.-H., KIM, D.-H., XIAO, J., KIM, B.H., PARK, S.-I., PANILAITIS, B., GHAFFARI, R., YAO, J., LI, M., LIU, Z., MALYARCHUK, V., KIM, D.G., LE, A.-P., NUZZO, R.G., KAPLAN, D.L., OMENETTO, F.G., HUANG, Y., KANG, Z., ROGERS, J.A. Waterproof

- AllInGaP Optoelectronics on Stretchable Substrates with Applications in Biomedicine and Robotics. *In: Nature Mater* 2010, Vol. 9, p. 929–937, doi:10.1038/nmat2879.
65. MONAICO, E.V., BUSUIOC, S., TIGINYANU, I.M. Controlling the Degree of Hydrophilicity/Hydrophobicity of Semiconductor Surfaces via Porosification and Metal Deposition. In Proceedings of the 5th International Conference on Nanotechnologies and Biomedical Engineering; Tiginyanu, I., Sontea, V., Railean, S., Eds.; Springer International Publishing: Cham, 2022; pp. 62–69.
 66. MONAICO, E.I., MONAICO, E.V., URSAKI, V.V., TIGINYANU, I.M. Controlled Electroplating of Noble Metals on III-V Semiconductor Nanotemplates Fabricated by Anodic Etching of Bulk Substrates. *In: Coatings* 2022, Vol. 12, p. 1521, doi:10.3390/coatings12101521.
 67. PRISLOPSKI, S.Y., NAUMENKO, E.K., TIGINYANU, I.M., GHIMPU, L., MONAICO, E., SIRBU, L., GAPONENKO, S.V. Anomalous Retroreflection from Strongly Absorbing Nanoporous Semiconductors. *In: Opt. Lett., OL* 2011, Vol. 36, p. 3227–3229, doi:10.1364/OL.36.003227.
 68. GAPONENKO, S.V., GERMANENKO, I.N., PETROV, E.P., STUPAK, A.P., BONDARENKO, V.P., DOROFEEV, A.M. Time-resolved Spectroscopy of Visibly Emitting Porous Silicon. *In: Appl. Phys. Lett.* 1994, Vol. 64, p. 85–87, doi:10.1063/1.112004.
 69. PRISLOPSKI, S.Ya., TIGINYANU, I.M., GHIMPU, L., MONAICO, E., SIRBU, L., GAPONENKO, S.V. Retroreflection of Light from Nanoporous InP: Correlation with High Absorption. *In: Appl. Phys. A* 2014, Vol. 117, p. 467–470, doi:10.1007/s00339-014-8683-x.
 70. MADELUNG, O. *Semiconductors: Data Handbook*; Springer Berlin Heidelberg: Berlin, Heidelberg, 2004; ISBN 978-3-642-62332-5.
 71. SERGENTU, V.V., PRISLOPSKI, S.Y., MONAICO, E.V., URSAKI, V.V., GAPONENKO, S.V., TIGINYANU, I.M. Anomalous Retroreflection from Nanoporous Materials as Backscattering by ‘Dark’ and ‘Bright’ Modes. *In: Journal of Optics* 2016, Vol. 18, p. 125008.
 72. SERGENTU, V.V., URSAKI, V., MONAICO, Ed., TIGINYANU, I.M., PRISLOPSKI, S.Ya., GAPONENKO, S.V. Dark Modes Backscattering as Possible Rationale for Anomalous Retroreflection from Strongly Absorbing Porous Nanostructures. In *Physics, Chemistry and Application of Nanostructures*; WORLD SCIENTIFIC, 2017; pp. 30–33 ISBN 978-981-322-452-0.
 73. GAPONENKO, S.V., MONAICO, E., SERGENTU, V.V., PRISLOPSKI, S.Y., TIGINYANU, I.M. Possible Coherent Backscattering of Lightwaves from a Strongly Absorbing Nanoporous Medium. *In: J. Opt.* 2018, Vol. 20, p. 075606, doi:10.1088/2040-8986/aac841.
 74. PRISLOPSKI, S.Ya., GAPONENKO, S.V., MONAICO, E., SERGENTU, V.V., TIGINYANU, I.M. Polarized Retroreflection from Nanoporous III–V Semiconductors. *In: Semiconductors* 2018, Vol. 52, p. 2068–2069, doi:10.1134/S1063782618160248.
 75. SERGENTU, V.V., MONAICO, E.V., URSAKI, V.V. Scattering Indicatrix for Absorbing Porous Medium with Dark Modes. In Proceedings of the International Conference on Nanotechnologies and Biomedical Engineering; Springer, Cham, 2019; pp. 775–778.
 76. BRANISTE, T., CIERS, J., MONAICO, Ed., MARTIN, D., CARLIN, J.-F., URSAKI, V.V., SERGENTU, V.V., TIGINYANU, I.M., GRANDJEAN, N. Multilayer Porous Structures of HVPE and MOCVD Grown GaN for Photonic Applications. *In: Superlattices and Microstructures* 2017, Vol. 102, p. 221–234, doi:10.1016/j.spmi.2016.12.041.
 77. VESELAGO, V.G. The Electrodynamics of Substances with Simultaneously Negative Values of ϵ and μ . *In: Sov. Phys. Usp.* 1968, Vol. 10, p. 509, doi:10.1070/PU1968v010n04ABEH003699.
 78. SERGENTU, V.V., TIGINYANU, I.M., URSAKI, V.V., ENACHI, M., ALBU, S.P., SCHMUKI, P. Prediction of Negative Index Material Lenses Based on Metallo-Dielectric Nanotubes. *In: physica status solidi (RRL) – Rapid Research Letters* 2008, Vol. 2, p. 242–244, doi:10.1002/pssr.200802130.

79. TIGINYANU, I., MONAICO, E., SERGENTU, V., TIRON, A., URSAKI, V. Metallized Porous GaP Templates for Electronic and Photonic Applications. În: *ECS J. Solid State Sci. Technol.* 2015, Vol. 4, p. P57, doi:10.1149/2.0011503jss.
80. TIGINYANU, I., URSAKI, V., MONAICO, E. Template Assisted Formation of Metal Nanotubes. In *Nanostructures and Thin Films for Multifunctional Applications: Technology, Properties and Devices*; Tiginyanu, I., Topala, P., Ursaki, V., Eds.; NanoScience and Technology; Springer International Publishing: Cham, 2016; pp. 473–506 ISBN 978-3-319-30198-3.
81. LI, L.-M., ZHANG, Z.-Q. Multiple-Scattering Approach to Finite-Sized Photonic Band-Gap Materials. În: *Phys. Rev. B* 1998, Vol. 58, p. 9587–9590, doi:10.1103/PhysRevB.58.9587.
82. TIGINYANU, I., MONAICO, E., URSAKI, V. Two-Dimensional Metallo-Semiconductor Networks for Electronic and Photonic Applications. În: *ECS Trans.* 2012, Vol. 41, p. 67, doi:10.1149/1.4718392.
83. MONAICO, E.V. Engineering of Semiconductor Compounds via Electrochemical Technologies for Nano-Microelectronic Applications. În: *J. Eng. Sci.* 2022, Vol. 29, p. 8–16, doi:10.52326/jes.utm.2022.29(1).01.
84. MONAICO, E., POSTOLACHE, V., BORODIN, E., URSAKI, V.V., LUPAN, O., ADELUNG, R., NIELSCH, K., TIGINYANU, I.M. Control of Persistent Photoconductivity in Nanostructured InP through Morphology Design. În: *Semicond. Sci. Technol.* 2015, Vol. 30, p. 035014, doi:10.1088/0268-1242/30/3/035014.
85. VOLCIUC, O., MONAICO, E., ENACHI, M., URSAKI, V.V., PAVLIDIS, D., POPA, V., TIGINYANU, I.M. Morphology, Luminescence, and Electrical Resistance Response to H₂ and CO Gas Exposure of Porous InP Membranes Prepared by Electrochemistry in a Neutral Electrolyte. În: *Applied Surface Science* 2010, Vol. 257, p. 827–831, doi:10.1016/j.apsusc.2010.07.074.
86. MONAICO, E. Structuri Hibride Metal-Semiconductor În Baza Nanoșabloanelor de InP Și GaAs Pentru Aplicații Electronice Și Fotonice. Teza de doctor în științe inginerești., Universitatea Tehnică a Moldovei: Chișinău, Republica Moldova, 2023.
87. MONAICO, E.V., MORARI, V., KUTUZAU, M., URSAKI, V.V., NIELSCH, K., TIGINYANU, I.M. Magnetic Properties of GaAs/NiFe Coaxial Core-Shell Structures. În: *Materials* 2022, Vol. 15, p. 6262, doi:10.3390/ma15186262.
88. MONAICO, E.V., MORARI, V., KUTUZAU, M., URSAKI, V.V., NIELSCH, K., TIGINYANU, I.M. Ferromagnetic Core-Shell Coaxial Nanostructures on Gallium Arsenide Substrates. În: *Rom. J. Phys.* 2022, Vol. 67, p. published on-line: <https://rjp.nipne.ro/accpaps/23773438A554DFDDC177E6DC5EC0288760A92556.pdf>.
89. PLESCO, I., CIOBANU, V., BRANISTE, T., URSAKI, V., RASCH, F., SARUA, A., RAEVSCHI, S., ADELUNG, R., DUTTA, J., TIGINYANU, I. Highly Porous and Ultra-Lightweight Aero-Ga₂O₃: Enhancement of Photocatalytic Activity by Noble Metals. În: *Materials* 2021, Vol. 14, p. 1985, doi:10.3390/ma14081985.
90. MISHRA, Y.K., KAPS, S., SCHUCHARDT, A., PAULOWICZ, I., JIN, X., GEDAMU, D., FREITAG, S., CLAUS, M., WILLE, S., KOVALEV, A., GORB, S.N., ADELUNG, R. Fabrication of Macroscopically Flexible and Highly Porous 3D Semiconductor Networks from Interpenetrating Nanostructures by a Simple Flame Transport Approach. În: *Particle & Particle Systems Characterization* 2013, Vol. 30, p. 775–783, doi:10.1002/ppsc.201300197.
91. MONAICO, E.V., REIMERS, A., CIOBANU, V., ZALAMAI, V.V., URSAKI, V.V., ADELUNG, R., TIGINYANU, I.M. ZnO Microtetrapods Covered by Au Nanodots as a Platform for the Preparation of Complex Micro-Nano-Structures. In *Proceedings of the 6th International Conference on Nanotechnologies and Biomedical Engineering*; Sontea, V., Tiginyanu, I., Railean, S., Eds.; Springer Nature Switzerland: Cham, 2024; pp. 197–205.
92. AZIZ, B., MAJID, A., GHANI, L., AZIZ, I. Photoluminescence Effect on Phosphorous Irradiated Zinc Oxide (ZnO) Nanotetrapods Synthesized by Simple Thermal Oxidation

Method. În: *Journal of Physics and Its Applications* 2020, Vol. 3, p. 107–112, doi:10.14710/jpa.v3i1.8271.

93. MYNDRUL, V., COY, E., BABAYEVSKA, N., ZAHORODNA, V., BALITSKYI, V., BAGINSKIY, I., GOGOTSI, O., BECHELANY, M., GIARDI, M.T., IATSUNSKYI, I. MXene Nanoflakes Decorating ZnO Tetrapods for Enhanced Performance of Skin-Attachable Stretchable Enzymatic Electrochemical Glucose Sensor. În: *Biosensors and Bioelectronics* 2022, Vol. 207, p. 114141, doi:10.1016/j.bios.2022.114141.
94. CIOBANU, V., URSAKI, V.V., REIMERS, A., MIHAI, G., ZALAMAI, V.V., MONAICO, E.V., ADELUNG, R., ENACHESCU, M., TIGINYANU, I.M. Controlling Hydrophobic/Hydrophilic Properties of ZnO Microtetrapods Structures by Means of Thermal Treatment. In Proceedings of the 6th International Conference on Nanotechnologies and Biomedical Engineering; Sontea, V., Tiginyanu, I., Railean, S., Eds.; Springer Nature Switzerland: Cham, 2024; pp. 284–292.

THE LIST OF PUBLISHED SCIENTIFIC ARTICLES ON THE TOPIC OF SYNTHESIS WORK

1. Specialized books

1.1. monograph

1. **MONAICO, E.V.** *Micro- and nano-engineering of III-V and II-VI semiconductor compounds and metal nanostructures based on electrochemical technologies for multifunctional applications*. Technical University of Moldova. Chisinau: S. n., Bons Offices, **2022**, 286 p. ISBN 978-9975-166-63-8. <http://repository.utm.md/handle/5014/21913>

1.2. chapters in monographs

2. TIGINYANU, I.M., **MONAICO, E.V.** Self-organized porous semiconductor compounds. In: *Encyclopedia of Condensed Matter Physics (Second Edition)*; Chakraborty, T., Ed.; Academic Press: Oxford, **2024**; Vol. 5, p. 350–374. ISBN 978-0-323-91408-6. <https://doi.org/10.1016/B978-0-323-90800-9.00105-0>
3. TIGINYANU, I., URSAKI, V., **MONAICO, E.** Template assisted formation of metal nanotubes. In: *Nanostructures and Thin Films for Multifunctional Applications: Technology, Properties and Devices*; Tiginyanu, I., Topala, P., Ursaki, V., Eds.; NanoScience and Technology; Springer International Publishing: Cham, **2016**; Chapter 15, pp. 473–506. ISBN 978-3-319-30198-3. https://doi.org/10.1007/978-3-319-30198-3_15

2. Articles in scientific journals

2.1. in journals from the Web of Science and SCOPUS databases

4. **MONAICO, E.V.**, MONAICO, E.I., URSAKI, V.V., TIGINYANU, I.M. Porous semiconductor compounds with engineered morphology as a platform for various applications. In: *Physica status solidi (RRL) – Rapid Research Letters*, **2023**, 2300039, <https://doi.org/10.1002/pssr.202300039>
5. **MONAICO, E.V.**, URSAKI, V. V., TIGINYANU, I. M. Gold coated microstructures as a platform for the preparation of semiconductor-based hybrid 3D micro-nano-architectures. In: *The European Physical Journal Plus*. 138, 827. **2023**. <https://doi.org/10.1140/epjp/s13360-023-04462-8>. <https://rdcu.be/dmINN>
6. URSAKI, V.V., LEHMANN, S., ZALAMAI, V.V., MORARI, V., NIELSCH, K., TIGINYANU, I.M., **MONAICO, E.V.** Planar and coaxial core-shell nanostructures prepared by atomic layer deposition on semiconductor substrates. In: *Romanian Journal of Physics* **2023**, Vol. 68, 601. https://rjp.nipne.ro/2023_68_1-2/RomJPhys.68.601.pdf
7. **MONAICO, E.V.**, MORARI, V., URSAKI, V.V., NIELSCH, K., TIGINYANU, I.M. Core-shell GaAs-Fe nanowire arrays: fabrication using electrochemical etching and deposition and study of their magnetic properties. In: *Nanomaterials* **2022**, 12, 1506, doi:[10.3390/nano12091506](https://doi.org/10.3390/nano12091506)

8. MOISE, C.C., MIHAI, G.V., ANICĂI, L., **MONAICO, E.V.**, URSAKI, V.V., ENĂCHESCU, M., TIGINYANU, I.M. Electrochemical deposition of ferromagnetic Ni nanoparticles in InP nanotemplates fabricated by anodic etching using environmentally friendly electrolyte. In: *Nanomaterials* **2022**, *12*, 3787, doi:[10.3390/nano12213787](https://doi.org/10.3390/nano12213787)
9. **MONAICO, E.V.**, MORARI, V., KUTUZAU, M., URSAKI, V.V., NIELSCH, K., TIGINYANU, I.M. Magnetic properties of GaAs/NiFe coaxial core-shell structures. In: *Materials* **2022**, *15*, 6262, doi:[10.3390/ma15186262](https://doi.org/10.3390/ma15186262)
10. MONAICO, E.I., **MONAICO, E.V.**, URSAKI, V.V., TIGINYANU, I.M. Controlled electroplating of noble metals on III-V semiconductor nanotemplates fabricated by anodic etching of bulk substrates. In: *Coatings*, **2022**, *12*, 1521, doi:[10.3390/coatings12101521](https://doi.org/10.3390/coatings12101521)
11. URSAKI, V.V., LEHMANN, S., ZALAMAI, V.V., MORARI, V., NIELSCH, K., TIGINYANU, I.M., **MONAICO, E.V.** Core-shell structures prepared by atomic layer deposition on GaAs nanowires. In: *Crystals* **2022**, *12*, 1145, doi:[10.3390/cryst12081145](https://doi.org/10.3390/cryst12081145)
12. **MONAICO, E.V.**, MORARI, V., KUTUZAU, M., URSAKI, V.V., NIELSCH, K., TIGINYANU, I.M. Ferromagnetic core-shell coaxial nanostructures on gallium arsenide substrates. In: *Rom J Phys* **2022**, *67*, 611. Disponibil: <https://rjp.nipne.ro/accpaps/23773438A554DFDDC177E6DC5EC0288760A92556.pdf>
13. ZALAMAI, V.V., COLIBABA, G.V., MONAICO, E.I., **MONAICO, E.V.** Enhanced emission properties of anodized polar ZnO crystals. In: *Surf. Engin. Appl. Electrochem.* **2021**, *57*, 117–123, doi:10.3103/S1068375521010166.
14. **MONAICO, E.**, TIGINYANU, I., URSAKI, V. Porous semiconductor compounds. In: *Semicond. Sci. Technol.* **2020**, *35*, 103001, 62 pages. doi:10.1088/1361-6641/ab9477. **Articol de sinteză.**
15. **MONAICO, E.**, MOISE, C., MIHAI, G., URSAKI, V.V., LEISTNER, K., TIGINYANU, I.M., ENACHESCU, M., NIELSCH, K. Towards uniform electrochemical porosification of bulk HVPE-grown GaN. In: *J. Electrochem. Soc.* **2019**, *166*, H3159, doi:10.1149/2.0251905jes.
16. WOLFF, N., JORDT, P., BRANISTE, T., POPA, V., **MONAICO, E.**, URSAKI, V., PETRARU, A., ADELUNG, R., MURPHY, B.M., KIENLE, L., TIGINYANU, I. Modulation of electrical conductivity and lattice distortions in bulk HVPE-grown GaN. In: *ECS J. Solid State Sci. Technol.* **2019**, *8*, Q141, doi:10.1149/2.0041908jss.
17. GAPONENKO, S.V., **MONAICO, E.**, SERGENTU, V.V., PRISLOPSKI, S.Y., TIGINYANU, I.M. Possible coherent backscattering of lightwaves from a strongly absorbing nanoporous medium. In: *J. Opt.* **2018**, *20*, 075606, doi:10.1088/2040-8986/aac841.
18. PRISLOPSKI, S.Ya., GAPONENKO, S.V., **MONAICO, E.**, SERGENTU, V.V., TIGINYANU, I.M. Polarized retroreflection from nanoporous III–V semiconductors. In: *Semiconductors* **2018**, *52*, 2068–2069, doi:10.1134/S1063782618160248.
19. **MONAICO, E.V.**, TIGINYANU, I.M., URSAKI, V.V., NIELSCH, K., BALAN, D., PRODANA, M., ENACHESCU, M. Gold Electroplating as a tool for assessing the conductivity of InP nanostructures fabricated by anodic etching of crystalline substrates. In: *J. Electrochem. Soc.* **2017**, *164*, D179, doi:10.1149/2.1071704jes.
20. BRANISTE, T., CIERS, J., **MONAICO, Ed.**, MARTIN, D., CARLIN, J.-F., URSAKI, V.V., SERGENTU, V.V., TIGINYANU, I.M., GRANDJEAN, N. Multilayer porous structures of HVPE and MOCVD grown GaN for photonic applications. In: *Superlattices and Microstructures* **2017**, *102*, 221–234, doi:10.1016/j.spmi.2016.12.041.
21. SERGENTU, V.V., PRISLOPSKI, S.Y., **MONAICO, E.V.**, URSAKI, V.V., GAPONENKO, S.V., TIGINYANU, I.M. Anomalous retroreflection from nanoporous materials as backscattering by ‘dark’ and ‘bright’ modes. In: *J. Opt.* **2016**, Vol. 18, p. 125008, doi:10.1088/2040-8978/18/12/125008
22. TIGINYANU, I., STEVENS-KALCEFF, M.A., SARUA, A., BRANISTE, T., **MONAICO, E.**, POPA, V., ANDRADE, H.D., THOMAS, J.O., RAEVSCHI, S., SCHULTE, K., ADELUNG, R. Self-organized three-dimensional nanostructured architectures in bulk GaN generated by spatial

- modulation of doping. In: *ECS J. Solid State Sci. Technol.* **2016**, 5, P218, doi:[10.1149/2.0091605jss](https://doi.org/10.1149/2.0091605jss)
23. TIGINYANU, I., **MONAICO, E.**, NIELSCH, K. Self-assembled monolayer of Au nanodots deposited on porous semiconductor structures. In: *ECS Electrochem. Lett.* **2015**, 4, D8, doi:[10.1149/2.0041504eel](https://doi.org/10.1149/2.0041504eel)
 24. TIGINYANU, I., **MONAICO, E.**, SERGENTU, V., TIRON, A., URSAKI, V. Metallized porous GaP templates for electronic and photonic applications. In: *ECS J. Solid State Sci. Technol.* **2015**, 4, P57, doi:[10.1149/2.0011503jss](https://doi.org/10.1149/2.0011503jss)
 25. **MONAICO, E.**, POSTOLACHE, V., BORODIN, E., URSAKI, V.V., LUPAN, O., ADELUNG, R., NIELSCH, K., TIGINYANU, I.M. Control of persistent photoconductivity in nanostructured InP through morphology design. In: *Semicond. Sci. Technol.* **2015**, 30, 035014, doi:[10.1088/0268-1242/30/3/035014](https://doi.org/10.1088/0268-1242/30/3/035014)
 26. **MONAICO, E.**, TIGINYANU, I., VOLCIUC, O., MEHRTENS, T., ROSENAUER, A., GUTOWSKI, J., NIELSCH, K. Formation of InP nanomembranes and nanowires under fast anodic etching of bulk substrates. In: *Electrochemistry Communications* **2014**, 47, 29–32, doi:[10.1016/j.elecom.2014.07.015](https://doi.org/10.1016/j.elecom.2014.07.015)
 27. PRISLOPSKI, S.Ya., TIGINYANU, I.M., GHIMPU, L., **MONAICO, E.**, SIRBU, L., GAPONENKO, S.V. Retroreflection of light from nanoporous InP: correlation with high absorption. In: *Appl. Phys. A* **2014**, 117, p. 467–470, doi:[10.1007/s00339-014-8683-x](https://doi.org/10.1007/s00339-014-8683-x)
 28. **MONAICO, E.**, COLIBABA, G., NEDEOGLO, D., NIELSCH, K. Porosification of III–V and II–VI semiconductor compounds. In: *Journal of Nanoelectronics and Optoelectronics* **2014**, 9, p. 307–311, doi:[10.1166/jno.2014.1581](https://doi.org/10.1166/jno.2014.1581)
 29. COLIBABA, G., GONCEARENCO, E., NEDEOGLO, D., NEDEOGLO, N., **MONAICO, E.**, TIGINYANU, I. Obtaining of II-VI compound substrates with controlled electrical parameters and prospects of their application for nanoporous structures. In: *Physica status solidi c* **2014**, 11, 1404–1407, doi:[10.1002/pssc.201300590](https://doi.org/10.1002/pssc.201300590)
 30. COLIBABA, G.V., **MONAICO, E.V.**, GONCEARENCO, E.P., NEDEOGLO, D.D., TIGINYANU, I.M., NIELSCH, K. Growth of ZnCdS single crystals and prospects of their application as nanoporous structures. In: *Semicond. Sci. Technol.* **2014**, 29, 125003, doi:[10.1088/0268-1242/29/12/125003](https://doi.org/10.1088/0268-1242/29/12/125003)
 31. TIGINYANU, I., **MONAICO, E.**, URSAKI, V. Two-dimensional metallo-semiconductor networks for electronic and photonic applications. In: *ECS Trans.* **2012**, 41, 67, doi:[10.1149/1.4718392](https://doi.org/10.1149/1.4718392)
 32. LANGA, S., TIGINYANU, I.M., **MONAICO, E.**, FÖLL, H. POROUS II-VI vs. Porous III-V semiconductors. In: *Physica status solidi c*. **2011**, 8, 1792–1796, doi:[10.1002/pssc.201000102](https://doi.org/10.1002/pssc.201000102)
 33. TIGINYANU, I.M., URSAKI, V.V., **MONAICO, E.**, ENACHI, M., SERGENTU, V.V., COLIBABA, G., NEDEOGLO, D.D., COJOCARU, A., FÖLL, H. Quasi-ordered networks of metal nanotubes embedded in semiconductor matrices for photonic applications. In: *Journal of Nanoelectronics and Optoelectronics* **2011**, 6, 463–472, doi:[10.1166/jno.2011.1197](https://doi.org/10.1166/jno.2011.1197)
 34. PRISLOPSKI, S.Y., NAUMENKO, E.K., TIGINYANU, I.M., GHIMPU, L., **MONAICO, E.**, SIRBU, L., GAPONENKO, S.V. Anomalous retroreflection from strongly absorbing nanoporous semiconductors. In: *Opt. Lett., OL* **2011**, 36, 3227–3229, doi:[10.1364/OL.36.003227](https://doi.org/10.1364/OL.36.003227)
 35. VOLCIUC, O., **MONAICO, E.**, ENACHI, M., URSAKI, V.V., PAVLIDIS, D., POPA, V., TIGINYANU, I.M. Morphology, luminescence, and electrical resistance response to H₂ and CO gas exposure of porous InP membranes prepared by electrochemistry in a neutral electrolyte. In: *Applied Surface Science* **2010**, 257, 827–831, doi:[10.1016/j.apsusc.2010.07.074](https://doi.org/10.1016/j.apsusc.2010.07.074)
 36. GOLOGAN, V.F., BOBANOVA, Zh.I., **MONAICO, E.V.**, MAZUR, V.A., IVASHKU, S.Kh., KIRIYAK, E. Peculiarities of the influence of an inductance-capacitance device on the initial stage of the crystallization of electrolytic coatings of copper. In: *Surf. Engin. Appl. Electrochem.* **2010**, 46, 9–15, doi:[10.3103/S1068375510010023](https://doi.org/10.3103/S1068375510010023)

2.2. in journals from other databases accepted by ANACEC

37. **MONAICO, E.**; Tighineanu I. Nanofire și nanotuburi: Tehnologii și perspective de utilizare. In: *Fizica și Tehnologiile Moderne*, **2012**, vol. 10, nr. 1-2, pp. 4 – 12. Disponibil: https://ibn.idsi.md/vizualizare_articol/29460

2.3. in journals from the National Register of professional journals

38. **MONAICO, E.** Engineering of semiconductor compounds via electrochemical technologies for nano-microelectronic applications. In: *Journal of Engineering Science*, **2022**, Vol. XXIX, no. 1, pp. 8 – 16. doi:[10.52326/jes.utm.2022.29\(1\).01](https://doi.org/10.52326/jes.utm.2022.29(1).01) Categoria B+
39. ГОЛОГАН, В, БОБАНОВА, Ж, **МОНАЙКО, Э.**, МАЗУР, В, ИВАШКУ, С., ШИРИАС, Е. Особенности влияния индуктивно-емкостного устройства на начальную стадию кристаллизации электролитических покрытия меди. In: *Электронная обработка материалов*, **2010**, No. 1 (261), pp. 12-18. Disponibil: <http://www.repository.utm.md/handle/5014/10399> Categoria C

3. Articles in conference proceedings and other scientific events

3.1. in the works of scientific events included in the Web of Science and SCOPUS databases

40. **MONAICO, E.V.**, REIMERS, A., CIOBANU, V., ZALAMAI, V.V., URSAKI, V.V., ADELUNG, R., TIGINYANU, I.M. ZnO microtetrapods covered by Au nanodots as a platform for the preparation of complex micro-nano-structures. In: *IFMBE Proceedings* 91, pp. 197–205, 2024. https://doi.org/10.1007/978-3-031-42775-6_22
41. CIOBANU, V., URSAKI, V.V., REIMERS, A., MIHAI, G., ZALAMAI, V.V., **MONAICO, E.V.**, ADELUNG, R., ENACHESCU, M., TIGINYANU, I.M. Controlling hydrophobic/hydrophilic properties of ZnO microtetrapods structures by means of thermal treatment. In: *IFMBE Proceedings* 91, pp. 284–292, 2024. https://doi.org/10.1007/978-3-031-42775-6_32
42. **MONAICO, E.V.**, BUSUIOC, S., TIGINYANU, I.M. Controlling the degree of hydrophilicity/hydrophobicity of semiconductor surfaces via porosification and metal deposition. In: *IFMBE Proceedings*, 2022; pp. 62–69. doi: [10.1007/978-3-030-92328-0_9](https://doi.org/10.1007/978-3-030-92328-0_9)
43. SERGENTU, V.V., **MONAICO, E.V.**, URSAKI, V.V. Scattering indicatrix for absorbing porous medium with dark modes. In: *IFMBE Proceedings*, vol 77, pp. 775-778, 2020. Springer, Cham. https://doi.org/10.1007/978-3-030-31866-6_137
44. BRANISTE, T., **MONAICO, E.**, MARTIN, D., CARLIN, J.-F., POPA, V., URSAKI, V.V., GRANDJEAN, N., TIGINYANU, I.M. Multilayer porous structures on GaN for the fabrication of Bragg reflectors. In: *Proceedings of the Nanotechnology VIII*; SPIE, May 30 **2017**; Vol. 10248, 102480R, pp. 83–89. doi:[10.1117/12.2266280](https://doi.org/10.1117/12.2266280)
45. COLIBABA, G.V., **MONAICO, E.V.**, GONCEARENCO, E.P., INCULET, I., TIGINYANU, I.M. Features of nanotemplates manufacturing on the II-VI compound substrates. In: *Proceedings of the 3rd International Conference on Nanotechnologies and Biomedical Engineering*, **2016**; pp. 188–191. doi: [10.1007/978-981-287-736-9_47](https://doi.org/10.1007/978-981-287-736-9_47)

3.2. in the works of scientific events included in other databases accepted by ANACEC

46. **MONAICO, E.V.**, COLIBABA, G.V. Impact of the electrolyte and electrochemical parameters upon the morphology of anodized zinc oxide. In: *International Scientific Conference “Materials and Structures of Modern Electronics” MSME-2022*, 12 — 14 October 2022, Minsk, Belarus. p. 316-321. Comunicare orală. <https://elib.bsu.by/handle/123456789/292849>
47. **MONAICO, E.V.**, BRINCOVEANU, O., MESTERCA, R., URSAKI, V., PRODANA, M., ENACHESCU, M., TIGINYANU, I. Pulsed electroplating of metal nanoparticles form DODUCO electrolytes. In: *9th International Conference on Microelectronics and Computer Science*, Chisinau, Republic of Moldova, pp. 16 - 20, October 19-21, 2017 https://ibn.idsi.md/en/vizualizare_articol/55237
48. ANICAI, L., GOLGOVICI, F., **MONAICO, E.**, URSAKI, V., PRODANA, M., ENACHESCU, M., TIGINYANU, I. Influence of metal deposition on electrochemical impedance spectra of porous GaP and GaN semiconductors. In: *9th International Conference on Microelectronics and*

- Computer Science*, Chisinau, Republic of Moldova, pp. 60 - 64, October 19-21, 2017
https://ibn.idsi.md/en/vizualizare_articol/55278
49. SERGENTU, V.V., URSAKI, V., **MONAICO, Ed.**, TIGINYANU, I.M., PRISLOPSKI, S.Ya., GAPONENKO, S.V. Dark modes backscattering as possible rationale for anomalous retroreflection from strongly absorbing porous nanostructures. In: *Physics, Chemistry and Application of Nanostructures*; WORLD SCIENTIFIC, 2017; pp. 30–33 ISBN 978-981-322-452-0. https://doi.org/10.1142/9789813224537_0006
 50. **MONAICO, E.V.**, MONAICO, E.I., COLIBABA, G. Obținerea straturilor poroase în baza cristalelor de $Zn_xCd_{1-x}S$ cu banda interzisă largă. In: *Conferința Științifică a Colaboratorilor, Doctoranzilor și Studenților UTM*, Vol. 1, pp. 123-126, 18 noiembrie 2016
 51. **MONAICO E.** Formation of low-dimensional object obtaining via ultra-fast anodic etching of InP. In: *Conferința Științifică a Colaboratorilor, Doctoranzilor și Studenților UTM*, 27 noiembrie 2015 vol. 1, pp. 179-182. <http://repository.utm.md/handle/5014/697>
 52. POSTOLACHE, V., **MONAICO, E.**, BORODIN, E., LUPAN, O., URSAKI, V., ADELUNG, R., NIELSCH, K., TIGINYANU, I. Photoconductivity relaxation in nanostructured InP. In: *8th International Conference on Microelectronics and Computer Science*, Chișinău, Republic of Moldova, October 22-25, 2014. pp. 94 – 97. https://ibn.idsi.md/ro/vizualizare_articol/75603
 53. **MONAICO, E.**, TIGINYANU, I., NIELSCH, K., URSAKI, V., KOLIBABA, G., NEDEOGLO, D., COJOCARU, A., FOLL, H. Comparative study of porosification in InAs, InP, ZnSe and ZnCdS. (*Invited paper*) In: *2nd International Conference on Nanotechnologies and Biomedical Engineering*, Chișinău, Republic of Moldova, pp. 51-55, April 18-20, 2013. ISBN 978-9975-62-343-8. https://ibn.idsi.md/ro/vizualizare_articol/79319
 54. PRISLOPSKI, S., NAUMENKO, E., TIGINYANU, I., GHIMPU, L., **MONAICO, E.**, SIRBU, L., GAPONENCO, S. Retroreflection from nanoporous InP. In: *Nanotechnologies and Biomedical Engineering*, Ed. 2, 18-20 aprilie 2013, Chișinău. Technical University of Moldova, 2013, Editia 2, pp. 278-280. ISBN 978-9975-62-343-8. https://ibn.idsi.md/vizualizare_articol/79499
 55. GONCEARENCO E.P., COLIBABA G.V., **MONAICO E.V.** Obtaining of the substrates of II-VI compounds and solid solutions for nanoporous structures. In: *Proc. of International Conference CYSENI 2013*, 29-31 May 2013, Kaunas, Lithuania, pp. 448-456. ISSN 1822-7554. https://cyseni.com/wp-content/archives/proceedings/Proceedings_of_CYSENI_2013.pdf
 56. **MONAICO, E.**, TIGINYANU, I.M., URSAKI, V., KOLIBABA, G., NEDEOGLO, D., COJOCARU, A., FOLL, H. Porosification of narrow and wide band gap semiconductor compounds: comparative study of InAs, InP, and ZnSe. In: *4th International Conference "Telecommunications, Electronics and Informatics" ICTEI 2012*. Chișinău, Republic of Moldova, 17—20 May 2012. pp. 240 – 245. <http://repository.utm.md/handle/5014/7315>
 57. TIGINYANU, I., **MONAICO, E.**, POPA, V. Electrochemistry-based maskless nanofabrication. In: *Proceedings of the CAS 2012*; October 2012; Vol. 1, pp. 21–26. 15-17 October, Sinaia, Romania. Doi: [10.1109/SMICND.2012.6400703](https://doi.org/10.1109/SMICND.2012.6400703)
 58. **MONAICO, E.**, URSAKI, V., ZALAMAI, V., MASNIK, A., SYRBU, N., BURLACU, A. Electrochemical nanostructuring of $CuInS_2$ bulk crystals. In: *7th International Conference on Microelectronics and Computer Science*, Chișinău, Republic of Moldova, September 22-24, 2011, pp. 139-143. Disponibil: <http://repository.utm.md/handle/5014/6309>
 59. **MONAICO, E.**, TIGINYANU, I., KOLIBABA, G., NEDEOGLO, D., COJOCARU, A., FOLL, H. Development of conductive nanotemplates on ZnSe. In: *Nanotechnologies and Biomedical Engineering*, Ed. 1, 7-8 iulie 2011, Chișinău. Technical University of Moldova, 2011, Editia 1, pp. 39-42. ISBN 978-9975-66-239-0. https://ibn.idsi.md/vizualizare_articol/80288
 60. TIGINYANU, I.M., **MONAICO, E.**, BADINTER, E., IOISHER, A., ENACHI, M. Dielectric and metallo-dielectric 2D quasi-periodic nanomaterials for photonic and electronic applications. (*Invited paper*) In: *10th Expert Evaluation & Control of Compound Semiconductor Materials & Technologies* (EXMATEC), May 19-21, 2010, Darmstadt/Seeheim, Germany. Pp. 173 – 176.

3.3. in the works of scientific events included in the Register of materials published on the basis of scientific events organized in Republic of Moldova

61. LANGA, S., MONAICO, E., FOLL, H., TIGINYANU, I. Porous morphologies in Si, III-V and II-VI compounds: a comparative study. In: *Microelectronics and Computer Science: The 6th International Conference*, Ed. 6, 1-3 octombrie 2009, Chisinau. Bălți, Republica Moldova. Ediția 6, pp. 175-179. ISBN 978-9975-45-122-2. https://ibn.idsi.md/vizualizare_articol/184635
62. TIGINYANU, I., MONAICO, E., URSAKI, V., KOLIBABA, G., NEDEOGLO, D., LEPORTA, N. Electrochemically nanostructured ZnSe for photonic and optoelectronic applications. In: *Microelectronics and Computer Science: The 6th International Conference*, Ed. 6, 1-3 octombrie 2009, Chisinau. Bălți, Republica Moldova. Ediția 6, pp. 146-149. ISBN 978-9975-45-122-2. https://ibn.idsi.md/vizualizare_articol/184614
63. MONAICO, E., COSEAC, V., URSAKI, V., SYRBU, N., TIGINYANU, I. Photoluminescence of ZnTe nanowires prepared by electrochemical etching of bulk ZnTe. In: *Microelectronics and Computer Science: The 6th International Conference*, Ed. 6, 1-3 octombrie 2009, Chisinau. Bălți, Republica Moldova. Ediția 6, pp. 150-153. ISBN 978-9975-45-122-2. https://ibn.idsi.md/vizualizare_articol/184615
64. SPRINCEAN, V., COJOCARU, A., MONAICO, E., TIGINYANU, I., FOLL, H. Comparison of morphologies of porous InP layers obtained in different electrolytes. In: *Microelectronics and Computer Science: The 6th International Conference*, Ed. 6, 1-3 octombrie 2009, Chisinau. Bălți, Republica Moldova. Ediția 6, pp. 179-181. ISBN 978-9975-45-122-2. https://ibn.idsi.md/vizualizare_articol/184637

4. Patents and other intellectual property objects

4.1. issued by the State Agency for Intellectual Property

65. MONAICO Eduard, URSACHI Veaceslav, MORARI Vadim, TIGHINEANU Ion. *Procedeu de obținere a nanostructurilor magnetice*. Brevet de invenție 4869. Universitatea Tehnică a Moldovei. Nr. depozit a2020 0012. Data depozit 22.02.2022. In: BOPI. 2023, nr. 1, pp. 38 – 39. https://agepi.gov.md/sites/default/files/bopi/BOPI_09_2023.pdf
66. MONAICO Eduard, MONAICO Elena, URSACHI Veaceslav, TIGHINEANU Ion. *Procedeu de obținere a nanomembranei perforate de Au*. Brevet de invenție 4830. Universitatea Tehnică a Moldovei. Nr. depozit a2020 0052. Data depozit 09.06.2020. In: BOPI. 2022, nr. 11, pp. 52. https://agepi.gov.md/sites/default/files/bopi/BOPI_11_2022.pdf
67. GOLOGAN Viorel, IVAȘCU Sergiu, SIDELINICOVA Svetlana, MONAICO Eduard. *Procedeu de depunere a acoperirilor din electrolit pe bază de nichel*. Brevet de invenție 4721. Institutul de fizică aplicată. Nr. depozit a2019 0002. Data depozit 02.01.2019. In: BOPI. 2020, nr. 10, pp. 50 – 51. https://agepi.gov.md/sites/default/files/bopi/BOPI_10_2020.pdf

5. Theses at national and international conferences

68. MONAICO, E.V. Porous semiconductor compounds: obtaining and functionalization with metallic nanostructures for multifunctional applications. (*Invited paper*). In: *Abstract Book of Invited Papers at the 7th International Colloquium "Physics of Materials" (PM-7)*, 10 — 11 November 2022, Bucharest, Romania. http://www.physics.pub.ro/Site_Conferinta_PM-7/INVITED_PAPERS.pdf p.1. Comunicare orală. <http://cris.utm.md/handle/5014/1547>
69. MONAICO, E.V. Semiconductor matrices and templated electrodeposition of metal dots and nanotubes. (*plenary session, invited*). In: *The fifth International Colloquium 'Physics of Materials' - PM-5*. November 10-11, 2016. Bucharest, Romania. Comunicare orală
70. SERGENTU, V.V., URSAKI, V., MONAICO, Ed., TIGINYANU, I.M., PRISLOPSKI, S.Y., GAPONENKO, S.V. "Dark" modes backscattering as possible rationale for anomalous retroreflection from porous strongly absorbing Nanostructures. (*Invited paper*) In: *International Conference on Coherent and Nonlinear Optics/ International Conference on Lasers, Applications and Technologies 2016 (ICONO/LAT 2016)*. 26-30 September 2016 Minsk, Belarus. (Журнал прикладной спектроскопии. – 2016. – Vol. 83, Nr 6-16). – P. 281-282. –

71. **MONAICO, E.V.** Porous semiconductor compounds: characterization and applications. In: *Book of Abstracts of BPU11 CONGRESS. The 11th International Conference of the Balkan Physical Union.* 28 August 2022 - 1 September 2022, Belgrade, Serbia. pp. 209-210. S12-PSSAP-100/Comunicare orală. <https://indico.bpu11.info/event/1/contributions/111/http://cris.utm.md/handle/5014/1421>
72. **MONAICO, E.V.,** TIGINYANU, I.M. Nano-engineering of III-V semiconductor compounds and metal nanostructures based on electrochemical technologies. In: *Book of abstracts 4th conference "Nanotechnology and Innovation in the Baltic Sea Region" (NIBS2021)*, page 5, Kiel, Germany, 4th-6th august 2021. (Oral presentation) Disponibil: https://nibs.nina-sh.de/wp-content/uploads/2021/08/NIBS2021_Technical_Digest_final.pdf
73. MORARI, V., **MONAICO, E.V.,** LEISTNER, K., TIGHINEANU, I., NIELSCH, K. Porous GaAs layers and nanostructures decorated with magnetic materials. In: *Energy Efficient Magnetolectric Materials by Ionic Approaches: Fundamentals, Challenges and Perspectives.* 26 - 29 January 2020, Physikzentrum Bad Honnef, Bonn, Germany p.48
74. COLIBABA G., **MONAICO E.,** RUSNAC D. Obtaining highly conductive oxide single crystals for manufacturing nanotemplates. In: *NANO-2019: Limits of Nanoscience and Nanotechnologies + Humboldt Kolleg Conference, 24-27 September 2019, Chisinau, Moldova* pp. 78 https://ibn.idsi.md/ro/vizualizare_articol/92980/
75. PRISLOPSKI, S.Ya., GAPONENKO, S.V., **MONAICO, E.,** SERGENTU, V.V., TIGINYANU I.M. Polarized retroreflection from nanoporous III-V semiconductor. (poster). In: *26th International Symposium "Nanostructures: Physics and Technology"* Minsk, Belarus, June 18–24, 2018
76. **MONAICO, E.,** MOISE, C., MIHAI, G., URSAKI, V., TIGINYANU, I., ENACHESCU, M., NIELSCH, K. Control of HVPE grown GaN nanostructuring by anodization. In: *9th International Conference Materials Science and Condensed Matter Physics*, Chisinau, Republic of Moldova, p. 207, September 25-28, 2018. https://ibn.idsi.md/ro/vizualizare_articol/71753
77. **MONAICO, E.V.** Development of optically transparent and electrically conductive nanotemplates for nanofabrication. In: *Humboldt Kolleg, Multidisciplinary in Modern Science for the Benefit of Society*, Chisinau, Moldova, pp. 19, September 21-22th, 2017. https://ibn.idsi.md/vizualizare_articol/60460
78. BRANISTE, T., **MONAICO, E.,** MARTIN, D., CARLIN, J.-F., POPA, V., URSAKI, V.V., GRANDJEAN, N., TIGINYANU, I.M. Fabrication and characterisation of multilayer porous GaN structures. In: *Humboldt Kolleg, Multidisciplinary in Modern Science for the Benefit of Society*, Chisinau, Moldova, pp. 48, PS-7, September 21-22th, 2017. https://ibn.idsi.md/vizualizare_articol/60525
79. TIGINYANU, I., BRANISTE, T., **MONAICO, E.,** POPA, V., STEVENS-KALCEFF, M.A., SARUA, A., THOMAS, J., ANDRADE, H.D., MARTIN, D., CARLIN, J.-F., GRANDJEAN, N. Impact of defects upon the morphology of GaN nanoporous layers and membranes (oral presentation). In: *2016 European Materials Research Society Spring Meeting*, May 2-6, 2016, Lille, France. Symposium BB: Defect-induced effects in nanomaterials, Report BB-10.2
80. G.V. COLIBABA, **E.V. MONAICO, E.P. GONCEARENCO, I. INCULET, I.M. TIGINYANU.** Features of nanotemplates manufacturing on the II-VI compound substrates. In: *3rd International Conference on Nanotechnologies and Biomedical Engineering.* Chisinau, Moldova, September 23-26th, 2015. p. 76. https://ibn.idsi.md/sites/default/files/imag_file/76-76a.pdf
81. **MONAICO, E.V.** 2D semiconductor-metal quasi-periodic structures for photonics. In: *Humboldt Kolleg "Science and society- the use of light"*, Chisinau, Moldova, September 23-26th, 2015, p. 42. <http://repository.utm.md/handle/5014/20306>
82. COLIBABA, G., **MONAICO, E.,** TIGINYANU, I., GONCEARENCO, E., INCULET, I. Obtaining of II-VI compound single crystal substrates with controlled electrical properties and

- prospects of their application for manufacturing nanotemplates. In: *Fifth European Conference on Crystal Growth (ECCG5)*, Bologna, 9-11 September 2015.
83. COLIBABA, G., GONCEARENCO, E., NEDEOGLO, D., TIGINYANU, I., **MONAICO, E.V.** Obtaining of II-VI compound substrates with controlled electrical parameters and prospects of their application for nanotemplates. In: *XII International Conference on Nanostructured Materials (NANO 2014)*, Lomonosov Moscow State University, Moscow, Russia, July 13 – 18, 2014
 84. PRISLOPSKI, S.Y., TIGINYANU, I.M., GHIMPU, L., **MONAICO, E.**, SIRBU, L., GAPONENKO, S.V. Retroreflection of light from nanoporous InP: Correlation with high absorption. In: *Proc. of META '14, the 5th International Conference on Metamaterials, Photonic Crystals and Plasmonics. META 2014 CONFERENCE*, 20 – 23 MAY 2014, SINGAPORE.
 85. PRISLOPSKI, S.Y., NAUMENKO, E., TIGINYANU, I.M., GHIMPU, L., **MONAICO, E.**, SIRBU, L., GAPONENKO, S.V. Retroreflection of light from nanoporous InP. In: *Proc. of META '14, the 5th International Conference on Metamaterials, Photonic Crystals and Plasmonics. META 2014 CONFERENCE*, 20 – 23 MAY 2014, SINGAPORE
 86. COLIBABA, G.V., **MONAICO, E.V.**, GONCEARENCO, E.P., COVALCIUC, G. Growth of wide band-gap II-VI semiconductor compounds with controlled electrical properties. In: *7th International conference of Material Science and Condensed Matter Physics (MSCMP-2014)*, Chisinau, Moldova, 16-19 September 2014, Abstract, p.106 https://ibn.idsi.md/ro/vizualizare_articol/72989
 87. COLIBABA, G.V., **MONAICO, E.V.**, GONCEARENCO, E.P., NEDEOGLO, D.D., TIGINYANU, I.M. Wide band-gap II-VI semiconductor compounds: fabrication of nanotemplates and prospects of their application for optoelectronics and photonics. In: *2nd International Symposium on Optics and its Applications*, 1-5 September 2014, Yerevan-Ashtarak, Armenia, Abstracts, p. 123
 88. **MONAICO, E.**, TIGINYANU, I.M., NIELSCH, K., URSAKI, V.V., COLIBABA, G., NEDEOGLO, D.D., COJOCARU, A., FÖLL, H. Porosification of III-V and II-VI semiconductor compounds. In: *Humboldt Kolleg 2013. Knowledge Society: mutual influence and interference of science and society - NANO-2013*, 13-16 September 2013, Chisinau, Moldova
 89. COLIBABA, G.V., GONCEARENCO, E.P., **MONAICO, E.V.**, NEDEOGLO, D.D., NEDEOGLO, N.D. Obtaining of II-VI compound substrates with controlled electrical parameters and prospects of their application for nanoporous structures. In: *E-MRS Fall Meeting 2013, Fall Meeting Warsaw University of Technology*, Warsaw (Poland), 16th - 20st September, 2013
 90. PRISLOPSKI, S., NAUMENKO, E., TIGINYANU, I., GHIMPU, L., **MONAICO, E.**, SIRBU, L., GAPONENKO, S. Anomalous retroreflection from strongly absorbing nanoporous semiconductors. In: *Fundamental and Applied NanoElectroMagnetics. FANEM-2012*, May 22-25, 2012, Belarusian State University, Minsk, Belarus. - Minsk: BSU, 2012. - P. 24. Disponibil: <https://elib.bsu.by/bitstream/123456789/230042/1/24.pdf>
 91. **MONAICO, E.V.** Electrochemical deposition of nanodots, nanotubes, and nanowires in porous III-V and II-VI compounds. In: *German-Moldova Workshop on Electrochemical Nano-Structuring of Materials*. Kiel, Germany, July 23, 2012.
 92. TIGINYANU, I.M., **MONAICO, E.V.** URSAKI, V.V. Two-dimensional metallo-semiconductor networks for electronic and photonic applications. In: *220th ECS Meeting & Electrochemical Energy Summit in Boston*, Massachusetts (October 9-14, 2011)
 93. PRISLOPSKI, S., TIGINYANU, I.M., GHIMPU, L., **MONAICO, E.**, SIRBU, L., ZHUKOVSKY, S.V., GAPONENKO, S.V. Retroreflection from disordered porous semiconductors. In: *13th International Conference on Transparent Optical Networks ICTON 2011*, Stockholm, 26-30 June 2011.
 94. COLIBABA, G., **MONAICO, E.**, NEDEOGLO, D., TIGINYANU, I.M., GONCEARENCO, E. Obtaining A²B⁶ compound substrates with controlled conductivity and prospects of their application for fabrication of nanoporous structures. In: *2nd International Conference of*

Luminescent Processes in Condensed State of Matter (LUMCOS), Kharkov, Ukraine, p. 98-99, 14-18 November 2011.

95. LANGA, S., TIGINYANU, I.M., **MONAICO, E.**, FÖLL, H. Porous II-VI vs. porous III-V semiconductors. In: *7th Int. Conf. „Porous Semiconductors: Science and Technology“*, Valencia, Spain, March 14-19, 2010 (Abstract Booklet, Paper P1-13)
96. **MONAICO E.** Optically transparent and electrically conductive nanotemplates on ZnSe. In: *German-Moldova Workshop on Electrochemical Nano-Structuring of Materials*. Kiel, Germany, November 12, 2010.

Participation at international salons for invention

97. **MONAICO, E.V.**, URSAKI, V.V., MORARI V., TIGINYANU, I.M. Process for fabrication of magnetic nanostructures. In: *Proceedings of the 15th Edition of European Exhibition of Creativity and Innovation, “EUROINVENT 2023”* 11-13 MAY 2023, Iasi, Romania. **Diplomă și Medalie de aur**. Disponibil: <http://cris.utm.md/handle/5014/1692>
98. **MONAICO, E.V.**, URSAKI, V.V., MORARI V., TIGINYANU, I.M. Process for fabrication of magnetic nanostructures. In: *Salonul Internațional al Cercetării Științifice, Inovării și Inventicii PRO INVENT*, ediția a XXI-a, 25-27 octombrie 2023, CLUJ-NAPOCA, Romania. **Diploma de excelență și Medalie de aur**. Disponibil: <http://ncmst.utm.md/images/stories/medalii/ProInvent%202023%20Diploma%20aur.pdf>
99. **MONAICO, E.V.**, MONAICO, E.I., URSAKI, V.V., TIGINYANU, I.M. Nanomembranes constituées d'une monocouche de nanoparticules d'or. Geneva, “Geneva 2023” 26-30 April 2023, Geneva, Elvetia. **Diplomă și Medalie de bronz**. Disponibil: <http://cris.utm.md/handle/5014/1683>
100. **MONAICO, E.V.**, URSAKI, V.V., MORARI, V., TIGINYANU, I.M. Process for fabrication of magnetic nanostructures. In: *The International Fair of Innovation and Creative Education for Youth (ICE-USV) the VIIth edition*, 07-09 July 2023, Suceava, Romania. **Diplomă și Medalie de aur**. Disponibil: <http://cris.utm.md/handle/5014/1748>
101. **MONAICO, E.V.**, URSAKI, V.V., TIGINYANU, I.M. Process for obtaining several non-connected pore networks in a semiconductor wafer for fluidic applications. In: *The 26th International Exhibition of Inventions “INVENTICA 2022”* 23-24 June 2022, Iași, România. **Diploma de excelență și Medalie de argint**. Disponibil: <http://cris.utm.md/handle/5014/1494>
102. **MONAICO, E.V.**, URSAKI, V.V., TIGINYANU, I.M. Process for independent pore networks obtaining in semiconductor wafers. In: *Proceedings of the 14th Edition of European Exhibition of Creativity and Innovation, “EUROINVENT 2022”* 26-28 MAY 2022, Iasi, Romania. pp. 150-151, 2022. **Diplomă și Medalie de aur**. Disponibil: <http://cris.utm.md/handle/5014/1339>
103. **MONAICO, E.V.**, URSAKI, V.V., TIGINYANU, I.M. Procedeu de obținere a mai multor rețele de pori independente în substrat semiconductor pentru aplicații fluidice. In: *Salonul Internațional al Cercetării Științifice, Inovării și Inventicii PRO INVENT*, ediția a XXI-a, 26-28 octombrie 2022, Iasi, Romania. **Diplomă și Medalie de aur**. Disponibil: <http://cris.utm.md/handle/5014/1461>

DECLARATION OF RESPONSIBILITY

I, the undersigned, declare under personal responsibility that the materials presented in the synthesis work for the title of Dr. Habilitat in Physics, developed on the basis of published scientific papers, are the result of my own research and scientific achievements. I am aware that, otherwise, I will bear the consequences in accordance with the legislation in force.

dr., research assoc. prof. Eduard MONAICO

Signature:



Date: 22.04.2024

CURRICULUM VITAE

Name, Surname:

MONAICO Eduard Vladimir

<https://orcid.org/0000-0003-3293-8645>
<https://scholar.google.com/citations?hl=ru&user=Z1bfsSkAAAAJ>

Scopus Author ID: 8979938300



Citizenship:

Republic of Moldova

Studies:

2021 – 2022 – Postdoc, Technical University of Moldova

2017 – research associated professor, Technical University of Moldova

2009 – PhD in physics and mathematics, Moldavian State University. Specialty 01.04.10 –

Physics and semiconductor engineering

2002 – 2005 – PhD studies, Technical University of Moldova

1997 – 2002 – Engineer in Electronics and Communications, Technical University of Moldova

Studies:

03.2018 – 05.2018 – Leibniz Institute for Solid State and Materials Research (IFW Dresden), Germany. Alexander von Humboldt Fellowship

01.2012 – 01.2014 – Hamburg University, Hamburg, Germany. Alexander von Humboldt Fellowship

05.2004 – Oxford Instruments, London, UK

Fields of scientific interest:

Semiconductor physics and engineering, Nano-Microelectronics and Optoelectronics

Participation in national and international scientific projects:

Director in 9 scientific projects: 1- CRDF / MRDA individual (2009); 2 - for young researchers (2009-2010, 2011-2012); 1 - State Program #16.00353.50.08.A (2016-2017); 1 - STCU #6222 (2017-2019), 1 - institutional project #15.817.02.29A (2016-2019), 1- bilateral Belarus-Moldova #19.80013.50.07.03A/BL (2019-2020), postdoctorat #21.00208. 5007.15/PD (2021-2022), State Program #20.80009.5007.20 (2020-2023) and executor in several national and international projects (INTAS, CRDF, SCOPES, STCU, FP7, H2020)

Participation in scientific events (national and international):

Organizer of International Conferences:

– Organizing committee: The 6th International Conference on Nanotechnologies and Biomedical Engineering (ICNBME-2023), 20-23 September 2023, Chisinau, Republic of Moldova

– Organizing Committee: The 5th International Conference on Nanotechnologies and Biomedical Engineering (ICNBME-2021), 3-5 November 2021, Chisinau, Republic of Moldova;

– Co-chairman of Humboldt Kolleg 2015 "Science and society: the use of light" 24 – 25 September 2015, Republic of Moldova.

Published scientific works:

1 monograph, 1 review article, 2 chapters in monographs, 85 published scientific articles, participation in international and national scientific conferences with 118 oral and poster communications, 19 invention patents registered at AGEPI, Moldova.

Awards, mentions, distinctions, honorary titles, etc.:

– Laureate of the Prize for Youth in the fields of Science, Technology, Literature and Arts, 2006 edition, for the cycle of works "Study of nanostructured materials and electronic devices developed on the basis of semiconductor compounds" in the field of physics.

– Diplomas with gold, silver and bronze medals at International Exhibitions: Euroinvent 2023, 2022, 2021, 2020; Inventica 2021; Proinvent 2022, 2021; EUREKA Brussels (Gold Medal in 2007,

2006, 2005); Gold Medal at IMPEX 2005 USA; and at Geneva International Exhibitions in 2023, 2008, 2007 and 2005.

Membership of national and international scientific societies/associations:

- Moldavian Physical Society, 2022 – present, President, <https://sfm.utm.md/>
- Society of Biomedical Engineering from Moldova, member
- Balkan Physical Union (BPU), member
- European Physical Society (EPS), member

Activities within the editorial boards of scientific journals:

„Fizica și Tehnologii Moderne” member of the editorial/advisory boards from 18.10.2021

Didactic activity:

Associated professor at the Department of Microelectroelectronics and Biomedical Engineering: 2 disciplines. MicroNanoElectronic Devices (Cycle I), NanoElectronic Devices (Cycle II).

Knowledge of languages:

Mother tongue: Romanian;

English language: Advanced level;

Russian language: Advanced level;

German: Intermediate level.

Contact details:

National Center for Materials Study and Testing

Technical University of Moldova

Bd. Ștefan cel Mare 168, Chisinau 2004, Republic of Moldova

Tel. +373 (22) 50-99-20

e-mail: eduard.monaico@cnstm.utm.md

www.ncmst.utm.md

ADNOTARE

Monaico Eduard Vladimir, Micro- și nano-ingineria compușilor semiconductori și a structurilor metalice în baza tehnologiilor electrochimice. Specialitatea 134.01 – Fizica și tehnologia materialelor. Lucrarea de sinteză pentru titlul de doctor habilitat în științe fizice (în baza lucrărilor științifice publicate), Chișinău 2024.

Structura lucrării de sinteză: reperele conceptuale ale cercetării, conținutul publicațiilor expuse în 4 capitole, concluzii generale și recomandări. Lucrarea cuprinde 94 referințe bibliografice, 84 pagini, 26 figuri și 3 tabele. În baza rezultatelor obținute au fost publicate 103 lucrări științifice, inclusiv 41 articole științifice din bazele de date Web of Science și SCOPUS.

Cuvinte-cheie: structuri poroase, dirijarea direcției de creștere a porilor, electrodepunere în salturi, dispozitiv varicap, retroreflexie anormală, fotodetector IR, lentile fotonice integrate, anizotropie magnetică, structuri hibride miez-înveliș, proprietăți hidrofile/hidrofobe.

Scopul lucrării de sinteză: elaborarea conceptelor teoretice și elaborarea abordărilor tehnologice pentru micro- și nano-ingineria compușilor semiconductori poroși și a nanostructurilor metalice prin metode electrochimice pentru aplicații multifuncționale.

Obiective cercetării: obținerea templatelor semiconductoare cu bandă interzisă largă; analiza comparativă a nanostructurării compușilor semiconductori III-V (InP, GaAs, GaN) și compușilor II-VI (CdSe, ZnSe, $Zn_xCd_{1-x}S$); elaborarea mecanismului de depunere; dezvoltarea și optimizarea tehnologiilor electrochimice de trecere de la straturi poroase la rețele de nanofire; cercetarea proprietăților nanostructurilor elaborate cu scopul de a demonstra aplicabilitatea în micro- și nano-dispozitive în electronică, optoelectronică, fonică, feromagnetism.

Noutatea și originalitatea științifică: dezvoltarea abordărilor tehnologice electrochimice ce permit de a dirija cu direcția porilor atât în adâncime, cât și pori paraleli cu suprafața cristalelor; a fost elaborat și demonstrat mecanismul „electrodepunerii în salturi” ce duce la depunerea unui monostrat de nanopuncte de Au pe compuși semiconductori poroși; în premieră a fost demonstrată retroreflexia „anormală” a luminii de pe straturile ultra-poroase în baza compușilor semiconductori de InP și GaAs, observată și cu ochiul liber; în premieră a fost propusă o abordare cost-eficientă și originală de estimare a conductibilității electrice în nanostructuri semiconductoare de InP cu grosime diferită, prin depunerea electrochimică a metalului în impulsuri; a fost demonstrat că ingineria suprafețelor semiconductoare prin metode electrochimice (corodare și/sau depunere electrochimică) permite de a schimba în mod dirijat proprietățile hidrofile/hidrofobe.

Rezultatele științifice principale noi sunt: (i) conceptul elaborat și demonstrat experimental pentru ingineria morfologiei straturilor poroase în compuși semiconductori prin aplicarea pe suprafața semiconductorului a măștilor fotolitografice cu o configurație specială, urmată de corodarea electrochimică; (ii) mecanismul de „electrodepunere în salturi” elaborat a stat la baza conceptului de demonstrare experimentală a conductibilității electrice diferite în nanostructuri semiconductoare cu grosime diferită și utilizat pentru demonstrarea experimentală cu evidențierea dopării neuniforme în timpul creșterii HVPE a substraturilor de GaN; (iii) dirijarea formei geometrice a porilor sau a nanofirelor semiconductoare permite de a obține structuri hibride miez-înveliș cu geometrii triunghiulare, pătrate sau rotunde prin depunerea unui strat subțire de metal cu ajutorul depunerii electrochimice în impulsuri în interiorul porilor sau în jurul nanofirelor.

Semnificația teoretică constă în elaborarea și demonstrarea: mecanismului de „electrodepunere în salturi”; conceptului ingineriei direcției de creștere a porilor prin folosirea proceselor fotolitografice.

Valoarea aplicativă este accentuată prin: demonstrarea perspectivelor pentru elaborare de noi elemente de focalizare și separatoare de fascicule în baza nanostructurilor GaP/Pt sau ZnSe/Pt pentru aplicații în regiunea vizibilă a spectrului, reflectoare Bragg; elaborarea dispozitivelor: varicap, senzor de gaz, fotodetectori de radiație IR.

Implementarea rezultatelor științifice. Rezultatele obținute au fost prezentate la saloane internaționale de invenție fiind apreciate cu diplome și medalii de aur, argint și bronz. Rezultatele au fost implementate în procesul didactic la Facultatea CIM, departamentul MIB la predarea cursurilor „Dispozitive nanoelectronice” ciclul 2, „Dispozitive micronanoelectronice” ciclul 1.

ANNOTATION

Monaico Eduard Vladimir, Micro- and nano-engineering of semiconductor compounds and metal nanostructures based on electrochemical technologies. Specialty 134.01 Physics and Materials Technology. Synthesis work for the degree of doctor habilitat in Physics (based on published works), Chisinau, 2024.

The structure of the synthesis work: the conceptual benchmarks of the research, the content of the publications presented in 4 chapters, general conclusions and recommendations. The work includes 94 bibliographic references, 84 pages, 26 figures and 3 tables. Based on the obtained results, 103 scientific papers were published, including 41 scientific articles from the Web of Science and SCOPUS databases.

Keywords: porous structures, pore growth direction, jumping electrodeposition, varicap device, anomalous retroreflection, IR photodetector, integrated photonic lenses, magnetic anisotropy, core-shell hybrid structures, hydrophilic/hydrophobic properties.

The goal of the study: the development of theoretical concepts and the development of technological approaches for the micro- and nano-engineering of porous semiconductor compounds and metallic nanostructures by electrochemical methods for multifunctional applications.

Research objectives: obtaining of the wide bandgap semiconductor templates; comparative analysis of the nanostructuring of III-V semiconductor compounds (InP, GaAs, GaN) and II-VI compounds (CdSe, ZnSe, $Zn_xCd_{1-x}S$); the development of the electrodeposition mechanism; development and optimization of electrochemical technologies for transition from porous layers to nanowire networks; investigation of the developed nanostructures properties with the aim of demonstrating their applicability in micro- and nano-devices for electronics, optoelectronics, photonics, ferromagnetism.

Scientific novelty and originality: the development of electrochemical technological approaches that allow controlling the direction of pores growth, both in depth and parallel to the surface of the crystals; the "jumping electrodeposition" mechanism leading to the deposition of a monolayer of Au nanodots on porous semiconductor compounds was developed and demonstrated; for the first time was demonstrated the "abnormal" retroreflection of light from ultra-porous layers based on InP and GaAs semiconductor compounds, also observed with the naked eye; for the first time, a cost-effective and original approach was proposed to estimate the electrical conductivity in InP semiconductor nanostructures with different thicknesses, via pulsed electrochemical deposition of metal; it has been demonstrated that the engineering of semiconductor surfaces by electrochemical methods (electrochemical etching and/or pulsed electrochemical deposition) allows to change the hydrophilic/hydrophobic properties in a controlled fashion.

The main new scientific results are: (i) the developed and experimentally demonstrated concept for the morphology engineering of porous layers in semiconductor compounds by applying on the surface of the semiconductor photolithographic masks with a special configuration, followed by electrochemical etching; (ii) the elaborated "hopping electrodeposition" mechanism served as the basis of the concept of experimental demonstration of different electrical conductivity in semiconductor nanostructures with different thickness and used for experimental demonstration highlighting non-uniform doping during HVPE growth of GaN substrates; (iii) controlling the geometric shape of the semiconductor pores or nanowires allows one to obtain core-shell hybrid structures with triangular, square or round geometries by depositing a thin metal layer by means of pulsed electrochemical deposition inside the pores or around the nanowires.

The theoretical significance lies in the development and demonstration of: the "hopping electrodeposition" mechanism; the concept of engineering the direction of pore growth using photolithographic processes.

The applicative value is emphasized by: demonstration of the perspectives for the development of new focusing elements and beam splitters based on GaP/Pt or ZnSe/Pt nanostructures for applications in the visible region of the spectrum, Bragg reflectors; device development: varicap, gas sensor, IR radiation photodetectors.

Implementation of scientific results. The obtained results were presented at international invention salons, being appreciated with gold, silver and bronze diplomas and medals. The results were implemented in the didactic process at the Faculty CIM, the MIB department at courses "Nanoelectronic Devices" master level, "Micronanoelectronic Devices" licentiate level.

MONAICO, EDUARD

**MICRO- AND NANO-ENGINEERING OF
SEMICONDUCTOR COMPOUNDS AND METAL STRUCTURES
BASED ON ELECTROCHEMICAL TECHNOLOGIES**

134.01 – PHYSICS AND MATERIALS TECHNOLOGY

**Synthesis work for the title of Doctor Habilitat in Physics
(elaborated on the basis of published scientific papers)**

Approved for printing: *16.05.2024*

Paper size 60x84 1/16

Offset paper. RISO Typing

Circulation 30 ex.

Print sheets: 5.25

Order number

MD-2004, Chisinau, bd. Ștefan cel Mare și Sfânt, 168, UTM
MD-2045, Chisinau, str. Studenților 9/9, Editorial Department “Tehnica – UTM”